CHARACTERISATION AND REACTION KINETICS OF HIGH ASH CHARS DERIVED FROM INERTINITE–RICH COAL DISCARDS

by

Rufaro Kaitano
MSc. (Chem. Eng.) (Wits)

Thesis submitted in fulfilment for the requirements for the degree Philosophiae Doctor in Chemical Engineering in the School of Chemical and Minerals Engineering at the North-West University, Potchefstroom Campus, South Africa.

Promoter:	Professor R.C. Everson (North-West University)
Assistant promoter:	Professor H.W.J.P. Neomagus (North-West University)
Co-promoter:	Professor R. Falcon (University of the Witwatersrand)

January 2007
Potchefstroom

DECLARATION

This thesis is submitted in fulfilment of the requirements for the degree of the Philosophiae Doctor in Engineering at the School of Chemical and Minerals Engineering of the North-West University.

I, Rufaro Kaitano, hereby declare that the dissertation with the title: CHARACTERISATION AND REACTION KINETICS OF HIGH ASH CHARS DERIVED FROM INERTINITE-RICH COAL DISCARDS is my own work and has not been submitted at any other university either in whole or in part.

Signed at Potchefstroom on the ..... day of January 2007

.....

R. Kaitano

ACKNOWLEDGEMENTS

The author wishes to gratefully acknowledge and deeply express his appreciation to the following people for their role during the course of this project:

- Professor R.C. Everson, Professor H.W.J.P. Neomagus and Professor R. Falcon without their expert guidance, critical evaluation of this work and inspiration during every stage of this study, this thesis would have been only a dream.
- Mr. Jan Kroeze, Mr. Hennie van Zyl and Mr Adrian Brock for the maintenance of the experimental apparatus.
- Dr. Quentin Campbell and Dr. Delani Njapha, for the fruitful discussions we held on the subject of coal.
- Ms Vivien du Cann and Dr Chris van Alphen were of great help with the characterisation work and the interpretation thereof.
- All the personnel of the School of Chemical and Minerals Engineering who were always willing to help when called to.
- My Grade 1 teacher, Ms Machiri who gave me a foundation for education.
- Eskom and the National Research Foundation (NRF), for providing financial support for this project.
- My family for their patience and continuous encouragement.
- All my friends, for the moral support.

ABSTRACT

An investigation was undertaken to determine the gasification and combustion characteristics of chars derived from an inertinite-rich coal discard sample with a high ash content. Fundamental knowledge of the reaction rate kinetics for char conversion at reactions conditions used in fluidised bed gasification and combustion was obtained. For this purpose, characterisation of the parent coal and derived chars, reactivity determinations of the chars and detailed reaction rate modelling was undertaken.

The characterisation performed consisted of standard coal analytical methods, petrographic techniques, CCSEM image analysis and a surface adsorption method. The parent coal consists of 32% by volume of inertinite, 7% of vitrinite, 13% of bi- and tri-macerite, 30% of maceral/mineral mixtures (carbominerite) with 18% of mineral-rich material. Reflectances obtained from measurements taken on vitrinites and total maceral reflectance scans increased dramatically on charring at 900°C and is accompanied by an extension of vitrinite-class distribution. Volatiles were liberated essentially from the original parent vitrinites, creating fine pores. Inertinites increased in reflectance but not in porosity and are characterised as dense char fractions in the final charred product, which was established according to a coal form analysis. Structural change due to low temperature thermal stress fracturing ("passive deflagration") occurred early on in the temperature regimes, creating increased surface areas and porosity. The chars consist of a high proportion (52%) of extraneous rock fragments together with minerals mainly as fine inclusions in carbon rich particles. The chars have very low porosities and surface areas created by devolatisation of maceral associations and deflagration.

Combustion and gasification reactivity experiments were carried out in a thermogravimetric analyser at 87.5 and 287.5 kPa pressures between 700 and 900°C and with varying mixtures of oxygen/nitrogen and carbon dioxide/nitrogen mixtures respectively.

The effects of temperature, pressure, gas composition and particle size on reactivity were found to confirm well-established trends. The effect of temperature in the high temperature range was, however, strongly affected by pore and film diffusion during

combustion. Models based on the random pore model without and with pore diffusion incorporating the properties of the char (porosity, ash content, and derived structural parameter) and structural mechanisms concerning carbon removal, were successfully solved and validated against experimental results. As a result of the complexity of the models consisting of many unknown parameters, a procedure consisting of step-wise regression was developed and applied successfully. This procedure uses a unified carbon conversion versus a reduced time parameter plot with the latter defined as real time/time for 90% conversion.

It was found that for char particles with a mean diameter of 1mm prepared at 900°C, the random pore model (chemical reaction controlling) was applicable for predicting the gasification reaction rate with carbon dioxide-nitrogen mixtures at temperatures up to 900°C, whereas for the combustion reactions with oxygen-nitrogen mixtures an adapted chemical reaction-pore diffusion model was found to be applicable in the temperature range 450 to 600°C. The model is characterised by a variable Thiele modulus which can account for pore- diffusion and can undergo a transition to a chemically controlled reaction as a result of the depletion of carbon in the carbon/mineral matrix. Intrinsic reaction rate parameters for gasification and combustion are reported and compared with published results. and were found to be slightly different. Diffusion coefficients were also evaluated from the combustion reaction results and found to compare very well with predictions with the Knudsen diffusion model.

OPSOMMING

'n Ondersoek is gedoen om die vergassings– en verbrandingseienskappe van sintels, verkry vanaf 'n monster inertiniet-ryke afvalsteenkool met 'n hoë asinhoud, te bepaal. Hierdie studie is aangepak om fundamentele kennis van die reaksiekinetika te verskaf vir sintelomsetting onder reaksiekondisies wat geld in gefluïdiseerde–bed vergassing en verbranding. Vir hierdie doel is karakterisering van die oorspronklike steenkool en verkreë sintels, reaktiwiteitbepalings van die sintels en detail–reaksiesnelheid modellering onderneem.

Die karakterisering wat uitgevoer is, het standaard steenkool analitiese metodes, petrografiese tegnieke, CCSEM–beeldanalise en oppervlak–adsorpsiemetodes behels.

Die oorspronklike steenkool het bestaan uit 32% per volume inertiniet, 7% vitriniet, 13% bi– en tri–maseriet, 30% maseraal/mineraal mengsels (karbomineriet) met 18% mineraalryke materiaal. Reflektansiewaardes verkry van metings uitgevoer op vitriniete en totale maseraal reflektansie–aftastings het dramaties toegeneem na sinteling by 900°C en het gepaardgegaan met 'n uitbreiding van die vitrinietklas–verspreiding. Vlugtiges is essensieel vrygestel uit die oorspronklike vitriniete om sodoende fyn porieë te vorm. Inertiniete het 'n verhoging in reflektansie getoon, maar nie in porositeit nie en is gekarakteriseer as 'n digte sintel–fraksie in die finale gesintelde produk. Dit is vasgestel deur middel van steenkool–vormanalise. Strukturele verandering as gevolg van lae–temperatuur termiese spanningsbreking ("passiewe deflagrasie") vroeg in die temperatuur–regiems het aanleiding gegee tot vergrote oppervlakareas en porositeit. Die sintels het uit 'n hoë verhouding (52%) vreemde rotsfragmente saam met minerale, hoofsaaklik teenwoordig as fyn insluitsels in koolstofryke deeltjies, bestaan. Die sintels het baie lae porositeite en oppervlakareas gehad, soos veroorsaak deur ontgassing van maseraalassosiasies en deflagrasie.

Verbrandings– en vergassingsreaktiwiteit–eksperimente is uitgevoer in 'n termogravimetriese analiseerder by 87.5 en 287.5 kPa druk tussen 700 en 900°C en met verskeie mengsels van suurstof/stikstof en koolstofdioksied–/stikstofmengsels onderskeidelik.

Die effekte van temperatuur, druk, gassamestelling en deeltjiegrootte op reaktiwiteit het goed-gevestigde bevindings bevestig. Die effek van temperatuur in die hoë temperatuur–bereik is egter sterk beïnvloed deur porie– en filmdiffusie. Modelle gebaseer op die willekeurige poriemodel sonder en met poriediffusie en met insluiting van die eienskappe van die sintel (porositeit, asinhoud, afgeleide struktuurparameter) en strukturele meganismes betrokke by koolstofverwydering, is suksesvol opgelos en bevestig deur eksperimentele bevindings. As gevolg van die kompleksiteit van die modelle wat baie onbekende parameters bevat, is 'n prosedure wat stapsgewyse regressie behels, ontwikkel en suksesvol toegepas. Die prosedure gebruik 'n verenigde koolstofomsetting versus 'n gereduseerde tydparameter–stip met laasgenoemde gedefinieer as reële tyd/tyd vir 90% omsetting.

Daar is bevind dat, vir sintelpartikels met 'n gemiddelde deursnit van 1mm, voorberei by 900°C, die willekeurige poriemodel (chemiese reaksie–beherend) toepaslik is vir die voorspelling van die vergassingsreaksiesnelheid met koolstofdioksied–stikstof mengsels by temperature tot 900°C. Vir die verbrandingsreaksies met suurstof–stikstofmengsels, daarenteen, is gevind dat 'n aangepaste chemiese reaksie–poriediffusiemodel toepaslik is in die temperatuurbereik 450 tot 600°C. Die model is gekarakteriseer deur 'n veranderlike Thiele-modulus om voorsiening te maak vir poriediffusie wat kan oorgaan in 'n chemies–beheerde reaksie as gevolg van die uitputting van koolstof in 'n koolstof–mineraalmatrys. Intrinsieke reaksiesnelheidsparameters vir vergassing en verbranding word gerapporteer en vergelyk met gepubliseerde bevindings, waaruit verskille blyk. Diffusiekoëffisiënte is ook geëvalueer uit die verbrandingsreaksie–bevindinge en vergelyk goed met voorspellings van die Knudsen–diffusievergelyking.

TABLE OF CONTENTS

LIST OF FIGURES

LIST OF TABLES

NOMENCLATURE

a, b	constants	-
C	concentration of reacting gas in core	moles m^{-3}
C_o	concentration of reacting gas in surrounding	moles m^{-3}
C^*	dimensionless concentration C/C_o	-
d_p	pore diameter	m
D_e	average effective diffusivity of gas in core	m^{-2} s^{-1}
D_{eO}	initial value of D_e	m^{-2} s^{-1}
D_e^*	dimensionless diffusivity D_e / D_{eO}	-
D_{ki}	Knudsen diffusivity in micropores	m^{-2} s^{-1}
D_{kie}	effective Knudsen diffusivity in micropores	m^{-2} s^{-1}
E	activation energy	kJ $mole^{(-1}$
$f(X)$	structure factor	m^{-1}
T	temperature	K
k	reaction rate constant (Table 2.3)	s^{-1}
k_s	reaction rate constant, ($r_s = k_s C$)	m^{-4} $mole^{(-1}$ s^{-1} or m s^{-1} Pa
k_{so}	reaction rate constant, ($r_s = k_s C$)	m^{-4} $mole^{(-1}$ s^{-1} or m s^{-1} Pa
k'_{so}	lumped pre-exponential factor, $k_{so} S_O/.(1-\varepsilon_o)$	m^{-4} $mole^{(-1}$ s^{-1} or s^{-1} Pa
L_o	total pore length per unit volume	m m^{-3}
m	constant, (0, 1 or 2/3)	-
m_{ash}	mass of ash	g
m_o	initial mass of char	g
m_t	mass of char at time t	g
M	molecular weight of carbon	g $mole^{(-1}$
M_A	molecular weight of gas	g $mole^{(-1}$

n	order of reaction	-
p	partial pressure of reacting gas	kPa
R_r	vitrinite reflectance, %	-
R_{sc}	total (full) maceral reflectance, %	-
R_0	initial particle radius	m
r	radius of particle (spherical) at any time	m
r_1	radius of micropores	m
r_S	reaction rate	$m\ s^{-1}$
S_O	initial surface area	$m^{-2}\ m^{-3}$
T	temperature	°C and °K
t	time	s and min
t_f	time factor, $\frac{r_S S_O}{(1-\varepsilon_o)}$	s^{-1}
$t_{0.9}$	time for fractional carbon conversion of 0.9	s
χ_{ash}	ash fractional content	-
X	fractional conversion of carbon	-
$\overline{X}$	overall fractional conversion of carbon	-

Greek Letters

β	power dependence	-
γ	tortuosity	-
ε	porosity	-
ε_o	initial porosity	-
ε^*	dimensionless porosity, $\varepsilon/\varepsilon_o$	-
ρ	density of carbon	$g\ m^{-3}$
σ	standard deviation of reflectance measurements	-
τ	dimensionless time = $\tau = \frac{r_o S_o t}{(1-\varepsilon_o)}$	-
$\tau_{0.9}$	dimensionless time for fractional carbon conversion of 0.9	-

ϕ	Thiele modulus, $\phi = R_o\sqrt{k_s \rho C_{SO}/MD_e}$	-
ϕ_0	Initial Thiele Modulus, $\phi = R_o\sqrt{k_s \rho C_{SO}/MD_{eo}}$	-
ψ	structural parameter, $\frac{4\pi L_o(1-\varepsilon_o)}{S_o^2}$	-

Acronyms/Abbreviations

ar	as received
ASTM	American Society for Testing and Materials
BET	Brunauer, Emmett and Teller Isotherm
BFB	Bubbling Fluidised Bed
BJH	Barret Joyet Haleda method
BSI	Backscattered Electron Image
CCSEM	Computer Controlled Scanning Electron Microscope
CFB	Circulating Fluidised Bed
CHAR700	Char prepared at 700˚C
CHAR900	Char prepared at 900˚C
CSIR	Council for Scientific and Industrial Research (South Africa)
daf	dry and ash free
db	dry basis
FBC	Fluidised Bed Combustion
FMR	Full Maceral Reflectance
IGCC	Integrated Gasification Combined Cycle
ISO	International Standards Organisation
MMB	Visible Mineral Matter Basis
MMF	Visible Mineral Matter-Free Basis
NRF	National Research Foundation
PBBR	Packed Bed Balance Reactor
PBMR	Pebble Bed Modular Reactor
PCC	Pulverised Coal Combustion
PDEPE	Partial differential equation algorithm (MATLAB)

QEMSCAN	Automated image analysis system
SABS	South African Bureau of Standards
TGA	thermogravimetric analyser

See also Appendix C for terms and abbreviations used in petrographic results.

LIST OF PUBLICATIONS

(Accredited journals and conference proceedings)

Everson, R.C. Neomagus, H.W.J.P. and Kaitano, R. (2005). The modeling of the combustion of high-ash coal-char particles suitable for pressurised fluidised bed combustion: Shrinking Reacted Core Model. *Fuel*, 84(9), 1136-1143

Everson, R.C. Neomagus, H.W.J.P. and Kaitano, R. and Kalibantonga, P.D. (2006). Reaction kinetics of inertinite-rich coal particles at Fluidised bed combustion conditions. Presented at the Fossil Fuel Foundation Annual Indaba, Johannesburg. South Africa, Oct. 2006

Everson, R.C. Neomagus, H.W.J.P. Kaitano, R. Falcon, R. and Du Cann, V.M. (2005). The petrographic and combustion performance of high-ash coal-char particles derived from inertinite rich coal. Presented at the Fossil Fuel Foundation Annual Indaba, Jet Park, South Africa, Nov. 2005

Everson, R.C. Neomagus, H.W.J.P. Kaitano, R. Falcon, R. and Du Cann, V.M. (2005). Characteristics and reaction kinetics of high-ash coal-char particles suitable for bubbling fluidised bed combustion and gasification. Presented at Pittsburgh Coal Conference, Pittsburgh Sept 2005

Everson, R.C. Neomagus. H.W.J.P. and Kaitano R. (2003). Modeling of the combustion of high-ash coal/char particles involving chemical kinetics and diffusion. Coal Indaba 2003. 9th Coal Science and Technology Conference. Saxonwold, Johannesburg. 28-30 July 2003

Everson. R.C. Neomagus. H.W.J.P. Njapha, D. and Kaitano, R. (2002). Coal-char combustion and gasification kinetics using thermogravimetric analyser measurements. American Institute of Chemical Engineers. Annual Meeting. Indianapolis, Indiana. Nov. 2002

Njapha, D. Kaitano, R. Everson, R.C. and Neomagus, H.W.J.P. (2000). Evaluation of Combustion Kinetics of High Ash-Coal using a Thermogravimetric Analyser (TGA) and Packed Balance Reactor. Coal Indaba 2000-6th Coal Science and Technology Conference, Fourways. Nov. 2000

CHAPTER 1 GENERAL INTRODUCTION

This introductory chapter is sub-divided into three sections consisting of (1) Background information concerning the study and a motivation for executing the investigation given in Section 1.1 (2) The objectives of the investigation described in Section 1.2 and finally (3) The scope and outlay of the thesis presented in Section 1.3. The background information provided describes the availability and utilisation of coal reserves with particular reference to poor quality discards and the problems associated with the processing of these discards. The need for research on fundamental aspects of coal/char gasification and combustion using inertinite-rich coals with high ash content for the development of new industrial processes is motivated.

1.1 Background and Motivation

There is a universal increase in energy demand due to the global economic growth and it is generally accepted that fossil fuels will continue to dominate the world energy supplies for a great part of this century. This will prevail until political and environmental issues concerning the generation of nuclear energy have been overcome and that any new nuclear processes addressing especially safety has been proven feasible, for example the Pebble Bed Modular Reactor (PBMR). Coal as a result of its abundance, will thus play an increasing energy role and needs to be addressed to meet the increasing demands for different forms of energy (electricity and liquid fuels). The current worldwide known coal reserves (519000 million tons) are sufficient to provide energy for at least another one hundred and thirty years at the current production levels (Department of Minerals and Energy, South Africa 2003).
The projection for global crude oil usage and supplies shows a gap between supply and demand as consumption increases with time. With very few new oil discoveries anticipated in the near future, present oil reserves are estimated to be depleted by the year 2050 (Newsletter 28 of Association for Study of Peak Oil and Gas). As a consequence of this and other studies findings, together with events such as international political developments, renewed interest over the last decade has been devoted to the optimal use of coal for energy generation, especially in the United States, United Kingdom, China, Australia, Canada and South Africa (Childless,

2005). However, there is increasing environmental concern associated with coal utilisation, which include the emission of sulphur- and nitrogen compounds, carbon dioxide and the disposal of particulates (ash). Programs linked to cleaner utilisation of coal have been receiving much more attention in research laboratories than ever before.

South Africa has coal reserves amounting to 55 000 million tons and produces 220 million tons annually of which 69 million tons (low ash coal) are exported. The local coal usage distribution consists essentially of 59% for electrical power, 26% for synthetic fuels, 12% for metallurgical and other industries and 3% for domestic usage (Department of Minerals and Energy, South Africa, 2003). Power generation which uses most of the coal mined will increase in the near future as a result of the capacity expansion of the power stations operated by the South African major electricity generating company, Eskom. In order to meet the energy targets set by the South African government, Eskom will have to use the large quantities of poor quality bituminous coal mined as well as discards estimated at 950 million tons available in South Africa.

Discards originate from the classification/separation of different grades of mined bituminous coal, some for export and others for local consumption. The lowest grade of material which has been discarded presents a challenge to all coal-based industries (power and liquid fuels) and new technologies need to be developed and implemented to use this material. The poor quality discards available normally have a high sulphur and ash content and, as is the case with most South African coal reserves, a high inertinite content which is considered as an inert maceral with a low combustion and gasification efficiency. The combustion of this feedstock in pulverised coal combustion boilers is problematic because of the poor ignition and burnout properties of inertinite, the high ash content (> 50% wt) and the production of pollutants such as sulphur- and nitrogen compounds that require expensive down-stream processing. Therefore, there is need for alternative clean coal processes.

Fluidised bed combustion (FBC) of coal at atmospheric and pressurised conditions has been shown to be a viable alternative to pulverised coal combustion (PCC) because: (1) most of the pollutants can be removed inside the fluidised bed with the addition of sorbents for the capture of sulphur compounds and reduction of the nitrogen oxides formed during combustion; (2) the handling and disposal of the

associated ash from the high ash coal feed stocks can also be achieved more effectively as a result of the fluidised state of the ash particles. Both bubbling fluidised bed (BFB) and circulating fluidised bed (CFB) boilers have been developed operating at temperatures between 750 and 950°C and pressures between atmospheric and 100 atmospheres. Millimetre size particles (1 to 5mm diameter) are used in the bubbling bed whereas fine particles are used in the circulating bed.

The bubbling bed has the advantage that its operation is much simpler and is more suitable for poor quality feed stocks, which could require long residence times. Integrated Gasification Combined Cycle (IGCC) power generation involving both gas and stream turbines with fluidised bed gasification has been examined extensively and has been commercialised internationally for coal feed stocks very different (more reactive) to typical South African coals. As a result of this, Eskom (South Africa) is currently assessing the performance of a Bubbling Fluidised Bed Test Facility (pilot plant) using typical South African coal feed stocks and coal discards. It is well recognised by many investigators involved in fluidised bed combustion and gasification research that it is essential to develop an understanding of the reactions and associated micro-scale transport rates which become important at low and intermediate temperatures, much lower than for pulverised coal combustion and other gasification processes (Liu, 1999). This need was identified by Eskom (South Africa) seven years ago and a Research Group was established in the School of Chemical and Minerals Engineering at the North-West University, Potchefstroom (South Africa) in order to provide reaction kinetics information for their fluidised bed combustion development programme mentioned above. The results presented in this thesis are a consequence of this arrangement which originated from a project that was part of an extensive programme confined to reaction studies of many coal samples and the associated environmental issues.

The conversion of coal, such as gasification and combustion, involves essentially three stages consisting of, (1) pyrolysis of the coal to produce char and volatile species, (2) homogeneous reaction of the volatile species and the reacting gases, and (3) heterogeneous reactions of the char with both the reacting and product gases.

The initial pyrolysis process which involves devolatilisation of the coal has a marked effect on the morphology, structure and reactivity of the char formed and depends on (1) the parent coal rank and maceral composition, (2) the initial structure of the parent

coal which include the surface area and porosity, (3) the plastic properties of the coal and (4) the pyrolysis conditions.

Pyrolysis normally occurs very fast in comparison with the subsequent char-gas reactions and studies have been undertaken by different investigators concerning char formation using vitrinite-rich coals with low ash content. There is a lack of detailed results in literature on chars formed from inertinite-rich coals with high ash contents. The morphological classification of chars proposed by Bailey *et al.* (1990) and others accounts for chars derived from inertinite-rich coals, but needs to be expanded to include different carbon forms as a function of pyrolysis temperature in order to infer reactivity more accurately.

The homogeneous reactions involving reactions of the many different species formed by devolatilisation and the reacting gases are very complex, and reaction kinetics results reported in literature include both empirically rate-based and equilibrium reactions. The effect of combustion of volatiles together with many operating parameters on the in-bed combustion efficiency in FBC based on sound reaction kinetics still needs to be quantified more rigidly.

During the stage involving char-gas reactions, both chemical reaction and transport (diffusional) processes play a role in the overall conversion, which is dependent on the char properties as well as the reaction conditions. Different reaction regimes involving the relative importance of chemical reaction and diffusional rates (overall rate controlling) have been identified as a function of temperature (and pressure) with the transition temperatures between these regimes dependent on the properties of the char (Walker *et al.*, 1959).

At low temperatures, the overall reaction is determined by the chemical reaction (regime I) being characterised by a low reaction rate constant in comparison with the pore diffusion coefficient, small particles and a very porous structure. Gasification of chars with especially carbon dioxide is normally a chemical reaction controlled process even up to temperatures of 900°C. Over a higher intermediate temperature range (regime II) the overall reaction rate is controlled by pore diffusion, characterised by a fast reaction, low pore diffusional rates, and large particles with a low porosity. Fast combustion reactions with dense char particles up to 900°C could be classified in this regime. At very high temperatures (regime III), the effect of temperature is small and the overall reaction rate is completely determined by film

diffusion, being dependent essentially on the gas flow. Combustion of particles at very high temperatures (>1200°C) can fall within this regime. The overall reaction rates near the transition temperatures can be controlled by both chemical reaction and pore diffusion or pore diffusion and film diffusion, respectively. However, during the total reaction period, at a constant temperature, structural changes also occur which affects the relative importance of chemical reaction and diffusional rates and consequently the rate controlling mechanism(s). These changes include pore growth and coalescence, as well as the depletion of carbon in the carbon-mineral structure (Bhatia and Perlmutter, 1981).

Models to predict surface area and porosity changes have been developed and incorporated in overall reaction rate models and tested mainly for porous carbon-rich char particles, originating from vitrinite rich coal samples (Bhatia and Perlmutter, 1981; Liu *et al.* 2000). The presence of large amounts of different minerals and inertinites can be expected to have a major effect on surface area and porosity, as a result of the phase heterogeneity and the presence of non-uniform distributions of pores consisting of mainly micropores. There are many results reported in the literature on the effect of minerals on reactivity (catalytic), but mostly in association with reactive macerals (vitrinites) and in many cases involving coal with low ash contents (Radovic *et al.* 1985, Beamish *et al.* 1998, Miura *et al.* 1989). Publications concerning the effect of ash and inertinites present in large quantities on overall reaction rate kinetics, especially under fluidised bed conditions are limited. Regarding modeling there are also limited publications confined to the validation of advanced models consisting of chemical reaction and pore diffusion with experimental results.

The need for a thorough understanding of the effect of the properties of inertinite-rich coals with high ash contents and their associated chars on gasification and combustion reactivity and the detailed modeling thereof was considered important and was accordingly chosen as the subject for this thesis. For this purpose, a typical South African coal sample suitable for fluidised bed gasification and combustion was examined.

1.2 Objectives of this investigation

The objective of the investigation was to determine the reactivity with respect to gasification with carbon dioxide-nitrogen mixtures and combustion with oxygen-

nitrogen mixtures, respectively of coal chars derived from a typical South African inertinite-rich, high ash coal discard. This was undertaken to assess the effect of the large amount of inert macerals (inertinites) and minerals present on the char's properties that determine the reactivity and to quantify the reaction rate mechanism and associated parameters. In order to achieve this objective the following was carried out:

(1) Determination of relevant chemical, structural and petrographic properties of a typical coal discard and the chars produced from it at different charring temperatures in order to establish and quantify the internal structure and changes that have occurred.

(2) Determination of the reactivity (performance) of the coal chars formed using a laboratory scale reactor (Thermogravimetric analyser) which consists of the following:

- Gasification with carbon dioxide and nitrogen mixtures (slow reaction) at conditions between 750 and 900°C, at atmospheric pressure and at 287.5kPa.
- Combustion with oxygen-nitrogen mixtures (very fast reaction) over a suitable low temperature range (above ignition temperature) and atmospheric pressure and at 287.5kPa pressure in order to demonstrate the effect of the coal char structure on the combustion reactivity.

(3) Determination of overall reaction rate models with associated parameters using selected experimental results as described above. Models for reaction controlled and reaction pore diffusion models needed to be developed and evaluated against experimental results. The objective being to identify the temperature regions for the existence of essentially regimes I (reaction controlled) and II (reaction pore diffusion) kinetics which depends on the char structure properties.

1.3 Scope of this thesis

The research pathway followed in this study is given in the outlay shown in Figure 1.1. The research is divided into three core areas, Coal/char characterisation, char gasification/combustion experimentation and reaction rate modeling

(1) An overview of the background and motivating factors for the investigation, followed by a detailed description of the objectives of the research programme, is given in Chapter 1.

(2) In Chapter 2 (Literature Survey), an overview of the most relevant publications in the open literature on the three core areas of study, coal/char characterisation, char gasification and combustion and reaction rate modeling is given. This survey includes references to results published in journals, conference proceedings, special reports, doctoral theses and on Internet websites and were considered important for this study.

(3) In Chapter 3, details of the mathematical models used together with methods for validation and determination of associated parameters are described. These models are based on the Random Pore Model, which is included in the fundamental equations describing the chemical-pore diffusion model. All the models account for the structural properties of the char gasified or combusted.

(4) The characterisation of parent coal and derived chars is given in Chapter 4 (Coal and Char Characterisation). The focus was to investigate the effect of charring temperature on coal char properties. Besides the Proximate and Ultimate analysis normally done, Petrographic analysis, BET and Computerised Controlled Scanning Electron Microscopy analysis were among the other analyses carried out to give a comprehensive set of analytical data.

(5) The experimental apparatus (TGA) used for the gasification and combustion experiments is described in Chapter 5. Details of the procedure followed and the experimental programme are also described.

(6) The results obtained from gasification and combustion experimental data are presented and discussed in Chapters 6 and 7, respectively. The effect of a number of variables such as temperature, pressure, partial pressure of reaction gases and particle size, is demonstrated. The culmination of these chapters is the evaluation of suitable reaction rate models for both gasification and combustion

(7) In Chapter 8, the general conclusions for this study are drawn with an account of results from this investigation, which can be considered as contributing to the knowledge base of coal science and technology. Finally, recommendations for future research, based on the results obtained, are given.

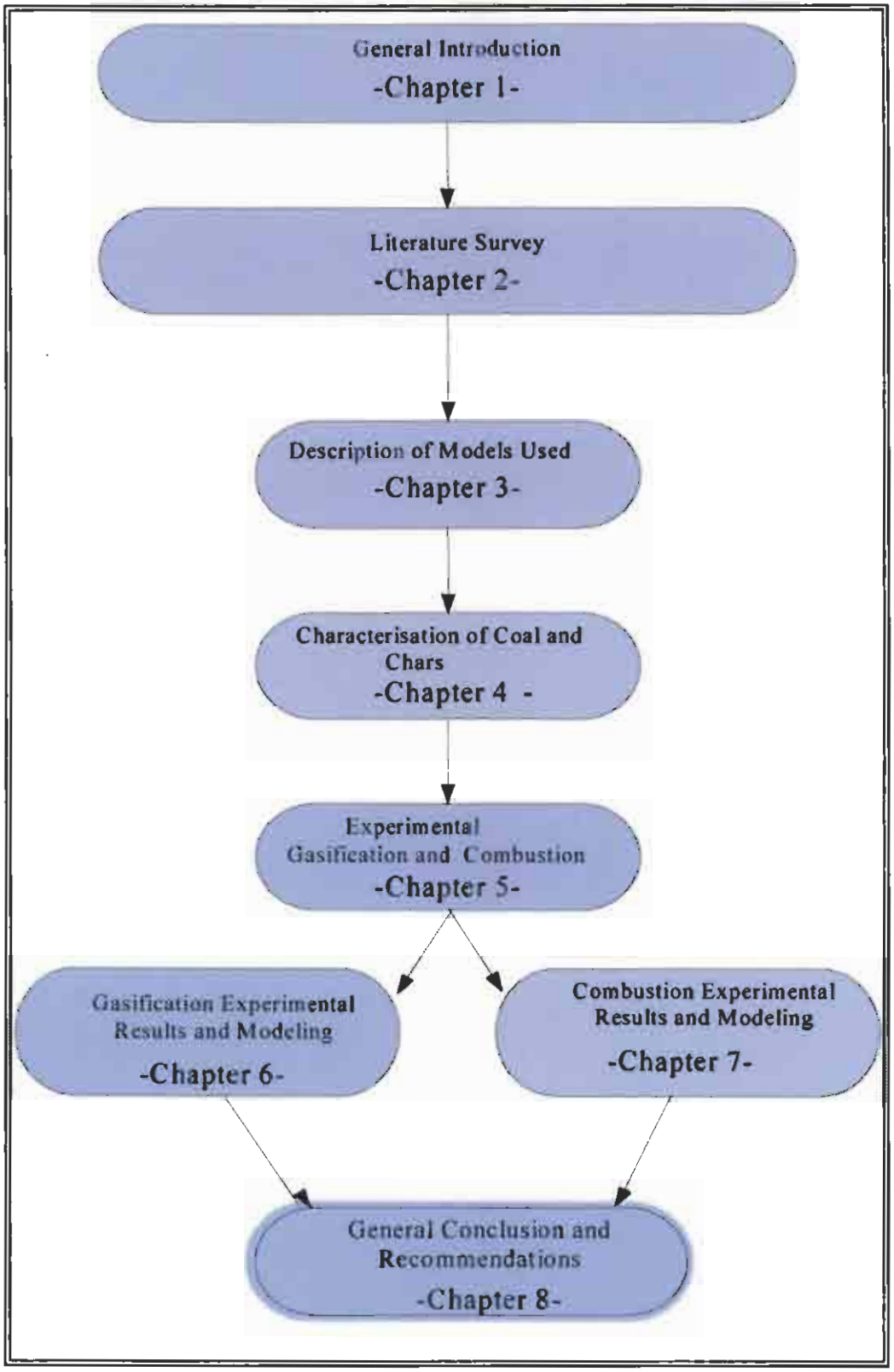

Figure1.1: Research path followed in this study

CHAPTER 2 LITERATURE REVIEW

2.1 Introduction

The objective of this chapter is to provide a literature review of research undertaken concerning the detailed characterisation of coal and chars, gasification and combustion reaction studies and the modeling of overall reaction rates based on advanced concepts (gas-char reactions). In Section 2.2.2, the chemical, petrographic and structural properties of coal are discussed while the morphology and structural properties of chars are discussed in Section 2.2.3. The operation variables affecting gasification and combustion as well as intrinsic kinetic equations are given in Sections 2.3.1 and 2.3.2. Finally, a survey of structural and overall models for coal/char conversion involving structural effects together with intrinsic reaction rates is given in Sections 2.3.3 and 2.3.4. The review presented in this chapter was considered to provide the necessary background for the execution of this investigation.

2.2 Coal and char properties

2.2.1 Introduction

The important properties of coal which need to be considered for application in combustion and gasification processes are very well documented in literature and consist of chemical analyses which include calorific values, minerals, structural and petrographic analyses. When examining the complete combustion or gasification of coal it is necessary to consider two distinct stages, namely (1) the fast process of coal devolatilisation (char formation), which depends on the coal properties, and (2) the slow gas-char combustion or gasification process involving the char formed. Consequently, the intermediate properties of the char need to be determined and examined especially with respect to structure, morphology and reflectance, which have an effect on the reactivity (Cloke and Lester, 1994).

2.2.2 Coal properties

The effects of the properties of coal that include, total carbon content, volatile matter, mineral composition and content, reflectance, macerals composition, plasticity,

surface chemical properties, surface area and pore structure on the properties and reactivity of the chars formed are summarised as follows:

2.2.2.1 Fixed carbon, volatile matter and minerals

Many publications have appeared covering the correlation of char activity with carbon content of the parent coal and it has been shown that the char reactivity decreases as the percentage carbon in the coal increases for both combustion and gasification (Cloke and Lester, 1994; Crelling *et al.*, 1988; Adschiri *et al.*, 1986; Oka *et al.*, 1987). Liu (1990) consolidated many results from different publications (Hashimoto *et al.*, 1986; Hippo and Walker, 1975) involving gasification and showed graphically, despite the presence of a large scatter of results, that there is a distinct decrease of the rate of carbon dioxide gasification with increasing percentage carbon in the coal. It is well known that the carbon content of coals correlate very well with its vitrinite reflectance properties (Berkowitz, 1985).

The volatile matter content (or fuel ratio) depends on the macerals present, which decreases from liptinite, vitrinite to inertinite and has a significant effect on the properties of the chars formed. The evolution of escaping volatiles under pyrolysis conditions affects char porosity (see Section 2.2.2.4) and hence overall reactivity and can cause fragmentation of the coal particles. A high volatile content ensures improved combustion efficiency in industrial boilers because of the rapid combustion of the volatiles.

Studies in connection with the effect of minerals (type and content) in coal or char combustion and gasification have been confined mostly to the catalytic aspects of the minerals present. Catalytically active minerals included in coal and char structures change the surface chemistry of the carbon and hence increases the number of active sites for reaction. The presence of particularly calcium, iron, potassium and sodium in minerals has been shown to catalyse gasification reactions (Huttinger and Natterman, 1994; Ye *et al.*, 1998; Walker *et al.*, 1983). Su and Perlmutter (1985) demonstrated that by doping coal samples with different inorganic materials intrinsic reaction rates can be increased by a factor of four. High rank chars show less influence of mineral matter on the char reactivity (Miura *et al.*, 1989) and it has been concluded that gasification reactivity of low rank coals with carbon content less than 80% is significantly affected by the presence of minerals. Catalytic effects are negligible at

high temperatures (Miura *et al.*, 1989). Menendez *et al.* (1994) showed that with high ash bituminous coals the char combustion rate increased with increasing mineral matter content and the effect is more pronounced at 500°C than at 1200°C. This result was attributed to a catalytic effect at the lower temperature and mass transfer at the higher temperature. Other relevant publications involving catalytic effects are those of Radovic *et al.*, (1985); Beamish *et al.*, (1998); Essenhigh, (1981); Cloke and Lester, (1994).

Other effects of high mineral content in coal on reactivity have been analysed by Smoot and Smith (1985) and Wigley *et al.* (1997): The difference in thermal expansion between included minerals and the organic components can cause fragmentation of particles because of internal stresses thus generating smaller particles. Publications consisting of in-depth studies of this effect are somewhat lacking in the literature. Mineral-rich particles have a larger specific heat capacity and will consequently absorb heat and slow down combustion as a result of a lower temperature in comparison with a carbon-rich particle. Included minerals in the carbon matrix may fuse and coat the surface of the particles thus reducing the surface area for reaction. A high mineral content will also increase the average density and lower the total porosity and surface area (Lu and Do, 1994) of the coal particles, which would affect fluidised bed operation and gas-solid reaction mechanisms.

It has been shown that a pulverised coal sample can consist of pure organic particles, pure mineral particles (excluded minerals) and particles consisting of mixtures of organic material and included minerals (mineral-organic association) with different compositions (Wrigley *et al.*, 1997; Liu *et al.*, 2005). This arises from preceding coal preparation, such as crushing, grinding and milling, during which liberation of minerals from the organic matrix occurs. It has been found that as particle size decreases, the mineral content (ash) of the particles increases, also different minerals occur in different size fractions (Liu *et al.*, 2005). The presence of mineral-carbon associations in a feedstock can contribute to the effects discussed in the above paragraph. Computer controlled scanning electron microscopy (CCSEM) (Wigley *et al.*, 1997; Van Alphen (2005a and 2005b) and QEMSCAN (Liu, *et al.*, 2005) has estimated these associations. A comparison between all methods for estimating mineral-organic associations is given by Vassilev *et al.* (2003).

2.2.2.2 Coal petrography

Petrographic properties that consist of reflectance (vitrinite- and total macerals reflectance) maceral and microlithotype compositions and their effect on char structure and morphology, are summarised as follows.

The reflectance is a measure of the state of coalification based on a scale from brown coal to anthracite, which increases in value with carbon content (Berkowitz, 1985). The maceral vitrinite (collotelenite or telovitrinite) can be selected as a reference material as its reflectance increases uniformly as the coalification process progresses. Vitrinite reflectance is a very reliable parameter, being independent of the vitrinite content and the grade of the coal but dependent on the carbon/hydrogen and carbon/oxygen ratios and the volatile matter, and is commonly used as a rank indicator (Cloke *et al.*, 1994). A total maceral reflectance scan can also be measured on coal samples with readings taken on all organic components, liptinite, vitrinites and inertinites (Benfell, 2001: O'Brien *et. al.*, 2003, Tang *et al.*, (2005a and 2005b) It has been suggested by Cloke and Lester, (1994); Tang *et al.* (2005a) that the vitrinite reflectance (rank) can be an accurate parameter for predicting combustion behaviour. Recently, O'Brien *et al.* (2003) and Tang *et al.* (2005a and 2005b) proposed a full maceral reflectance (FMR) parameter defined as the summation of each reflectance value multiplied by its frequency derived from the full reflectogramme, thus incorporating both rank and maceral compositions.

The reflectance and type of macerals present in the parent coal have an effect on char properties. Reflectance also has an effect on the combustion and gasification reactivity (Alonso *et al.*, 2001a; Bailey *et al.*, 1990; Cloke and Lester 1994; Crelling *et al.*, 1992; Hampartsoumain *et al.*, 1998; Hurt *et al.*, 1995; Jones *et al.*, 1985; Mendez *et al.*, 2003; Oka *et al.*, 1987; Rosenberg *et al.*, 1996).

It is well known that the porosity of most vitrinite-derived char decreases with increasing rank, and most inertinite-derived chars are less porous than the vitrinite derived char. This difference decreases with increase of reflectance and converges at high values (Jones *et al.*, 1985). The higher the temperature the more thick-walled are the char particles formed and networks are present in chars from lower rank coals which are related to coal aromaticity, and increase with coal rank (Cloke and Lester, 1994). Bend *et al.* (1992) also examined vitrinite-rich coal of increasing rank and

found that low rank coals generated multi-chambered and optical isotropic chars and that with increasing rank, hollow single-chambered optical anisotropic chars are formed. Some vitrinites are non-reactive, such as pseudo-vitrinite with a high reflectance (Bengtsson, 1987; Cloke and Lester, 1994).

The maceral inertinite has the highest carbon/hydrogen ratio and the lowest hydrogen content and volatile matter, and the highest degree of aromatic bonding in comparison to vitrinite and liptinite. Inertinite is capable of forming almost all of the types of chars from tenuispheres and networks to dense solids depending on the reflectance (rank) and plasticity (Cloke and Lester, 1994). Plasticity is related to aromaticity and low-rank inertinites, such as semi-fusinites swell during pyrolysis and is more reactive than other inertinites. It should be noted that many investigators considered high-ranking inertinites, which are non-reactive.

The maceral liptinite has the highest hydrogen and volatile content, the lowest aromaticity and the lowest reflectance and has been linked to flame stability and shorter combustion times and is only of significance during the pyrolysis period (Cloke and Lester, 1994).

The behaviour of microlithotypes (maceral associations) such as reactive vitrinite in association with inertinite is much different to that of the pure macerals and needs to be considered when assessing the chars (Bailey *et al.*, 1990; Cloke and Lester, 1994). Microlithotype particles consisting of vitrinite in association with other macerals are generally characterised by a high reflectance, high density and relatively low porosity in comparison with the pure vitrinite maceral. The pyrolysis temperature may influence the effect of the microlithotypes on the resultant char morphology. Char samples produced at temperatures above 1300°C from different lithotypes have similar morphology. While those produced at about 1423 K or lower are significantly different (Rosenberg *et al.*, 1996). Bailey *et al.*, (1990) correlated the formation of eleven different char types with coal microlithotypes and Bend (1991) related content of vitrinite-rich microlithotypes with porosity of chars formed under different conditions.

O'Brien *et al.* (2003) successfully correlated the full maceral reflectance parameter (FMR) with coal chemical properties (proximate and ultimate) while Tang *et al.*, (2005a) correlated this parameter with porosity for coals with pure macerals only. Tang *et al.* (2005b) estimated char reactivity kinetics from a coal reflectogramme and

thermogravimetric analyser experimental results and related the pre-exponential factor (Arrhenius equation) with FMR parameter with application to particularly chars derived from inertinite rich coals.

2.2.2.3 Surface properties

The influence of the carbon surface chemistry (atomic) on the coal- or char intrinsic reactivity is strongly related to the active sites present (Walker *et al.*, 1959). Laine *et al.* (1963) studied active surface area and its influence on the carbon-oxygen reaction using a highly graphitised carbon black and found that carbon crystallites on the edges were more reactive to oxygen than carbon crystallites on basal planes. The population and nature of the active sites and adsorbed molecules will affect the intrinsic kinetics, namely the activation energy, pre-exponential factor and dependence on reacting gases.

Thermal annealing effects during pyrolysis (and reaction), which lead to deactivation, has been analysed and reported in the literature, involving essentially, reordering of carbon with loss of carbon sites and changes in micro-pore structure (Lu *et al.*, 2000; Kuhl, *et al.*, 1992; Hurt and Gibbons, 1995; Davies, *et al.*, 1995; Senneca, *et al.*, 1998). Generally, the loss of reactivity due to the loss of sites increases with temperature and residence time with major changes occurring at very high temperatures (Salatino and Sennesa, 1998). Different macerals undergo different crystallite re-ordering, under similar conditions with vitrinite experiencing a larger degree of re-ordering the resultant being a lower reactivity. Chars from inertinite-rich coals have been shown to have a low overall reaction rate due to a high density (Davies, *et al.*, 1995; Hurt, *et al.*, 1995). Lu *et al.* (2000) examined the atomic structure, physical structure and chemistry of chars from coals as a function of pyrolysis temperature and coal properties. These authors found that for chars prepared at different temperatures, the crystallite size and aromaticity increased, the interlayer spacing decreased with increasing temperature and that the chars prepared at 1200°C have similar H/C and O/C ratios regardless of the coal properties. The chars become ordered and condensed with increasing temperature with the atomic structure (crystallite size and elemental composition) having an effect on the intrinsic combustion and gasification kinetics.

An annealing model incorporating the effect of decreasing number of carbon active sites on the surface, which affects the pre-exponential factor in the Arrhenius equation, has been developed by Hurt *et al.*(1998). These authors also included ash inhibition together with thermal annealing in a carbon burnout kinetic model (CBK) for predicting coal combustion performance.

2.2.2.4 Pore structure and surface area

Coal particles have a wide range of pore size distributions and the relative percentage of each pore type depends on the origin and coal rank (Gan *et al.* 1972). The pores in coal determine the rate of intra-particle mass transfer during pyrolysis, combustion and gasification. The accessibility of gas molecules to the micropore system can be attributed to diffusion through these pore systems (Walker and Mahajan 1993), which is an important factor determining the char structure, morphology and reactivity. The internal surface area of coals, which is attributed mainly to the presence of micropores, is generally lower than that of corresponding chars formed by pyrolysis as a result of the creation and opening of micropores, essentially as a result of the liberation of volatiles.

The measurement of these parameters characterising pore structure, can be achieved with mercury porosimetry, gas adsorption (BET analysis) (Gregg and Sing, 1982) and image analysis (Sorenson, *et al.*, 2000).

2.2.2.5 Plasticity of coal

The thermoplastic properties of the parent coal affect the pore size distribution, structure and morphology of the derived char (Soloman *et al.*, 1994; Normura, *et al.*, 2001; Kidena *et al.*, 2002; Van Krevelen, 1981). During devolatilisation, coal particles swell to different extents and as a result generate solid chars with different structures, which depend on the coal properties, such as, rank and petrographic composition, as well as pyrolysis conditions (Khan *et al.*, 1989). With respect to petrographic composition, the coal plasticity is determined by the presence of liptinite and vitrinite macerals (Van Krevelen, 1981). Inertinites exhibit no (or very little) plasticity at heating rates of 3°K/minute, while liptinites are very plastic and vitrinite

taking up the intermediate position (Van Krevelen, 1981). Both liptinite and vitrinite exhibit a maximum behaviour with respect to carbon content of the coal.

2.2.3 Char properties

2.2.3.1 Char morphology

Char morphological classification systems have been reported by a large number of investigators (Lightman and Street, 1968; Jones *et al.*, 1985; Oka *et al.*, 1987; Goodarzi and Vleekens, 1988; Bailey *et al.*, 1990; Menendez *et al.*, 1993, Roseberg *et al.* 1996; Cloke and Lester, 1994; Vleeskens *et. al.*, 1993). The classification proposed by Bailey *et al.,* (1990) that includes eleven different variables shown in Table 2.1, is referred to by many current researchers. Table 2.1 shows the parameters required for the classification as well as the microlithotypes involved. A summary and comparison of the different char classification systems have been published by Cloke and Lester (1994) and Benfell (2001) as shown in Table 2.2. This table compares six different systems grouped under similar char types labelled A to J which are illustrated diagrammatically in a number of publications (Cloke and Lester, 1994, Benfell, 2001, Bailley *et al.*, 1990). These systems are based on a combination of structural parameters such as particle size, porosity, wall thickness and anisotropy, which may be determined by image processing techniques. A simplified three-fold classification system (Groups I to II) based on the twelve-fold system of Bailey *et al.*, (1990) as indicated in Table 2.2 is also used (Liu, 1999: Benfell, 2001).

The overall porosity, wall thickness and surface carbon ordering determine the reactivity of the different char types that needs quantification. Many studies have, however, been reported involving the effect of structural properties, such as surface area and porosity (Section 2.3.3.2), which depend on the char morphology, for chemically controlled combustion and gasification char reactivity with surface reactions.

2.2.3.2 Pore structure and surface area

During pyrolysis of coal, pores evolve in a complex manner as described by Simon (1983), which consist of growth, coalescence, exposure, and generation of pores thus

generating a very complex structure consisting of a non-uniform distribution of micropores (<2nm), mesopores (2-50 nm) and macropores (> 50nm) (Liu *et al.*, 2000). Pores are randomly distributed in the carbon matrix with linkages and intersections occurring between each other with the micropores accounting for the largest portion of the internal surface area (Dutta *et al.*, 1977) while most of the porosity is in the macropores (Laurendeau, 1978). Pore structure and in particular pore distribution, play an important role in combustion and gasification of the char as it affects the char surface that may be reached by the reactant gases. This influences the overall reactivity where mass transfer of gases through the pores becomes limiting (regime II conditions). Pore structural models have been proposed to explain pore evolution during pyrolysis (Liu, 1999). It is generally understood that devolatilisation (char formation) is a process of organic removal from coal, which results in enlargement of existing micropores and generation of new micropores with the latter giving a higher internal surface area.

Table 2.1: Properties of char types (Bailey *et al.*, 1990)

Char type	**Shape**	**Porosity**	**Wall thickness**	**Char origin**
Tenuisphere	Spheroidal	> 80%	< 5 microns	vitrinite, clarite
Crassisphere	Spheroidal	60-90%	> 5 microns	vitinertite-V, duroclarite, clarodurite
Tenuinetwork	Spheroidal, elongated or irregular	60-95%	< 5 microns	vitrite, clarite
Meso-sphere	Spheroidal, elongated or irregular	40-60%	> 5 microns	vitrinertite-I
Inertoid	Sub-spherical, rectangular or irregular	5-40%	> 5 microns	durite, inertite
Solid	Rectangular or irregular	< 5%	solid	durite, inertite
Fusinoid	irregular	< 5%	solid	durite, inertite
Mixed porous	Spheroidal to irregular	> 50%	variable	vitrinertite-I, duroclarite, clarodurite
Mixed dense	Rectangular to irregular	< 50%	variable	durite, inertite
Fragment	Particle or group of particles < 10 microns	High	< 10 microns	vitrite, clarite
Mineroid	Spheroidal to rectangular	-	-	Minerals > 50%

The effect of temperature on surface area development during pyrolysis was examined by Lu (1991) involving coal discards and found that the surface area increases with temperature, then reaches a maximum and then decreases as the temperature increases for a residence time of 2.5 hours. This behaviour was also found by other investigators (Singla *et al.*, 1981; Gutierrez *et al.*, 1988) and can be attributed to the following two effects (Lu, 1991): (1) new pores are formed as volatile matter is liberated, creating greater accessibility to micropores with an increase of surface area. (2) at higher temperatures, a shrinking of the particle and narrowing of pore entrances occur, this results in a decrease of the accessible micropore surface area.

Measurement of surface area can be obtained by (1) gas adsorption (BET) using nitrogen or carbon dioxide, (2) mercury intrusion porosimetry and (3) image analysis. Kamahata and Walker (1962) combined porosimetry with adsorption methods to estimate porosity and surface area.

Table 2.2:Various char morphology classification systems (excluding mineroids)

Reference	Type A	Type B	Type C	Type D	Type E	Type F	Type G	Type H	Type I	Type J
Lightman and Street 1968	Thin-walled cenosphere	Thick-walled cenosphere	Lacy cenosphere	Solid	Solid	Solid	Solid	Solid	Solid	
Jones *et al.*, 1985a. 1985b	Cenosphere	Cenosphere	Honeycomb		Unfused	Unfused	Unfused	Solid		
Oka *et al.*, 1987	Thin-walled balloon	Thigh-walled balloon	Network		Unfused block	Unfused block	Skeleton			Micro disrupted
Goodarzi and Vleeskens, 1998	Thin-walled cenosphere	Thick-walled cenosphere	Cenophere with ribs			Non-reacted	Fusinoid			Fragment
Bailey *et al.*, 1990	Tenuisphere	Crassi-sphere	Tenuinetwork	Mesosphere	Inertinoid	Solid	Fusinoid	Mixed porous	Mixed dense	Fragment
Menedez *et al.*, 1993	Cenosphere	Cenosphere	Network	Network	Solid	Solid				
Vleeskens *et al.*, 1993	Plastic/ porous	Plastic/ porous	Plastic/ porous	Plastic/ porous	Inertinoid	Inertoid	Fusinoid			
Rosenberg *et al.*, 1996a, 1996b	Tenuisphere	Crassi-sphere	Tenui-network	Variable density type	Inertoid	Fusinoid/ solid	Fusinoid solid	Variable density type	Variable density type	
	GROUP I	GROUP II	GROUP I	GROUP II	GROUP III	GROUP III	GROUP III	GROUP II	GROUP II/III	N/A

2.2.3.3 Carbon form analysis

The relative proportions of the carbon-rich constituents/inorganic material can be established according to the method set out in the ISO Standard 7404-3, 1994. From these methods, a characterisation and quantification system was developed by Du Cann, (2005) and the description is given in Appendix B. This system comprises of six groups with different categories consisting of dense char, networks, coke, oxidised constituents, non-reacted coal, partially-reacted coal and inorganic matter, which originate from the macerals, microlithotypes and minerals present in the parent coal. The advantage of this system is that the different groups can be quantified for meaningful comparative studies. The system also accounts for reactive and non-reactive macerals in the parent coal as well as for the minerals present and gives estimates of relative proportions of dense and porous structures.

2.2.3.4 Pyrolysis conditions affecting char properties

The evolution of char structures and types (morphology) during coal pyrolysis or combustion depends on: (1) the parent coal rank and petrography (see Section 2.2.2.2.), (2) the initial structure of the parent coal (see Section 2.2.2.2), (3) the plastic properties of the coal (see Section 2.2.2.5), and (3) the pyrolysis conditions. This section gives a review of the effects of the pyrolysis conditions on the char properties, which include temperature, heating rate, pressure and nature of gases (Yu, 2002).

The effect of temperature on the char morphology has been reported in the literature (Bailey *et al.*, 1990; Cai *et al.*, 1998; Rosenberg *et al.*, 1996; Alonso *et al.*, 2001a; Alonso *et al.*, 2001b). As heat-treatment temperature increases, there is a decrease in the char micro-porosity (Cai *et al.* 1998), decreasing amounts of high density and thick-walled chars (Bailey *et al.*, 1990) and the formation of larger central pores and network voids (Griffin *et al.*, 1994). A reduction in accessible surface area was also observed by Lewellen (1975) with increasing temperature.

Alonso *et al.* (2001b) examined the petrography, reflectance and reactivity of chars derived from vitrinite- and inertinite-rich coals prepared at high temperatures (1000°C and 1300°C). The conclusion was that (1) the properties of the chars derived from the vitrinite-rich coal prepared at these temperatures do not differ much but are very much different to the chars derived from the inertinite-rich chars (2) the properties of

the chars derived from the inertinite-rich coal prepared at these temperatures were very much different, with the char prepared at the higher temperature having a much higher reflectance (5.42% as opposed to 4.09%) and containing larger amounts of isotropic fused fraction (porous and dense) material. As a result of this, the high temperature char has a lower reactivity and (3) the char derived from the inertinite-rich coal has a similar reactivity to that of the char derived from the vitrinite-rich coal under conditions favouring diffusion-controlled kinetics (regime II).

Heating rate effect studies by Cai *et al.* (1996) showed that chars produced at high heating rates contain more micro-pores and meso-pores and have larger internal surface areas. It was also reported by Gale *et al.* (1995) and Zygourakis (1993) that total porosity and swelling ratio increase with heating rate up to 1000 K/s, then levels off and finally decrease above 20000 K/s, which is attributed to a faster release rate of volatiles than relaxation time for expanding the char particle.

Increase in pressure results in the reduction of tar yield and an increase in gas yield. This is closely related to coal swelling and char morphology. High swelling ratios of solid chars at elevated pressures have been observed under a variety of heating conditions and consequently higher porosities may result (Benfell *et al.*, 1998; Khan and Jenkins, 1986). However, in combination with decreasing tar yield and increased gas yield a maximum swelling ratio can occur at an optimum pressure (Khan and Jenkins, 1989).

It was reported by Bailey *et al.* (1990) that chars obtained under combustion conditions are very similar to chars obtained under pyrolysis conditions although the proportions may vary. Rosenberg *et al.* (1996) reported that chars formed from vitrinite-rich microlithotypes under combustion conditions, consisted of tenuispheres and crassisphere char types. Inertinites fuse more readily under combustion conditions than under pyrolysis conditions producing tenuispheres (Bailey *et al.*, 1990).

2.3 Char-gas reaction rate kinetics

2.3.1 Reaction conditions affecting reaction rate

This section presents the important qualitative trends observed in combustion and gasification reactions with respect to temperature, pressure, and particle size and gas composition.

(1) *Temperature:* The effect of temperature on reaction rate kinetics is well documented in the literature (Walker *et al.*, 1959) consisting of the identification of reaction regimes (zones). These are controlled by either the intrinsic chemical reaction or pore diffusion or film diffusion. At low temperatures, chemical reaction determines the overall rate, while at higher temperatures the transport processes, pore and film diffusion is important. The relative ratio (Thiele modulus) of the reaction rate constants and diffusion coefficients that vary with reaction conditions (temperature, pressure and gas compositions) determines the controlling mechanism. At low temperatures the overall reaction, which is determined, by the chemical reaction (regime I) is characterised by a low reaction rate constant (slow reaction) in comparison with the diffusion coefficient rate, small particles and a very porous structure. At a higher intermediate temperature range (regime II), the overall reaction rate, which is controlled by pore diffusion, is characterised by a very fast reaction, low diffusion rates, and large particles with a low porosity. At high temperatures (regime III), the effect of temperature is small and the overall reaction rate is determined by film diffusion, being dependent essentially on the conditions surrounding the particle. A combination of controlling mechanisms can also determine the overall reaction rate, which would occur in a temperature range between regimes II and I.

(2) *Pressure:* Many publications have appeared concerning the effect of pressure on combustion reaction rates of coal in which both oxygen partial pressure and total pressure have been studied (Richard, *et al.*, 1994; Monson *et al.*, 1995; 1984, Lester *et al.*, 1981; Roberts *et al.*, 2000a and 2000b; Nikasa *et al.*, 2003). For a fixed total pressure the rate increased with partial pressure of oxygen, but for a constant partial pressure of oxygen an initial slight increase is observed as the total pressure is increased, which is followed by a decrease at the higher pressure, which then finally levels off to a constant value.

Richard *et al.* (1994) and Roberts *et al.* (2000a) who kept the partial pressure of oxygen constant while increasing the partial pressure of the diluents, confirm the latter result. All the other investigators found a similar result, but considered total pressure effects with variations in the partial pressure of oxygen. Monson *et al.* (1995) explained the latter phenomena by measuring

apparent reaction rate constants as a function of pressure and found that these values were dependant on pressure, which indicated that the intrinsic reaction rate is not applicable over a wide pressure range. Essenhigh (1991) explained this tendency in terms of an adsorption-desorption two-step reaction scheme with a rate equation consisting of three resistances and attributed the effect to a decreasing effectiveness factor accounting for internal diffusion. Lester *et al.* (1981) proposed that this effect is due to the decreasing pore area available for reaction with increasing total pressure. Niksa *et al.* (2003) presented a summary of the pressure effect involving large and small particles based on a number of relevant publications.

The effect of pressure on gasification reactions involving carbon dioxide and steam has been studied extensively especially with respect to the influence on surface chemical reactions (Blackwood and Ingeme, 1960; Nozaki *et al.*, 1992; Walker *et al.*, 1959; Muhlen *et al.*, 1985). Various Langmuir–Hinshelwood models have been analysed at low and high pressures to explain trends, but Roberts *et al.* (2000b) pointed out that the overall reaction is influenced by diffusion processes at the higher pressures and high temperatures as opposed to surface chemical reactions. At low temperatures, there is no dependence on total pressure and the partial pressure of reactant is only important for the determination of reactivity.

(3) *Particle size:* The effect of particle size on combustion and gasification can be a result of maceral disproportionation occurring during grinding and due to the physical structure of the particle (dimension and porosity). The cause of size segregation of macerals results from the differences in grindability between macerals with vitrinite being harder than inertinite. Thus, bigger particles will be rich in vitrinite and smaller particles rich in inertimite, which will have different pyrolysis and reaction properties despite being derived from the same parent coal sample (Jones *et al.*, 1985; Melendez, 2001). It is well-known that particle size (dimension) has an effect on the reaction controlling mechanisms and it has been found that the reaction rate (per unit surface area) becomes independent of the particle size when the overall reaction is chemical reaction controlled and inversely proportional to particle size when the reaction is film diffusion limited (Niksa *et al.*, 2003). This corresponds to the result of Wells

and Smoot (1985) who observed that reaction rate is independent of particle size at low temperatures for specific chars examined and that at high temperatures there is a dependence as a result of external diffusion effects (Liu, 1999). This property has an effect on the transition temperature between the different reaction regimes, which can be linked to the char porosity, and reactivity. Other investigators who also observed this behaviour include Kasaoka *et al.* (1985), Yang and Watkinson (1994), Weeda (1995), Knight and Sergeant (1982) and Kwon *et al.* (1988).

(4) *Gas composition:* Since large particles at high temperatures are expected to be limited by film diffusion, the overall reaction rate will increase with oxygen concentration since the diffusion of oxygen is dependent on the composition of the gases in the film. This effect is normally small and not easily detected. Product gases such as hydrogen and carbon monoxide in gasification with carbon dioxide and steam have an inhibiting effect on reaction rates and need to be accounted for (Blackwood and Ingeme, 1960; Muhlen *et al.*, 1985). This has been included successfully in the Langmuir-Hinshelwood reaction rate models by many investigators.

2.3.2 Intrinsic reaction rates

A review concerning the quantitative description of the intrinsic reaction rates is presented, which consists essentially of the power law and Langmuir-Hinshelwood rate equations.

2.3.2.1 Gasification

The gasification reaction (carbon dioxide and steam) has been expressed in an empirical form using the power law (nth order rate with respect to the gaseous reactant) for gasification reactions and is used by many investigators (Dutta *et al.* 1977; Knight and Sergeant, 1982; Liu, 1999). This is a simpler version of the Langmuir-Hinshelwood equations and is only valid for low partial pressures (Marsh and Kuo, 1989) and it has been found that the pressure order for carbon dioxide and steam is within the range 0.2 to 0.8 (Young and Smith, 1987).

Different forms of the Langmuir-Hinshelwood rate equations consisting of fundamental surface reaction mechanisms have been developed and successfully applied to results at different pressures (Blackwood and Ingeme, 1960, Walker and Mahajan, 1993, Muhlen *et al.*, 1985) with specific reaction rate equations for low and high pressures. Detailed derivations of the different models have also been extensively reported, which also include the inhibiting effects of carbon monoxide and hydrogen. A combination of oxidation and gasification mechanisms consisting of ten surface reactions has also been proposed for practical application in which oxygen reactions are accounted for (Niksa *et al.*, 2003). The major problem with the evaluation of the Langmuir-Hinshelwood equations for complex gas mixtures is the number of unknown parameters involved. A detailed summary of research done on carbon gasification with carbon dioxide is presented in a thesis by Liu (1999) involving some fifty publications in which pressures, temperatures, particle sizes, models, activation energies and equipment used are reported.

2.3.2.2 Combustion

The power-law reaction rate has been used preferably by many investigators for combustion reactions at all temperatures with varying values for the order. Hurt and Calo (2001) consolidated results from some eighteen noteworthy publications and showed that the reaction orders are (1) equivalent to 0.6 to 1 below 627°C (2) exceedingly low (nearly zero) above 927°C and, (3) close to 1 for above 1327°C. However, there is uncertainty of the values at the high temperatures, which could be affected by the presence of regime II and III kinetics, but despite that, there is a distinct transition as the temperature is increased. For temperatures below 727°C, Hurt and Hayes (2005) presented results from a fundamental study accounting for the occurrence of fractional power rate equations in terms of the surface or site heterogeneity based on a large activation energy distribution for adsorption and/or desorption.

Regarding the use of fundamental Langmuir-Hinshelwood equations for combustion kinetics, a number of different models based on a two-step mechanism have been proposed (Walker *et al.*, 1959; Lewis and Simons, 1979; Essenhigh and Mescher, 1997). However, these equations could not describe the temperature dependence

reported by Hurt and Calo (2001) and as result of this, these investigators proposed a three-step model (including a gaseous oxygen/surface complex reaction), which can predict high reaction orders at low temperatures.

2.3.3 Structural Models

2.3.3.1 Overview

The overall reaction rate for char-gas reactions depends on the intrinsic surface reaction r_s and the structure of the char particles (structure factor $f(X)$), which are determined by the coal properties, charring conditions, and operating conditions, which have been discussed in detail in this chapter. This equation can be thus written as follows (Lu and Do 1992)

$$\frac{dX}{dt} = r_s(T,C)f(X) \qquad (2.1)$$

In this section, the quantification of the structural property (structure factor) $f(X)$ is discussed for inclusion in a suitable overall reaction rate. Many structural factors have been developed and published of which only the most used are referred to and discussed where necessary. It should be noted the equations discussed in Sections 2.3.3.2 to 2.3.3.5 are applicable to chemical reaction controlled reactions.

2.3.3.2 Shrinking core model

The well-known model proposed by Yagi and Kunii, (1955) considers reaction(s) as occurring on the surface of a shrinking non-reacted core within the solid particle (grain). The shrinking surface can leave behind a layer of ash (if present in large amounts), which offers resistance to the transport of reactant and product gases. Under these conditions, it is assumed that there is negligible penetration and reaction in the core and that the reaction occurs within a very thin layer on the surface of the receding particle surface. Szekely and Evans (1970) assumed that a porous particle (negligible diffusion between individual grains) consists of an assembly of uniform non-porous grains and that the shrinking core behaviour is confined to these grains.

Most investigators, however, considered this behaviour applicable to the whole particle and have been found to be successful for predicting coal conversion kinetics (Weiss and Goodwin, 1963; Szekely and Evans 1970; Everson *et al.*, 2006 and 2006b). For a shrinking core model, with the surface reaction controlling, the structure factor is the following for spherical particles (Lu and Do, 1992):

$$f(X) = \frac{S_o(1-X)^{2/3}}{(1-\varepsilon_o)} \tag{2.2}$$

This model incorporates the initial structural properties of the char in terms of the initial porosity and external surface area, but fails to predict a maximum behaviour observed obtained for some combustion and gasification experiment (Kawahata and Walker, 1992; Hashimoto *et al.*, 1979). This model does not account for structural changes (surface area and porosity) occurring during reaction of the char.

2.3.3.3 Capillary and Random Pore Models

The models described include the structural changes that occur within the char particle during the reaction period. A model consisting of randomly intersecting cylindrical pores of uniform size was proposed by Petersen (1957) for calculating the surface area and porosity. Szekely *et al.* (1979) subsequently derived the conversion time equation from these equations, but the assumption of uniform pore sizes limits its applicability as chars normally have wide pore size distributions. A more rigorous model was derived independently by Bhatia and Perlmutter, (1980) and Gavalas (1980) based on the assumption that the volume enclosed by the moving pore and reaction surfaces is randomly distributed in the char. Bhatia and Perlmutter (1980) used a theory derived by Avrami (1940) for nucleation of crystals while Gavalas (1980) assumed a random distribution of the non-overlapped volume in accordance with a Poisson process.

These models incorporate both pore growth and coalescence during the reaction and can predict a surface area behaviour displaying a maximum and has been used for modeling char gasification and gasification. Results of the model of Bhatia and Perlmutter (1981) are given in chapter 3, which are characterised by a structural parameter ψ and a surface area equation which displays a maximum for structural

parameter values above a value of 2 with carbon conversions (X) less than 0.4. The structural parameter is calculated using the initial structural properties of the char which include the pore volume (porosity), - surface area and - length. The equivalent structure factor defined by Equation (2.1) is given as:

$$f(X) = \frac{S_o(1-X)\sqrt{1-\psi \ln(1-X)}}{(1-\varepsilon_0)} \qquad (2.3)$$

Modification/extension of the basic random pore model has been proposed in order to address certain particular properties of the chars used in gasification and combustion. These include the results of Liu et al. (2000), who considered non-uniform pore size distributions and Lu and Do (1992 and 1994), who expanded the theory to accommodate the presence of minerals (ash). The latter investigators considered the modeling of the gasification coal discards with high ash contents and developed models by considering the ash as an inactive inclusion in a carbon matrix, thus reducing the reactive surface. They used a modified random pore model with separate entities (carbon and ash) with different structural properties and a percolate including the fractional carbon content of the char particle. Ballal and Zygourakis (1987a and 1987b) also used an approximate equation relating ash surface area to ash content in a model for reactive surface area evolution during reaction.

Other noteworthy publications on modeling involving structural changes are those of Lindner and Simonson (1981), Sandman and Zygourakis (1986), Gupta and Bhatia, (2000) and Bhatia (1998).

2.3.3.4 Percolation Models

Structure models discussed above do not take into account connectivity properties that may be important under certain circumstances such as: (1) closed pore, which opens up during reaction; (2) disintegration of chars into small fractions at high conversions causing the loss of connectivity; (3) chars with low initial porosity with incomplete connectivity of the pore structure; (4) pore closure because of the closure of connecting pores. The occurrence of these features has been addressed by the percolation theory developed by Broadbent and Hamersley, (1957) and the

application of this theory to gasification processes has been reported (Mohanty *et al.*, 1982; Lu and Do, 1992 and 1994; Reyes and Jensen, 1986). The concepts of the percolation theory can also be integrated into reaction-diffusion models described below (Bhatia and Gupta 1992). Lu and Do (1992) used the Betha Lattice network for modeling gasification of a coal-reject-derived char and found the percolation model predicts the initial reaction rate changes better than a modified random pore model, which is attributed to the opening of initial closed pores.

2.3.3.5 Other models

Other equations (with different structure factors) used by a number of investigators are listed by Liliedahl *et al.* (1997) as shown in Table 2.3. Equation (2.4) is the traditional volume reaction model with m (fractional) corresponding to the order of reaction with respect to the carbon concentration. It should be noted that for m=1 this equation characterises the so-called volume or pseudo-homogeneous model that can be derived from first principles. For m=0 an independence of the carbon phase is implied and used by Ishida and Wen (1968), Ausman and Watson (1962) and Everson *et al.* (2005) for modeling carbon conversion based on reaction occurring homogeneously throughout a porous particle with dependence on gas concentration only. The equations proposed by Gardner *et al.*, (1979), and Johnson (1979) have an extra exponential term to allow for progressive deactivation or activation of the char surface. Equations (2.5) to (2.8) allow the conversion rate to exhibit a maximum with respect to conversion, which has been confirmed experimentally (Kawahata and Walker, 1992).

Table 2.3: Other reaction rate equations

Reference	Rate equation	
Szekely *et al.* (1976), Wen (1968) and Ishida and Wen (1968).	$k(1-X)^m$	(2.4)
Gardner *et al.* (1979)	$k\exp(-aX)(1-X)$	(2.5)
Johnson (1979)	$k\exp(-bX^2)(1-X)^{2/3}$	(2.6)
Chornet *et al.* (1979)	$kX^{1/2}(1-X)$	(2.7)
Simon (1980)	$k(X+\varepsilon_o(1-X))^{1/2}(1-X)$	(2.8)

2.3.4 Chemical Reaction-diffusion model

An excellent review by Bhatia and Gupta (1992) discusses models for internal (intra) diffusion and reaction with particular reference to details of pore structure. Bhatia and Perlmutter (1981) and Gavalas (1981) analysed reaction-diffusion models incorporating the random pore model equation with Bhatia and Perlmutter (1981) including diffusion through the product layer as well as particle size change due to reaction (product formation). These equations are described in detail in Chapter 3 with particular application to char combustion. Other investigators who have examined the solution of the reaction-diffusion models with some particle applications include (Weisz and Goodwin 1963; Everson *et al.* (2005), Ishida and Wen (1963); Blem *et al.* 1990).

2.3.5 Other semi-empirical overall reaction rates

Overall reaction rates for coal conversion reactions occurring in the presence of external and intra-particle diffusion based on simplifying assumptions consisting of effectiveness factors and other forms incorporating diffusion co-efficient, have been proposed and used. Effectiveness factors for gasification and combustion can be calculated using Langmuir-Hinshelwood rate equations and diffusion equations, which can be rather complex. An illustration is given by Liu and Niksa (2004) for an oxidation/gasification Langmuir-Hinshelwood type equation and in many cases a numerical evaluation can only be obtained (Niksa *et al.* 2003). Examples of overall

reaction rates based on kinetics and diffusion (effectiveness factor) for combustion reactions are given in the publication by Williams *et al.* (2000) who listed certain well-known reaction rates with a discussion of the limitations of each equation. These include the equations of Baum and Street (1971), Smith (1982), Hurt (1998), Sun and Hurt (2000), Essenhigh and Mescher (1996). The main limitation being that the dynamic behaviour of the coal structure is not accounted for.

2.4 Overview of reactivity of chars

In combustion and gasification processes involving chars, both chemical reaction and transport (diffusional) processes play a role in the overall conversions, which is dependent on the area and nature of the carbon surface (active sites) and the porosity of the char particles respectively, as well as the reaction conditions. The properties of the chars are dependent on the properties of the parent coal. The charring conditions are rather complex because of the nature of the coal and extensive research is still in progress to develop quantitative relationships between coal/char properties and overall reaction rate performance. The effect of reaction conditions has been extensively analysed by many investigators and results have been published, but there is still a lack of results concerning the effect of char properties on the existence of the different reaction regimes (zones) as defined by Walker *et al.* (1959).

During char combustion and gasification the char structure change significantly with carbon conversion in terms of internal surface area and porosity. Changes in surface area during combustion and gasification have been reported for many chars. It has been reported by most investigators that a maximum surface area occurs at carbon conversions of 20-50% (Kawahata and Walker, 1992; Liu *et al.*, 2000). Under chemically controlled conditions (regime I) the change in surface area can be explained by initial growth of pore with an increase in the surface area followed by pore interactions (coalescence) resulting in a decrease in surface area (Ballal and Zygourakis, 1987a; Ballal and Zygourakis, 1987b; Bhatia and Perlmutter, 1980 Gavalas, 1980). Models based on the initial char structure have been developed to account for surface area changes with conversion and have been successfully evaluated and incorporated in reaction rate models.

For combustion and gasification during regime II, the structural changes are more complex because of pore diffusion of reacting gases with accompanying gas concentration profiles inside the char particles. Results from studies involving intra-particle mass transfer have been reported by Mitchell (1988), Wheeler (1951) and Weeda (1995) and very low effectiveness factors have been reported (Mitchell 1988). Reaction-diffusion models have been developed by Gavalas (1981) and Bhatia and Perlmutter (1981). It is interesting to note that it was found that at high temperatures (regime II) the surface area decreases with increasing temperature (Hurt *et al.* 1991: Lin *et al.* 1994)) which was attributed to structural rearrangement occurring during carbon graphitisation at high temperatures. Pore size changes during char gasification have also been reported by Kawahata and Walker (1992) who showed that the behaviour with conversion was the same as for surface area and that it also decreases as temperature is increased.

The structural changes reported in literature have almost exclusively obtained from studies with carbon rich char particles (from low ash coal), which no doubt will be influenced by large amounts of minerals, if present, as a result of the phase heterogeneity introduced. Lu and Do (1992 and 1994) published results involving coal discards with high ash content and developed models by considering a modified random pore model with separate entities (carbon and ash) and a percolation model.

CHAPTER 3 DESCRIPTION OF MODELS USED

3.1 Introduction

The purpose of this chapter is to present details of the mathematical models used in this investigation and the procedures used for the validation of these models and associated parameters using experimental results. A literature survey of all the models developed and used by many investigators is given in Section 2.3 and it was decided to use the Random Pore Model (Bhatia and Perlmutter, 1980 and 1981; Gavalas, 1980a Gavalas, 1981) without and with pore diffusion. The motivation for this choice can be summarised as follows:

(1) The model accounts for intraparticle reaction and since coal char particles are porous as a result of devolatilisation and thermal cracking; it cannot be neglected as surface area for chemical reaction is available and has a major effect on the overall reaction. This overcomes the limitation of the unreacted shrinking core model

(2) The variation of surface area during reaction is accounted for in terms of the initial surface area and other structural properties of the char reacted. This feature establishes the effect of char physical properties on variation of active surface area with carbon conversion.

(3) The model and modifications have been successfully used by many investigators for coal chars gasification and combustion and other gas-solid reactions.

(4) The general model incorporating internal and product layer (pore) diffusion, and external film diffusion can be solved numerically. The model can be used to identify the different reaction regimes quite easily by considering limiting values for dimensionless groups characteristic of the different controlling mechanisms.

The generalised chemical reaction-pore diffusion model consists of a number of unknown parameters, which need to be determined for the evaluation of a suitable model. In the absence of film diffusion these parameters are (1) the structural parameter in the random pore model characterising the surface area variation rate (2) the intrinsic reaction rate parameters, and (3) the Thiele Modulus accounting for

effect of reaction rate and pore diffusion. Special procedures were developed for evaluation of these parameters, which are also described in this chapter.

3.2 Intrinsic reaction rates

The models described below incorporate surface-based intrinsic reaction rates in addition to other parameters mentioned above and the relevant parameters need to be estimated. (See also Section 2.3.2).

3.2.1 Gasification with carbon dioxide/nitrogen mixtures

Both nth order power rate equations with dependence on carbon dioxide concentration only and Langmuir-Hinshelwood type equations with dependence on carbon dioxide- and other products concentrations have been used by many investigators for describing the carbon dioxide-char gasification reaction rate. The power rate equation has been found to be applicable to low pressures gasification results and was accordingly used in this investigation, which consisted of experimentation at relatively low concentrations of carbon dioxide (total pressures of 87.5 and 287.5kPa with dilute carbon dioxide gas mixtures) (See also Section 2.3.2.2).

3.2.2 Combustion with oxygen/nitrogen mixtures

The nth order power rate law with dependence on oxygen concentration was used for the combustion of coal chars, which has also been derived from fundamental principles (Hurt and Hayes, 2005) and has been shown to be temperature dependent with high orders below 627 °C and lower orders above 927 °C (Hurt and Calo, 2001). In this investigation, a first order dependence was used (see also Section 2.3.2).

3.3 Random pore model

This model is described in detail in Section 2.3.3.3. The basic equation describes the reaction rate as a function of conversion inside a porous particle with a constant gas composition throughout the particle, that is without any pore diffusional effects (regime I) and which is characterised by a dimensionless structural parameter. This

parameter can be calculated using initial structural properties of the char under consideration, which include the surface area, porosity and pore length.

For cases where chemical reaction and pore diffusion effects are important (regimes I and II) this equation would be applicable at a particular point in the particle with a varying gas concentration profile along the radius and the Thiele Modulus would be used to characterise the diffusion effect.

3.3.1 Chemical reaction controlled regime (Regime I)

For the evaluation of an overall reaction rate model for regime I kinetics, the intrinsic kinetics, the structural changes which include the surface area dependant on the char properties and the reaction conditions need to be considered. The following equations and derivatives were used for the analysis of the results reported in chapter 6 and 7.

3.3.1.1 Model equations

The overall reaction rate is: (Bhatia and Perlmutter, 1980)

$$\frac{dX}{dt} = \frac{r_s(1-X)S_o\sqrt{1-\psi\ln(1-X)}}{(1-\varepsilon_O)} \qquad (3.1)$$

ψ being the structural parameter characteristic of the initial char structure and defined as:

$$\psi = \frac{4\pi L_0(1-\varepsilon_o)}{S_o^2} \qquad (3.2)$$

Equation (3.1) can be written in terms of the dimensionless parameter as follows:

$$\frac{dX}{d\tau} = (1-X)\sqrt{1-\psi\ln(1-X)} \qquad (3.3)$$

Relationships for carbon conversion X in terms of time t or dimensionless time τ (implicit and explicit) obtained by integration of the above equations are as follows:

In terms of time t:

$$t = \frac{2(1-\varepsilon_o)}{r_s S_o \psi}(\sqrt{1-\psi \ln(1-X)} - 1) \tag{3.4}$$

In terms of dimensionless time τ

$$\tau = \frac{2}{\psi}(\sqrt{1-\psi \ln(1-X)} - 1) \tag{3.5}$$

and explicitly as

$$X = 1 - \exp[-\tau(1 + \frac{\psi\tau}{4})] \tag{3.6}$$

Defining the time factor as:

$$t_f = \frac{r_s S_O}{(1-\varepsilon_O)} \tag{3.7}$$

Equation (3.6) in terms of time t becomes

$$X = 1 - \exp[-t_f t(1 + \frac{\psi t_f t}{4})] \tag{3.8}$$

A reduced time t/t_X with t_X the time for a fractional conversion of X, being the upper limit for reliable experimental results, can be defined, which is independent of the parameters appearing before the square root term (Equation (3.4)) and only dependant on ψ as shown in equation (3.9) where $t_{0.9}$ is the time for 90% conversion. Thus, all results for a particular coal-char gasified or combusted should be the same, which enables this property to be used for determination of the structural parameter.

$$\frac{t}{t_{0.9}} = \frac{\sqrt{1-\psi \ln(1-X)} - 1}{\sqrt{1-\psi \ln(1-0.9)} - 1} \tag{3.9}$$

It should be noted that $\frac{t}{t_{0.9}} = \frac{\tau}{\tau_{0.9}}$

Intrinsic reaction rate equation r_s given by Equation (3.10) for both gasification and combustion based on an nth order power rate relationship as discussed in Section 3.2 was used. In this investigation the dependence for gasification and combustion were based on the partial pressure of carbon dioxide and oxygen concentration respectively. The equations are:

Gasification: $r_s = k_{SO} \exp(-E/RT) p^n$

Combustion: $r_s = k_{SO} \exp(-E/RT) C^n$ (3.10)

3.3.1.2 Validation procedure

The evaluation of the chemical reaction controlled model requires estimates of the structural parameter ψ and the time factor t_f Equations (3.2) and (3.7). The structural parameter can be determined from BET results and image analysis (Bhatia and Perlmutter, 1980; Liu *et al.*, 2000a) and from experimental reaction rate results (Liu *et al.*, 2000b). However, it has been found that with non-uniform pore size distribution, the use of surface areas and pore volume estimates from BET measurements and image analysis was not accurate enough because of the approximations required to describe the non-uniformity of the pore sizes as well as the accuracy of the pore size estimates within the micro-pore range. Some investigators (Lu and Do, 1992; Liu *et al.*, 2000a) estimated this parameter from the maximum of experimental reaction rate curves obtained from conversion results. These estimates, however, depend upon the accuracy of the numerical differentiation of the experimental results, which could be subject to errors as a result of the discrete intervals chosen.

In this investigation, this problem was overcome by fitting Equation (3.9) by regression with the unknown structural parameter to corresponding experimental results. By using an upper limit of 90% for the conversion, the uncertainty of the experimental conversion results, which are normally asymptotic near the end of the reaction, is eliminated. With a regressed value for the structural parameter, a second

regression calculation was carried out involving Equation (3.8) with real time conversion results with t_f as the unknown parameter. With t_f values determined from experimental results, at different gas concentrations or partial pressures and temperatures the intrinsic reaction rate parameters were determined using the logarithmic form of Equations (3.7) and (3.10) which are the following:

Gasification: $\ln t_f = -E/RT + n\ln p + \ln(k'_{so})$

Combustion: $\ln t_f = -E/RT + n\ln C + \ln(k'_{so})$ (3.11)

With $k'_{so} = k_{so} S_o /(1-\varepsilon_o)$ (3.12)

For the determination of the reaction order parameter n, isothermal results were used with a linear regression procedure involving a plot of $\ln(t_f)$ versus ln(p) or ln(C). For the activation energy, E and lumped pre-exponential factor k'_{so} a plot of $\ln(t_f)$ versus $1/T$ for constant gas concentrations or partial pressures was used, also with a linear regression procedure.

3.3.2 Chemical reaction – Pore diffusion controlled regime (Regimes I and II)

The evaluation of an overall reaction rate model for regimes I and II kinetics the intrinsic kinetics and structural changes, which include surface area and porosity changes, which are all dependant on the char properties and reaction conditions need to be incorporated in the model. Surface area variation can be accounted for using the random pore model equations and the porosity variations can be calculated from a carbon material balance. Pore diffusion, which is dependant on porosity is very complex as a result of the presence of a non-uniform distribution of pore sizes and can consist of a combination of Knudson and molecular diffusion because of the presence of micro-, meso- and macro-pores that changes with conversion of carbon.

3.3.2.1 Model equations

The overall model incorporating the features mentioned above consists of the following equations.

The equations (dimensionless) for consumption of reacting gas inside the particle are the following, (Bhatia and Perlmutter, 1981):

$$\frac{1}{\xi^2}\frac{\partial}{\partial \xi}\left(D_e^{*}\xi^2\frac{\partial C^{*}}{\partial \xi}\right)=\phi^2\frac{dX}{d\tau} \tag{3.13}$$

$$\frac{dX}{d\tau}=C^{*}(1-X)\sqrt{1-\psi\ln(1-X)} \tag{3.14}$$

$$\frac{dX}{d\tau}=(1+\frac{\psi C^{*}\tau}{2})\exp\{-\tau(1+\frac{\psi C^{*}\tau}{4}\} \tag{3.15}$$

Boundary and initial conditions being:

$$C^{*}=C_O^{*} \text{ at } \xi=1\text{; (assuming negligible gas film diffusional resistance)} \tag{3.16}$$

$$\frac{\partial C^{*}}{\partial \xi}=0 \text{ at } \xi=0;\ C^{*}=0 \text{ at}\tau=0\text{, for } 0\le\xi\le1 \tag{3.17}$$

The following important characterising parameters appear in these equations.

$$\phi = \text{Thiele modulus, } \phi = R_o\sqrt{k_s\rho S_o/MD_e} \tag{3.18}$$

$$\psi = \text{structural parameter, } \frac{4\pi L_O(1-\varepsilon_O)}{S_O^2} \tag{3.19}$$

$$\tau = \text{dimensionless time} = t_f t = \frac{r_s S_O t}{(1-\varepsilon_O)} \tag{3.20}$$

$$t_f = \text{time factor, } \frac{r_s S_O}{(1-\varepsilon_O)} \tag{3.21}$$

$$r_s = k_s C \qquad \text{(1st order combustion reaction)} \tag{3.22}$$

$$k_s = k_{so} \exp(-E / RT) \tag{3.23}$$

The dependence of the normalised effective diffusion co-efficient $D_e^* = D_e / D_{eo}$ appearing in Equation (3.13) during the combustion process needs to be quantified in terms of conversion X in order to yield an appropriate model.

In general, the effective diffusivity will vary with the structural parameters of the solid (coal char) according to (Bhatia and Perlmutter, 1981):

$$D_e = D\frac{\varepsilon}{\gamma(\varepsilon)} \tag{3.24}$$

Where the tortuosity γ is usually in the range 2 to 5 (Satterfield, 1970) which does not vary during the reaction process, with typical values for ε / τ being of the order of 0.15 (Gomez-Barea *et al.*, 2005). To account for variation during the reaction it has been proposed (Wakao and Smit, 1962) that it varies inversely with respect to the porosity, thus:

$$\gamma(\varepsilon) = \frac{1}{\varepsilon} \tag{3.25}$$

From these equations the following can be derived

$$\frac{D_e}{D_{eo}} = (\frac{\varepsilon}{\varepsilon_o})^2 \tag{3.26}$$

which can be written in general as (Wen, 1968)

$$\frac{D_e}{D_{eo}} = (\frac{\varepsilon}{\varepsilon_o})^\beta \tag{3.27}$$

In this investigation, the quadratic relationship given by Equation (3.26) was used. The determination of the normalised porosity ε^* needs to account for the ash present and the following equation can be derived by means of a material balance based on

the assumption that the bulk density of the ash remains constant and that the particle does not fracture so that the particle size remains constant (Brem and Brouwers, 1990).

$$\varepsilon^{*} = \{1-(1-\varepsilon_o)[1-(1-x_{ash})X]\}/\varepsilon_o \tag{3.28}$$

It should be noted that this would be applicable at different radii in the particle and that the initial porosity needs to be accurately determined.

Once the concentration profile inside the particle is known the local carbon conversion (X) at any point inside the particle can be calculated and consequently the overall carbon conversion at a certain time (dimensionless) instant, thus:

$$X = 1-\exp[-\tau C^{*}(1+\frac{\psi\tau C^{*}}{4})] \tag{3.29}$$

$$\bar{X} = 3\int_0^1 X\xi^2 d\xi \tag{3.30}$$

In terms of real time t, Equation (3.29) becomes

$$X = 1-\exp[-t_f t C^{*}(1+\frac{\psi t_f t C^{*}}{4})] \tag{3.31}$$

The following can be deduced from the model.

(1) For $\phi = 0$, that is for chemically controlled conversion, the gas concentration gradient of the reacting gas along the radius is constant (C = constant) and the carbon is consumed uniformly throughout the particle.

(2) For large values of ϕ, diffusional effects are important and can be such that the reaction is completely controlled by diffusion. For cases where there is diffusion, a gas concentration profile exists in the particle and carbon is depleted from the surface of the particle towards the centre.

(3) For chemical reaction controlled conversion the variation of surface area inside the particle is important whereas for pore diffusion controlled conversion the variation of porosity of the particle is important

(4) For chemical reaction and pore diffusion-controlled conversion, the variation of the porosity can be such that during combustion period the process becomes reaction controlled.

(5) For chemical reaction pore diffusion controlled conversion the overall carbon conversion can be determined from the intrinsic reaction kinetics based on a variable gas concentration profile in the particle, whereas for diffusion controlled conversion only the surface molar flux needs to be calculated from the derivative of the surface gas concentration profile, Equation (3.17).

3.3.2.2 Validation procedure

The set of equations describing the chemical reaction pore diffusion model given above were solved numerically using a MATLAB® programme for solving partial differential equations (PDEPE).

The evaluation of the chemical reaction-diffusion model with experimental results is complicated by the many unknown parameters, Equations (3.13) and (3.14) associated with the model and the uncertainty of the experimental conversion results at conversions levels near to completion, which are normally asymptotic. To overcome these problems the following procedure was developed.

The experimental results and model predictions (conversion) were plotted against a normalised time parameter $t/t_{0.9}$ where $t_{0.9}$ is the time required for 90% conversion, (see also Section 3.3.1.2). This avoids confusion regarding the determination of the time for complete conversion t_∞ and conveniently eliminates the effect of the chemical reaction rate. With this transformation, the result depends only on the structural parameter for chemically controlled conversions and on the Thiele modulus ϕ and the structural parameter for chemical reaction pore diffusion controlled conversions. Thus, these two parameters can be determined independently by considering a chemically controlled set of results for the determination of ψ and another set of chemical-diffusion controlled results for the determination of ϕ, using the same char in both cases.

The determination of these parameters (single parameter) can be achieved by manual curve fitting. The reaction rate parameters were evaluated from a plot of conversion of carbon versus real time using another regression procedure with subsequent linear plots for the evaluation of reaction rate constants, (see Section 3.3.2.2).

CHAPTER 4 COAL AND CHAR CHARACTERISATION

4.1 Introduction

This chapter describes the aspects concerned with the characterisation of the parent coal and the chars prepared for the reactivity and reaction rate modeling. The different sections address (1) The origin of the coal sample and the preparation of the chars, Sections 4.2 and 4.3.1 (2) The equipment used for the characterisation, Section 4.3.2, and (3) The results and discussion involving chemical, petrographic, image (CCSEM) and structural analyses of the parent coal and chars, Section 4.4.

4.2 Origin of Coal sample

A coal discard sample from a coal deposit from the South African Witbank coalfield (geologically part of the Karoo Basin, a coal rich area stretching between the Mpumalanga and KwaZulu Natal provinces of South Africa) was examined. Coal from this region is mainly utilised as a power station feedstock, for the production of synthetic petroleum products and some of it is exported to Europe and Asia mainly for industrial utilisation. The coal discard studied originated from a coal processing plant and has a high ash and high ash and inertinite content, which limits its application in most conventional combustion and gasification processes.

4.3 Experimental

4.3.1 Char preparation

The coal was received in mixed sizes from fine powder to large particles of up to 5cm in diameter. This sample was sieved to provide the required fraction sizes of 3.0(±0.3) mm and 1.0(±0.2) mm and these fractions were then charred separately using a Packed Bed Balance Reactor (PBBR), (see apparatus in Appendix A).

4.3.1.1 Charring apparatus

The reactor used for the charring consisted of a vertical tubular furnace mounted on an accurate microbalance by means of an aluminium tripod. A schematic drawing of the furnace and accessories is shown in Appendix A. Nitrogen gas from gas bottles

was admitted to the reactor at measured flow rates and the temperature of the reactor accurately controlled with a controlled unit. The temperature of the furnace could also be controlled to operate non-isothermally (ramp). The loss of mass due to devolatilisation was recorded by means of an on-line data acquisition system and the attainment of a constant mass indicated completion of the charring process. The reactor was capable of treating batches of 5 grams and was used for charring only. The charring in a separate reactor prior to the Themogravimetric determination was done in order to avoid condensation of volatiles in the very delicate TGA. Thus, the TGA experiments explained in Chapter 5 were confined to the accurate assessment of char combustion and gasification rates only.

4.3.1.2 Charring procedure

The method used for char preparation consisted of the following:

(1) The coal sample was sieved into the required fraction sizes and introduced into the oven.

(2) The sample temperature was equilibrated at ambient temperature and pressure in a nitrogen atmosphere.

(3) The sample was heated at a constant heating rate of $20^{\circ}Cmin^{-1}$ to either 700 or $900^{\circ}C$.

(4) The sample was held isothermally at the target temperature for 60 minutes.

(5) The resultant char sample was then cooled down to ambient temperature under nitrogen flow.

A final constant weight ensured that all the volatiles were driven off. The resultant char was finally cooled to room temperature under a constant nitrogen flow and stored under an atmosphere of nitrogen in airtight sample bottles and placed in a desiccator from which samples were taken for experimentation. The chars prepared at 700 and $900^{\circ}C$ are labelled Char700 and Char900

4.3.2 Experimental Equipment used for Characterisation

4.3.2.1 Chemical analysis

The chemical analysis was carried out by the Secunda Coal Laboratory of South African Bureau of Standards Laboratories (SABS) according to the methods outlined in Table 4.1 (Section 4.4.1). This consisted of proximate, ultimate and sulphur analyses as well as calorific value determinations of the coal and the chars.

4.3.2.2 Petrographic analysis

The petrographic analysis was carried out by Coal and Mineral Technologies (Pty) Ltd, a subsidiary of South African Bureau of Standards Laboratories, (SABS) (du Cann, 2005a and 2005b). The analysis undertaken by the microscopic examination of coals and chars, in conjunction with other analytical data provided information regarding organic composition, coal maturity (as indicated by the reflectance properties), associations of organic matter and minerals and the physical properties of the chars.

A petrographic block of coal was prepared in accordance with the ISO Standard 7404-2- (1985) and examined under a microscope. Reflectance measurements, which determine parent coal maturity and indicate subsequent reflectance changes with charring and analysis determine organic composition, were undertaken. Vitrinite random reflectance measurements to establish the coal rank were carried out in accordance with ISO Standard 7404-5 (1994), 100 readings were taken on the vitrinites in the coal sample. This method was also used to measure the reflectance properties of materials formed from vitrinites in the char samples. A total maceral reflectance scan, in which 250 reflectance readings were taken on all macerals over the polished surface of the petrographic block, was also undertaken on the coal and both chars.

For the coal sample, the group macerals were quantified by a 500-point count technique, in accordance with the ISO 7404-3 (1994) method. The reactive macerals were identified according to the method of Smith *et al.*, (1983) for South African coals. Microlithotype, carbominerite and minerite analyses, which determine the

coal's organic/inorganic associations, were carried out in accordance with ISO Standard 7404-4 (1988).

The microscopic constituents of the two chars were assessed by virtue of their colour, reflectance, degree of anisotropy, size, char morphology, extent of devolatilisation, and general response to heating. A quantitative analysis of the components present in the chars was carried out using the method set out in the ISO standard 7404-3 (1994). From this method, the relative proportions of the carbon-rich constituents/inorganic materials were established on a 500-point count basis.

A condition analysis was performed on the coal and char samples in which the same 500-point count technique was used to establish the extent of visible changes in the organic constituents due to charring.

4.3.2.3 Computer Controlled Scanning Electron Microscope Analysis

This analysis (CCSEM) was done by Van Alphen Consultancy (Van Alphen, 2005b). Samples of the char were mixed with iodinated epoxy resin and allowed to cure. The cured 30mm mount was polished exposing individual particles in cross-section. The studies of the particles provide information on mineral distribution in char particles. Information on the degree of association of minerals with the organic components present in the coal/char was also obtained, which is relevant for the understanding of the influence of mineral and carbon distribution within a particle on the combustion behaviour of the char sample.

The CCSEM analytical procedure was as follows:

(1) A cured and polished sample was divided into regularly spaced analytical fields of view or frames and was mounted onto the microscope. An appropriate magnification (based on particle sizes) was then selected.

(2) The sample was positioned at the first field of view and acquired a backscattered electron image (BSI). BSI is an atomic weight contrast image and ensures that coal and minerals can be identified by image processing routines.

(3) The image was processed by establishing a regular grid of analytical points for each field of view. The electron beam was positioned at each analytical point

and a 100 milli-second X-ray spectrum was acquired. Relative elemental composition of the phase was derived from the X-ray spectrum.

(4) The process was repeated by positioning the sample at the next field of view until all the fields of view were analysed.

4.3.2.4 Structural analysis

The BET adsorption method was used to determine the structural properties of the coal and chars, which was accomplished with a Micromeritics ASAP 2010 Analyser with nitrogen (BP = -196 °C) as the adsorbent. This instrument is capable of determining pore sizes in the range of 4 to 5000 Å (Gregg *et al.*, 1982; Stanley-Wood and Lines, 1992). Zhu (2007), however considers a lower limit of 10Å for accurate results with nitrogen.

4.4 Results and Discussion

4.4.1 Chemical analyses

Proximate and ultimate analyses together with calorific value determinations and total sulphur were determined involving the original coal sample (AR) and the chars (Char700 and Char900). The results are shown in Table 4.1. The parent coal is characterised as a high ash coal (ISO 1171-2005) with an ash content of 34.7% (dry basis) and graded in terms of the calorific value (CKS 561-1982) as a D-111 grade coal with a gross CV less than 21.5 MJ/kg, specifically 19.01 MJ/kg. The total sulphur content is 1.71% (dry basis), which together with the other properties would make this parent coal undesirable for combustion in conventional pulverised boilers because of the generation of especially sulphur dioxide and solids handling problems. The effect of charring temperature is also shown in Figure 4.1 and it can be seen that there is a significant reduction of the volatiles at 900°C to 7.4% as compared to 17.9% at 700°C from a parent coal with a value of 22% (dry basis).

Table 4.1: Chemical analysis of coal sample and chars

			Coal AR		Char700		Char900	
			Air Dry	Dry Basis	Air Dry	Dry Basis	Air Dry	Dry Basis
Proximate Analysis		Standard						
Inherent Moisture	%	ISO 11722	2.6	-	0.9		2.8	
Ash	%	ISO 1171	33.8	34.7	35.5	35.8	40.9	42.1
Volatiles	%	ISO 562	21.4	22.0	17.7	17.9	7.2	7.4
Fixed Carbon	%	By difference	42.2	43.3	45.9	46.3	49.1	50.5
Total Sulphur	%	ASTM D 4239	1.67	1.71	1.25	1.26	1.40	1.44
Calorific Value	MJ/kg	ISO 1928	19.01	19.52	19.34	19.52	19.15	19.70
Grade (on Cv ad basis)		CKS 561 1982	D-111					
Ultimate Analysis								
Carbon	%	ASTM 5373	50.89	52.25	51.06	51.52	52.19	53.68
Hydrogen	%	ASTM 5373	2.68	2.75	2.44	2.46	1.19	1.22
Nitrogen	%	ASTM 5373	1.23	1.26	1.18	1.19	1.17	1.20
Total Sulphur	%	ASTM D 42399	1.67	1.71	1.25	1.26	1.40	1.44
Oxygen	%	By difference	7.13	7.33	7.67	7.77	0.35	0.36

These changes resulting from the conversion of original macerals have a marked effect on the overall reactivity of the chars in terms of porosity (diffusional effects) and surface activity as a result of carbon ordering (See Section 2.2.2.2).

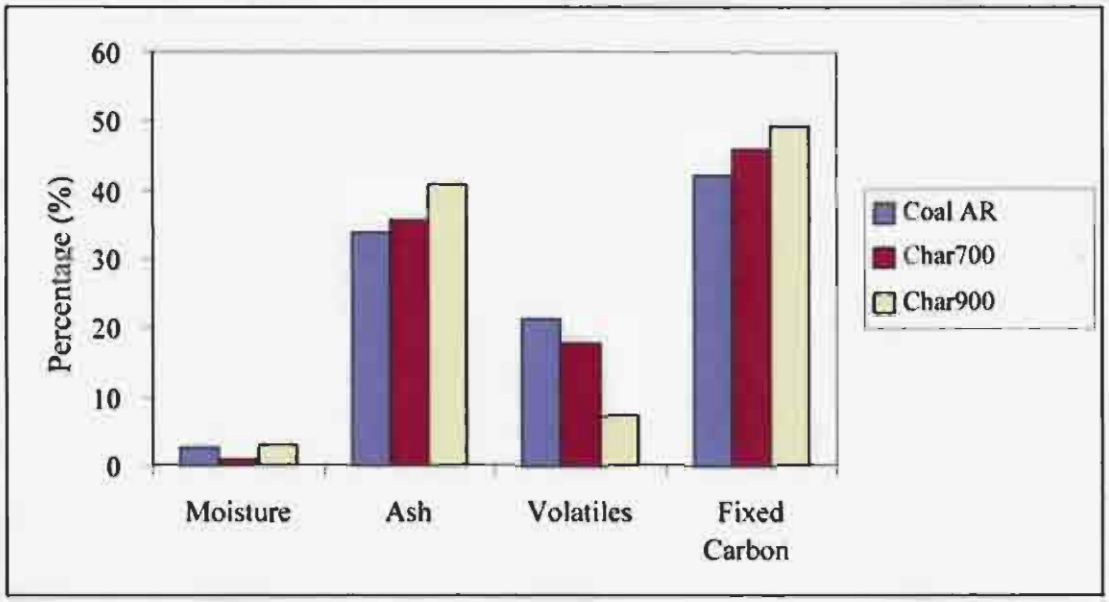

Figure 4.1: Comparison of proximate analyses of coal and chars

4.4.2 Petrographic analyses

The following results are reported: (1) Reflectance properties, which include both vitrinite and total maceral reflectance scans (2) Maceral and microlithotypes analysis of the parent coal (3) Carbominerite and minerite analysis of the parent coal (4) Petrographic composition of the chars, and (5) General condition analysis of the coal and chars.

4.4.2.1 Reflectance properties

Reflectance analyses involving (1) vitrinite as a reference material and (2) a total maceral reflectance scan analysis were carried out on each of the coal and char samples. Results from the vitrinite reflectance experiments are shown in Figure 4.2 and Table 4.2. The extent of the change in vitrinite reflectance as a result of the different charring temperatures was determined on char components clearly recognisable as originating from vitrinites in the parent coal. Very significant shifts were displayed in the levels and ranges of vitrinite reflectance in the char samples compared to those shown by the original coal.

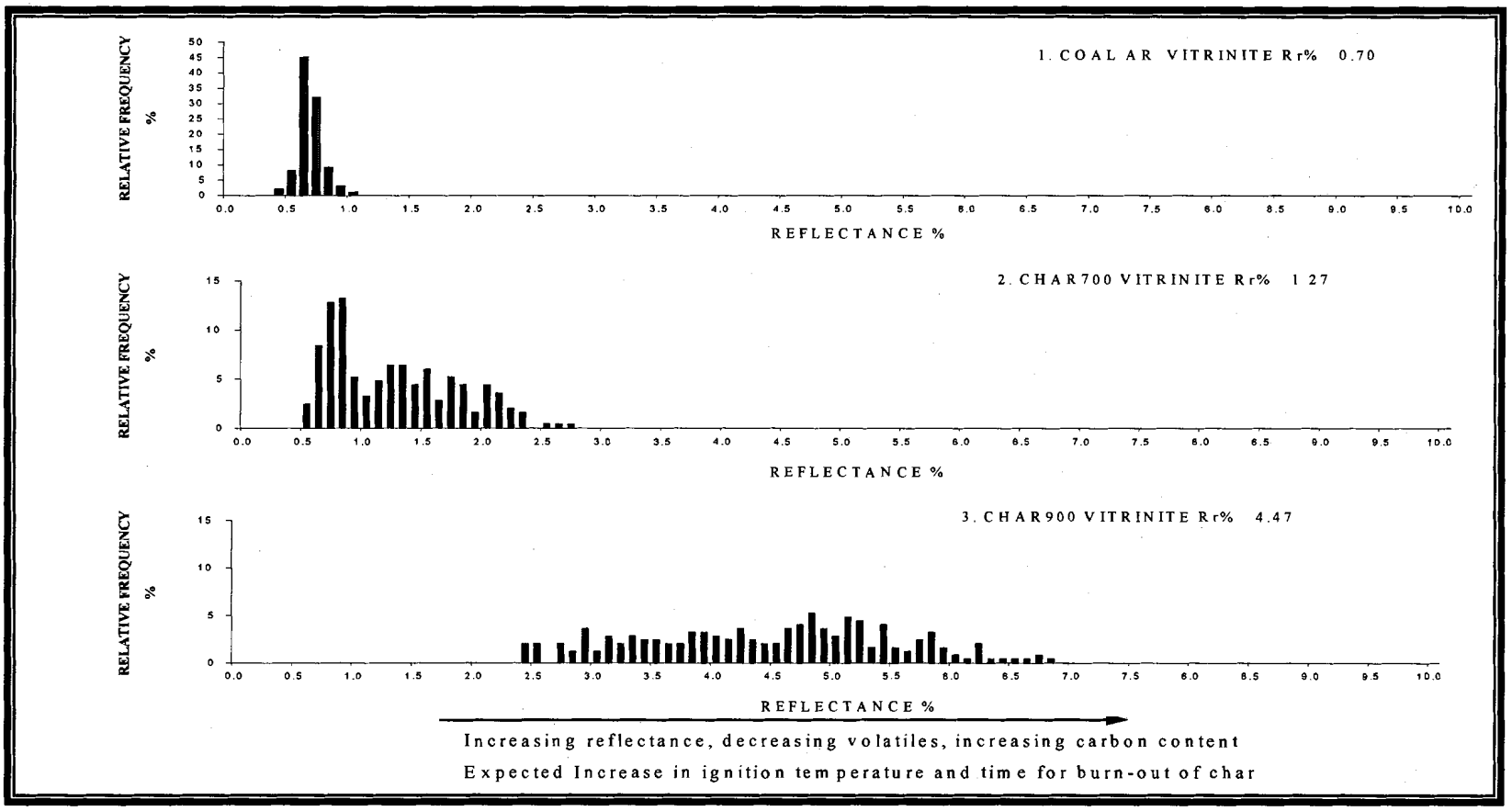

Figure 4.2: Coal/Char vitrinite reflectance histograms

Table 4.2: Coal/Char vitrinite reflectance results

	COAL AR			CHAR700			CHAR900		
	VITRINITE ONLY			VITRINITE ONLY			VITRINITE ONLY		
	MEAN Rr %		0.70	MEAN Rr %		1.27	MEAN Rr %		4.47
	σ		0.099	σ		0.517	σ		1.052
	RANGE %		0.4 - 1.0	RANGE %		0.5 - 2.7	RANGE %		2.4 - 6.8
Rr %	RELATIVE FREQUENCY %			RELATIVE FREQUENCY %			RELATIVE FREQUENCY %		
0.0									
0.1									
0.2									
0.3									
0.4		2.0							
0.5		8.0			2.4				
0.6	VITRINITE	45.0	100.0	< 1.1%	8.4	45.2	< 1.1%		0.0
0.7	PARENT	32.0			12.8				
0.8	COAL	9.0			13.2				
0.9		3.0			5.2				
1.0		1.0			3.2				
1.1					4.8				
1.2					6.4				
1.3					6.4				
1.4					4.4				
1.5					6.0				
1.6					2.8				
1.7					5.2				
1.8					4.4				
1.9				> 1 < 2%	1.6	42.0	> 1 < 2%		0.0
2.0					4.4				
2.1					3.6				
2.2					2.0				
2.3					1.6				
2.4								2.0	
2.5					0.4			2.0	
2.6					0.4				
2.7					0.4			2.0	
2.8								1.2	
2.9				> 2 < 3%		12.8	> 2 < 3%	3.6	10.8
3.0								1.2	
3.1								2.8	
3.2								2.0	
3.3								2.8	
3.4								2.4	
3.5								2.4	
3.6								2.0	
3.7								2.0	
3.8								3.2	
3.9				> 3 < 4%		0.0	> 3 < 4%	3.2	24.0

	COAL AR	CHAR700		CHAR900	
	VITRINITE ONLY	VITRINITE ONLY		VITRINITE ONLY	
	MEAN Rr % 0.70	MEAN Rr % 1.27		MEAN Rr % 4.47	
	σ 0.099	σ 0.517		σ 1.052	
	RANGE % 0.4 - 1.0	RANGE % 0.5 - 2.7		RANGE % 2.4 - 6.8	
Rr %	RELATIVE FREQUENCY %	RELATIVE FREQUENCY %		RELATIVE FREQUENCY %	
4.0				2.8	
4.1				2.4	
4.2				3.6	
4.3				2.4	
4.4				2.0	
4.5				2.0	
4.6				3.6	
4.7				4.0	
4.8				5.2	
4.9		> 4 < 5%	0.0	> 4 < 5% 3.6	31.6
5.0				2.8	
5.1				4.8	
5.2				4.4	
5.3				1.6	
5.4				4.0	
5.5				1.6	
5.6				1.2	
5.7				2.4	
5.8				3.2	
5.9		> 5 < 6%	0.0	> 5 < 6% 1.6	27.6
6.0				0.8	
6.1				0.4	
6.2				2.0	
6.3				0.4	
6.4				0.4	
6.5				0.4	
6.6				0.4	
6.7				0.8	
6.8				0.4	
6.9		> 6 < 7%	0.0	> 6 < 7%	6.0
7.0					
		> 7%	0.0	> 7%	0.0
TOTAL	100.0		100.0		100.0

The following can be deduced from the results obtained: For Char700 45% of the total vitrinite particles measured displayed reflectance levels still within the parent coal vitrinite reflectance range, representing non-reacted vitrinites and 55% of vitrinites represented partially-reacted material, with reflectance levels of above 1% but below 3%. These vitrinites would only have been devolatilised to a restricted extent. For Char900 the shift towards increased vitrinite reflectance levels was highly evident, there were no non-reacted vitrinite particles encountered and 65% of particles derived from vitrinites exhibited reflectance levels of above 4% of reflectance, comparable with the vitrinite reflectance level of meta-anthracite. The relatively highly reflecting vitrinites represented reacted material and would have devolatilised to a major extent.

A total maceral reflectance scan analysis was conducted on each of the samples, coal and chars, involving 250 readings being taken on all organic components, vitrinites, liptinites and inertinites.

The corresponding reflectance histogram and detailed results are given in Figure 4.3 and Table 4.3, respectively. The results for the coal sample revealed that: (1) the medium reflecting vitrinites represented approximately 19% (mineral matter-free basis) of the total organic constituents, within a reflectance ranges of 0.5 to 0.9%. (2) The relatively more highly reflecting inertinites predominated and represented around 77% of the total organic components, with reflectance levels mostly >1% and, (3) The relatively low reflecting liptinites (< 0.4%) represented around 4% of the coal. For Char700 a minor shift in mean reflectance value and distribution was observed in comparison to the parent coal. Approximately 20% of readings were still within the parent coal vitrinite range for Char900. The shift towards the higher reflectance ranges was far more pronounced. No organic material with less than 2% of reflectance was present. In addition, for Char900 the vitrinite reflectance and the total maceral scan reflectance distributions were very similar (Figures 4.2 and 4.3).

It should be noted that for the maceral scans involving the chars, the reflectances of the vitrinites and inertinites overlapped, falling within the same ranges, which made it difficult to distinguish between these macerals based on reflectance distribution as achieved with the coal sample.

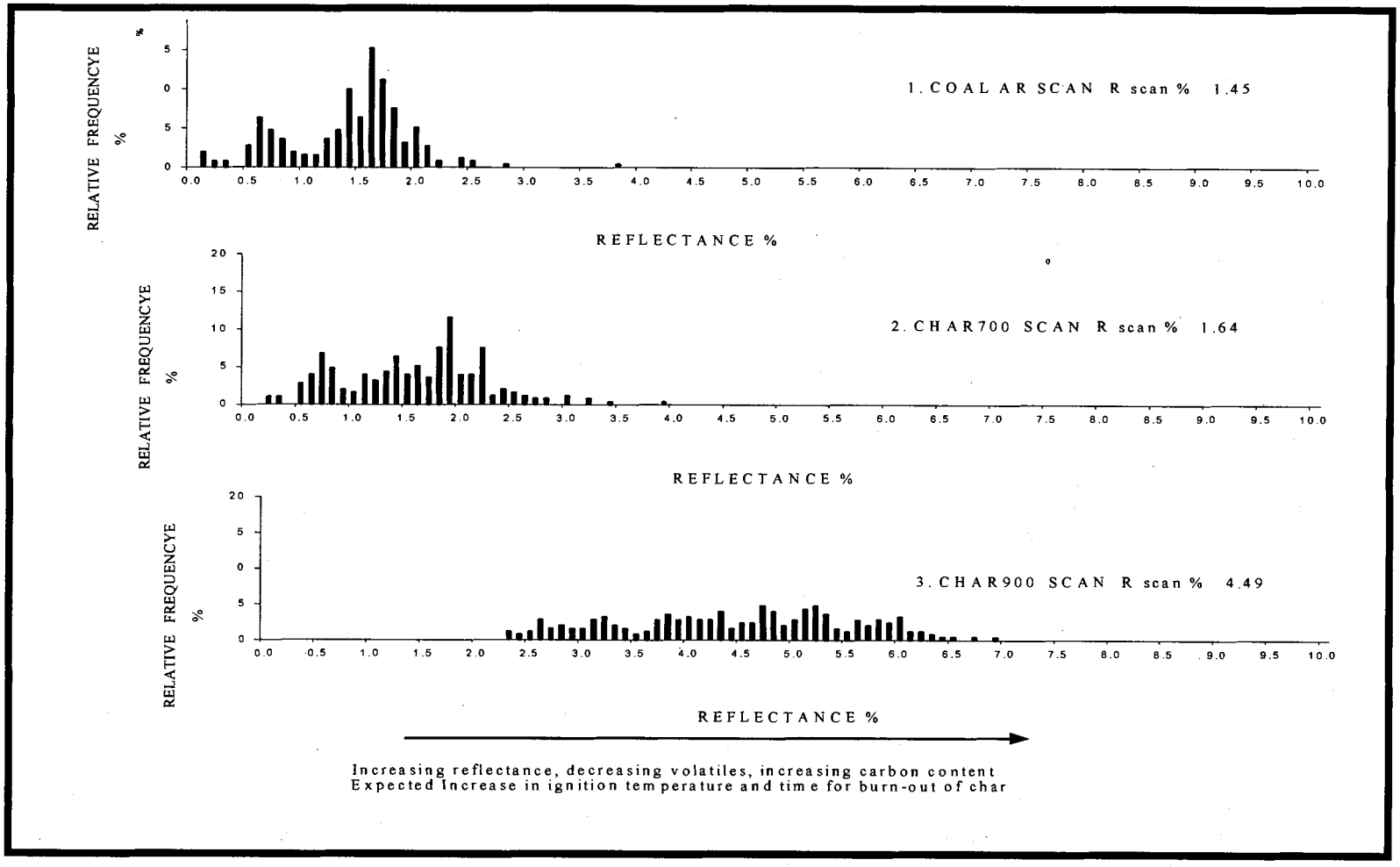

Figure 4.3: Coal/Char total maceral reflectance histogram.

Table 4.3: Coal/Char maceral reflectance results

	COAL			CHAR700			CHAR900		
	MACERAL			MACERAL			MACERAL		
	MEAN Rsc		1.45	MEAN Rsc		1.64	MEAN Rsc		4.49
	σ		0.538	σ		0.641	σ		1.081
	RANGE		0.1 - 3.8	RANGE		0.2 - 3.9	RANGE		2.3 - 6.9
	% TOTAL REACTIVES <		44.8						
Rsc %	RELATIV FREQUENCY			RELATIV FREQUENCY			RELATIV FREQUENCY		
0.0									
0.1	LIPTINIT	2.0	3.6	LIPTINIT		2.0	LIPTINIT		0.0
0.2		0.8			1.0				
0.3		0.8			1.0				
0.4									
0.5	VITRINIT	2.8		VITRINIT	2.8		VITRINIT		
0.6	< 1%	6.4	19.6	< 1%	4.0	20.4	< 1%		0.0
0.7		4.8			6.8				
0.8		3.6			4.8				
0.9		2.0			2.0				
1.0		1.6			1.6				
1.1		1.6			4.0				
1.2		3.6			3.2				
1.3		4.8			4.4				
1.4		10.0			6.4				
1.5		6.4			4.0				
1.6		15.2			5.2				
1.7		11.2			3.6				
1.8	INERTINIT	7.6			7.6				
1.9	> 1 < 2%	3.2	65.2	> 1 < 2%	11.6	51.6	> 1 < 2%		0.0
2.0		5.2			4.0				
2.1		2.8			4.0				
2.2		0.8			7.6				
2.3					1.2			1.2	
2.4		1.2			2.0			0.8	
2.5		0.8			1.6			1.2	
2.6					1.2			2.8	
2.7					0.8			1.6	
2.8		0.4			0.8			2.0	
2.9	> 2 < 3%		11.2	> 2 < 3%		23.2	> 2 < 3%	1.6	11.2
3.0					1.2			1.6	
3.1								2.8	
3.2					0.8			3.2	
3.3								2.0	
3.4					0.4			1.6	
3.5								0.8	
3.6								1.2	
3.7								2.8	
3.8		0.4						3.6	
3.9	> 3 < 4%		0.4	> 3 < 4%	0.4	2.8	> 3 < 4%	2.8	22.4

	COAL AR		CHAR700		CHAR900		
	MACERAL SCAN		MACERAL SCAN		MACERAL SCAN		
	MEAN Rsc %	1.45	MEAN Rsc %	1.64	MEAN Rsc %	4.49	
	σ	0.538	σ	0.641	σ	1.081	
	RANGE %	0.1 - 3.8	RANGE %	0.2 - 3.9	RANGE %	2.3 - 6.9	
	%TOTAL REACTIVES<1.5%	#REF!					
Rsc %	RELATIVE FREQUENCY %		RELATIVE FREQUENCY %		RELATIVE FREQUENCY %		
4.0						3.2	
4.1						2.8	
4.2						2.8	
4.3						4.0	
4.4						1.6	
4.5						2.4	
4.6						2.4	
4.7						4.8	
4.8						4.0	
4.9	>4<5%	0.0	>4<5%	0.0	>4<5%	2.0	30.0
5.0						2.8	
5.1						4.4	
5.2						4.8	
5.3						3.6	
5.4						1.6	
5.5						1.2	
5.6						2.8	
5.7						2.0	
5.8						2.8	
5.9	>5<6%	0.0	>5<6%	0.0	>5<6%	2.4	28.4
6.0						3.2	
6.1						1.2	
6.2						1.2	
6.3						0.8	
6.4						0.4	
6.5						0.4	
6.6							
6.7						0.4	
6.8							
6.9	>6<7%	0.0	>6<7%	0.0	>6<7%	0.4	8.0
	>7%	0.0	>7%	0.0	>7%		0.0
TOTAL		100.0		100.0			100.0

4.4.2.2. Maceral and microlithotype analysis of parent coal

A maceral and visible minerals analysis (percent by volume) of the parent coal is shown in Table 4.4; firstly as determined by a point-count procedure, and secondly as calculated from the total maceral reflectance scan (Tables 4.3). The high inertinite concentration (59% mineral matter basis) is evident and the total reactive macerals, defined as the propensity of the maceral constituents to react to heating, amount to 35% consisting of 15% vitrinite, 2% liptinite and 18% reactive inertinites. A close agreement between the point count analysis results (mineral matter-free basis) and the scan analysis on the relative proportions of the group macerals and the total reactives was obtained. The microlithotype analysis given in Table 4.5 shows that, the proportion of mono-macerals is much higher than that of bi- and tri- macerals. The latter maceral intermediates are the origin of a network of very high reflecting material with medium to high porosities when charred (see classification for char carbon forms given in Appendix B).

Photomicrographs of selected particles showing the macerals and microlithotypes present in the parent coal are given in Figures 4.4 to 4.7. The following are illustrated:

(1) The vitrinite present (Figure 4.4) appears to be relatively "fresh", with no marked features indicative of pronounced weathering, such as, extensive cracking, discoloration, oxidation rims or zones of abnormal reflectance levels. Weathering and/or oxidation can be regarded as a process of deterioration in coal quality with adverse effects on coal reactivity and gasification/combustion performance.

(2) Vitrinite, dark coloured liptinite (sporinite with some cutinite) and fragments of bright white inertinite in close association (microlithotype: tri-macerite) are shown in Figure 4.5. Reactives-rich microlithotypes can contribute to faster gasification and combustion reaction rates.

(3) The presence of inter-layered inertinites is shown in Figure 4.6. The inert semi-fusinites also exhibit well-preserved woody tissue cell structure and a markedly higher level of reflectance than the associated vitrinite in the coal. Inert inertinites and particularly fusinites, do not soften, degasify or develop into porous structures, but form quite dense chars, which are more difficult to ignite. They also tend to have lower burn-off rates. Inertinite group macerals

with colour and reflectance more similar to that of associated vitrinites are known to react to heating in a similar manner to vitrinites. Such reactive inertinites are quantified as reactive semi-fusinites and reactive inertodetrinites. The occurrence of densely packed inert inertodetrinite with some liptinite is shown in Figure 4.7.

Table 4.4: Maceral Analysis of coal sample AR

SAMPLES CODES	**MACERAL ANALYSIS (% VOLUME)**															**RANK REFLECTANCE**	
	Vitrinite			**Liptinite**			**Inertinite**							**Visible Mineral**	**Total Reactive**		
Company No	VIT* %	PV %	TV %	S/R/ C%	ALG %	TOT L%	RSF %	ISF %	F/SE C %	MIC %	R INT %	I INT %	Tot I %	%	%	Rr %	σ
Coal AR MMB	14	1	15	2	0	2	8	16	2	1	10	22	59	24	35	0.70	0.099
Coal AR MMF	18	1	19	3	0	3	11	21	3	1	13	29	78	0	46	0.70	0.099
Coal AR MMF Coal R Scan			19			4							77	0	45	0.70	0.538

*See Appendix C for explanation of abbreviations

MMB- Visible Mineral Matter Basis

MMF - Visible Mineral Matter-Free Basis

R Scan - Reflectance Scan

Total Reactives = Vitrinite + Liptinite + Semifusinite + Reactive Inertodetrinite

Table 4.5: Microlithotype analysis of coal sample AR

Microlithotype analysis (% Volume, Mineral Matter Basis)									
Monomacerals[1]				**Intermediates[2]**				**Carbominerite[3]**	**Minerite[4]**
Vitrite %	Liptite %	Inertite		Bi-Macerals			Tri-Macerals	%	%
		F/SF/S* %	M/IN/M** %	Clarite %	Durite %	Vitrinertite	Trimacerite		
7	0	11	21	1	2	4	6	30	18

[1,2,3,4] See Appendix C for details

*F/SF/S Fusite/Semifusite/Secretite

**M/IN/M Macrite/Inertodetrite/Micrite

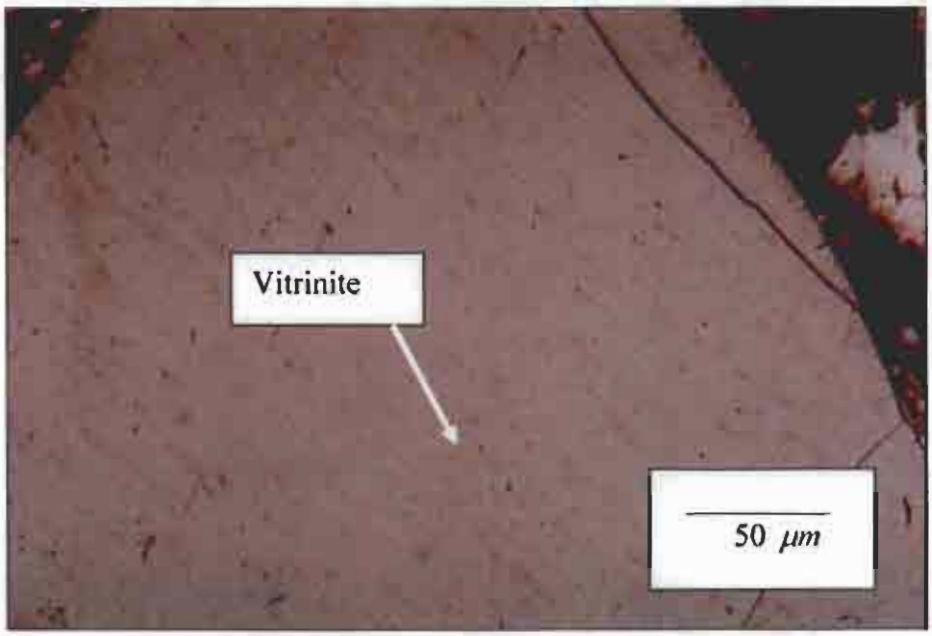

Figure 4.4: Parent Coal AR -Vitrinite (microlithotype: mono-maceral–vitrinite)

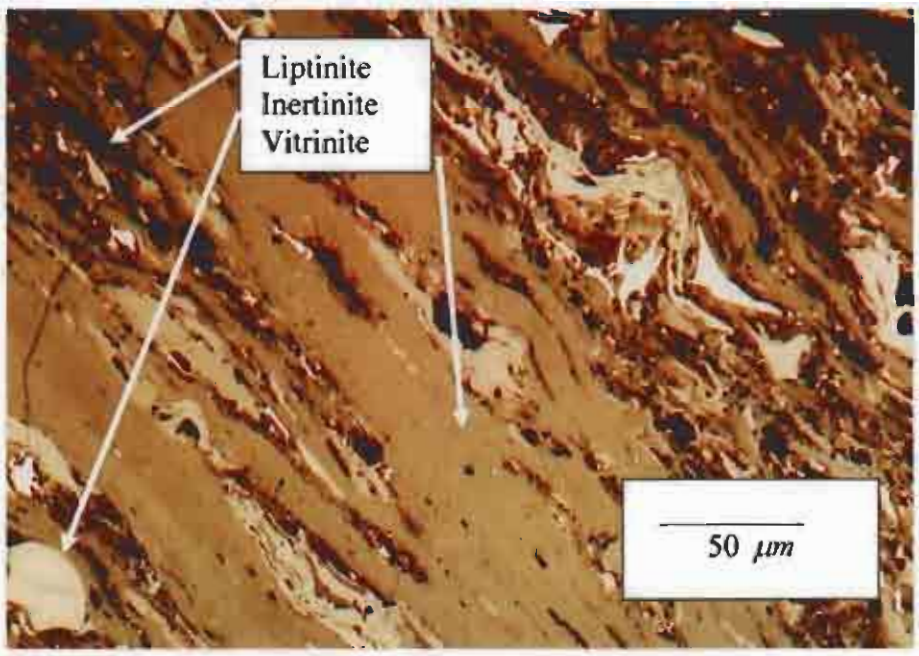

Figure 4.5: Parent Coal AR - Maceral associations (microlithotype: tri-macerite)

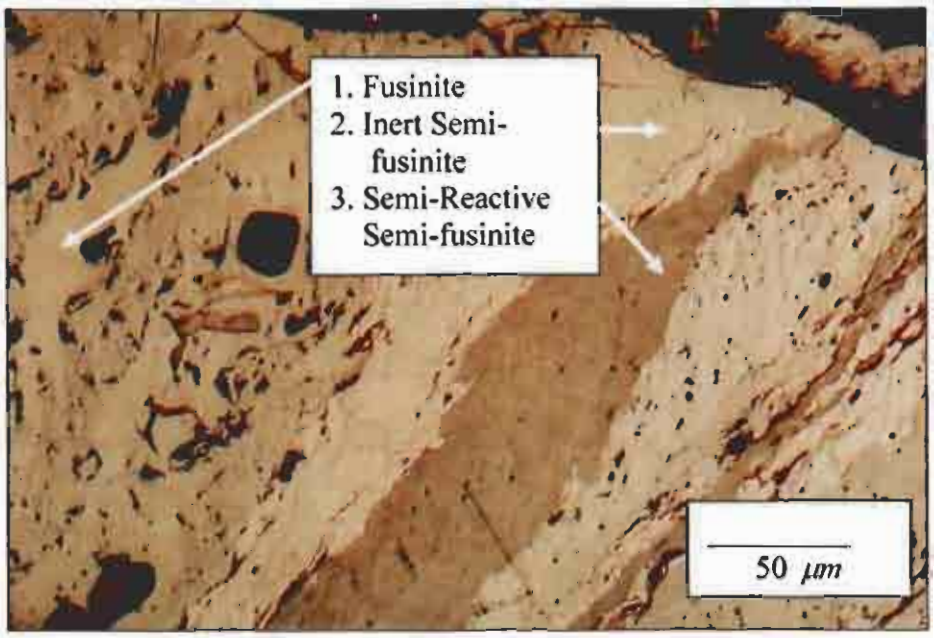

Figure 4.6: Inter-layered inertinites microlithotype: mono-maceral – inertinite.

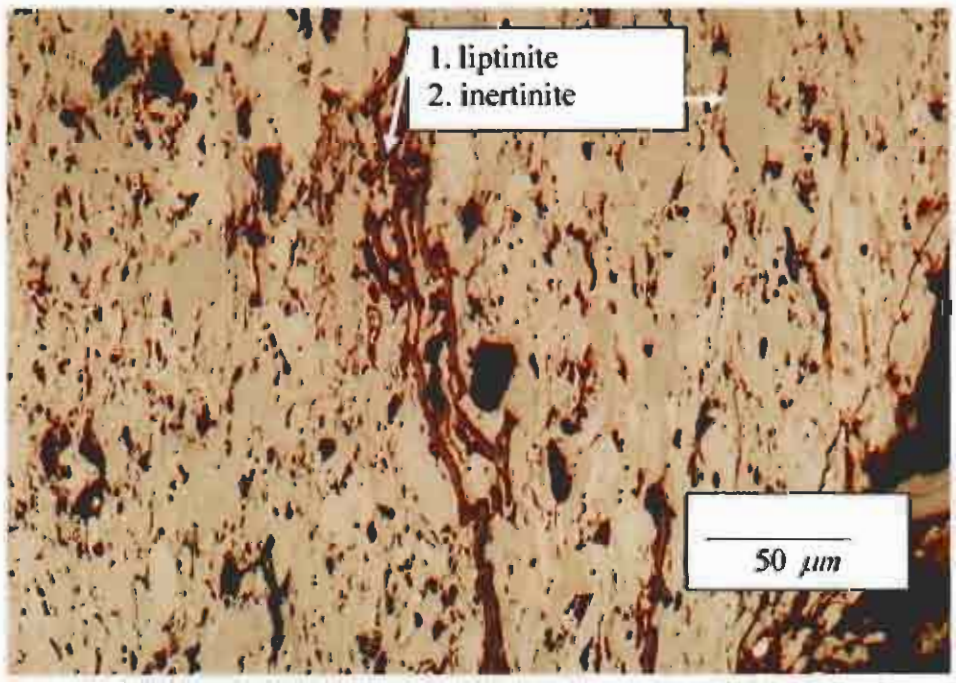

Figure 4.7: Densely packed inert inertodetrinites with fine fragment liptinite

4.4.2.3 Carbominerite and minerite analysis of parent coal

The carbominerite and minerite analysis of the coal is shown in Table 4.6. The visible minerals were found to be both finely dispersed and intimately associated with the coal macerals in carbominerite and occurring in a substantially lesser proportion in

mineral-rich particles. Finely dispersed clay group minerals (intimately mixed with coal macerals in carbargilite) occurred most commonly (13%). Fine grains and nodules of syngenetic pyrite were occasionally observed, closely associated with organic constituents as carbopyrite with replacement forms of pyrite occurring occasionally. Carbonates (calcite and siderite) were seen intimately mixed with organic material in carbankerite. Quartz minerals were also observed. However, the identification of quartz minerals in reflected light is problematic and the occurrence of these minerals may have been underestimated. Particles made up of intimately mixed organic/inorganic materials (carbominerite) made up 30% of the coal.

The mineral-rich particles amounted to 18% with the quartz group of minerals being the most abundant.

Table 4.6: Carbominerite and minerite analysis of coal sample AR

Carbominerite Analyses (by % Volume) [1]					**Minerite Analyses (by % Volume)**				
Organic/Inorganic Associations					Mineral rich Particles				
Carb-Argilite %	Carbo-Silicite %	Carbo-Pyrite %	Carb--Ankerite %	Total Carbo – Minerite[2] %	Clay Group %	Quartz Group %	Pyrite Group %	Carbonate Group %	Total Minerite %
13	7	4	6	30	4	7	4	3	18

[1]See Appendix C for explanation

[2]Total organic/inorganic microlithotypes

4.4.2.4 Petrographic composition of the chars

The classification system used for the characterisation is outlined in the Appendix B, (du Cann, 2005a and 2005b) and the results for the chars examined are shown in Table 4.7. These results revealed that the two char samples represented very different mixtures of unaffected coal, partially reacted coal, "char", "coke" and inorganic matter. The following categories of constituents were encountered (according to classification and Table 4.7):

(A) Char forms

(1) Dense "char" (25% in Char700 and 38% in the Char900)

These dense carbon forms were mainly derived from inertinites in the parent coal, which had not softened and expanded to any appreciable extent on charring, largely retaining their original coal maceral shape and form. A larger fraction is generated with a high charring temperature. A photomicrograph of dense char is shown in Figure 4.8 and is derived from the inertinite maceral with a charring temperature of 900°C. The material has remained virtually unchanged in its original coal inertinite maceral structure and form. Some small gas pores are visible.

(2 and 3) Char networks displaying varying degrees of porosity (6% in Char700 and 20% in Char900). Consisting of fine walled networks, developed from reactives-rich coal with high internal surface areas and thicker-walled networks that are less porous which are derived from inert-rich coal particles. Typical photomicrographs showing the occurrence of thick-walled char networks are shown in Figures 4.9 and 4.10 for the different charring temperatures. The reactive macerals have devolatilised leaving a slightly more porous carbon form.

(B) Coke forms (3% in Char700 and 7% in Char900)

(7) These forms were derived mainly from the pure vitrinite, i.e., vitrinite in the parent coal. When the coal is heated during the charring process, the vitrinites and other reactive macerals soften and degasify, creating pores. As the released gases within the pores increase in volume, the softening walls expand and the material increases in volume and surface area. The "coke" in these samples was represented by isotropic forms, displaying well-developed

devolatilisation vesicles and often quite thick "coke" walls. Typical photomicrographs of coke forms are shown in Figures 4.11 and 4.12. The parent coal vitrinite has increased markedly in reflectance in response to the charring process and forms both thick and thin-walled highly porous isotropic "coke". However, devolatilisation is incomplete and the pores are under-developed for Char700 (Figure 4.11). The original coal vitrinite has also passed through a plastic phase, released volatiles to form numerous vesicles, and produced highly porous cellular structures especially for Char900 (Figure 4.12).

(C) Oxidation effects

No signs of oxidation (e.g. dark rims and zones on particle edges and around gasification pores) were observed in either char.

(D) Non-reacted coal (30% in Char700 and 0% in Char900)

(11) Material unaffected by heat, displaying typical bituminous Medium Rank C vitrinite reflectance levels, was only encountered in the Char700.

(E) Partially reacted vitrinite (7% in Char700 and 4% in Char900)

(12) This material was found to have reflectance levels above those of the parent coal, but substantially lower than those of the fully charred components (i.e., intermediate reflectivities in the range of approximately 1% up to 4% Rr). Devolatilisation was limited and porosity was relatively poorly developed.

(F) Visible minerals from parent coal (29% at 700°C and 31% at 900°C)

(13) These included the minerals initially in the parent coal.

Table 4.7: Structural and textural analysis of chars

	Variable (Percentage Volume)	Char700	Char 900
A	1 Dense char (from coal inerts)	25	38
	2 Network-fine walled (from coal reactives)	1	6
	3 thick walled (from coal inerts)	5	14
	Sub Total	31	58
B	4 "Coke"-Circular Anisotropic-Fine	0	0
	5 "Coke"-Circular Anisotropic-Medium	0	0
	6 "Coke"-Incipient Anisotropic	0	0
	7 "Coke"-Isotropic (From Coal Vitrinite)	3	7
	Sub Total	3	7
C	8 "Oxidised"-Mainly from Vitrinite	0	0
	9 "Oxidised"-Mainly from Inertinite	0	0
	10 "Oxidised"-Low Reflecting Network	0	0
	Sub Total	0	0
D	11 Original Coal-Unaffected - Vitrinite	4	0
	- Inertinite	26	0
	12 Original Coal-Partially Reacted - Vitrinite	7	4
	(Low Temperature devolatilisation)		
	Sub Total	37	4
E	13 Inorganic Matter - From Coal	29	31
	14 Inorganic Matter – Other	0	0
F	15 Process Derived Depositional Carbons	0	0
	Total %	100	100
Organic Components Derived from Coal-Vitrinites - Inertinite Total Reacted/Partially Reacted Macerals		14 56 20	11 52 31
Mean Random Reflectance (%)		1.64	4.49
Range of Readings (%)		0.2-3.9	2.3-6.9
Standard Deviation		0.641	1.081

Groups A and B - Very highly Reflecting, Oxidation Restricted
Group C - Relatively Low Reflecting, Exhibiting Oxidation Rims
Group D - Low Reflecting, Little or No Change
Anisotropic - Exhibiting Optical Properties of Different Values When Viewed Under Crossed Nicols.
Isotropic - Exhibiting Optical Properties That Are The Same In All Directions When Viewed Under Crossed Nicols.

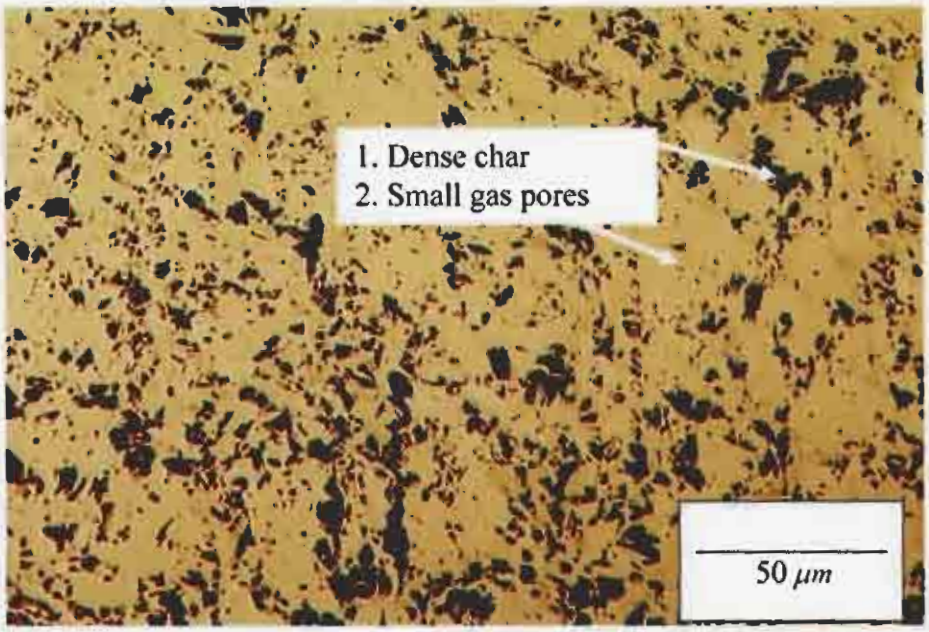

Figure 4.8: Char900 - Dense char from mono-maceral inertinite

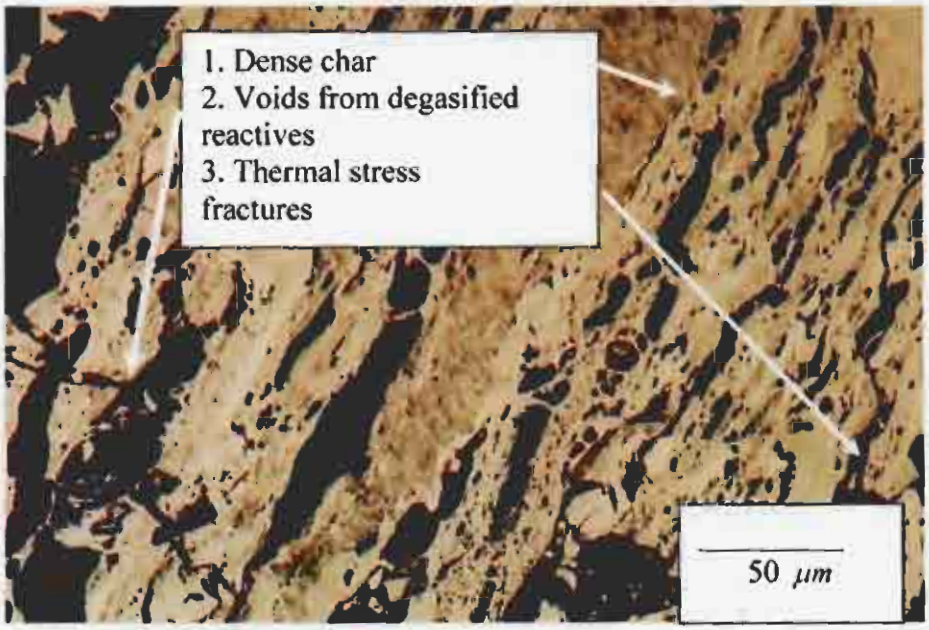

Figure 4.9: Char700 - Development of thick-walled char networks

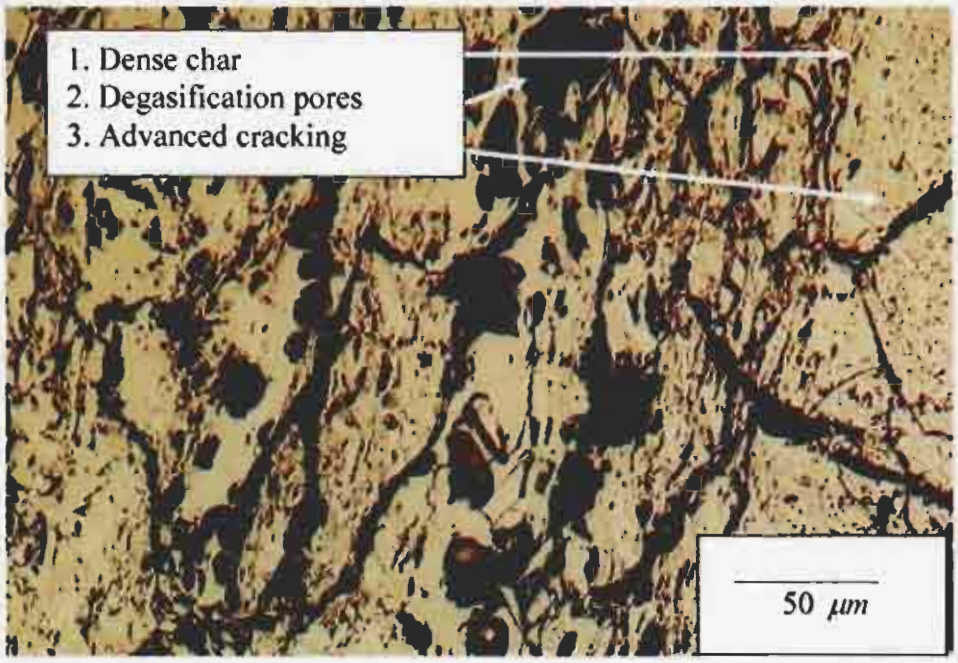

Figure 4.10: Char900 - Development of thick-walled char networks

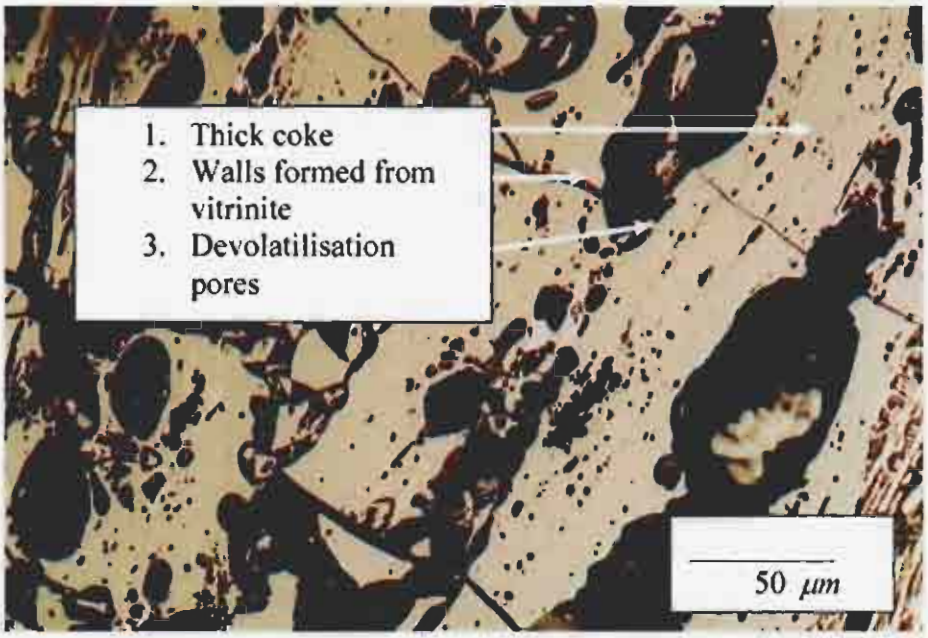

Figure 4.11: Char900 - Thick-walled isotropic "coke"

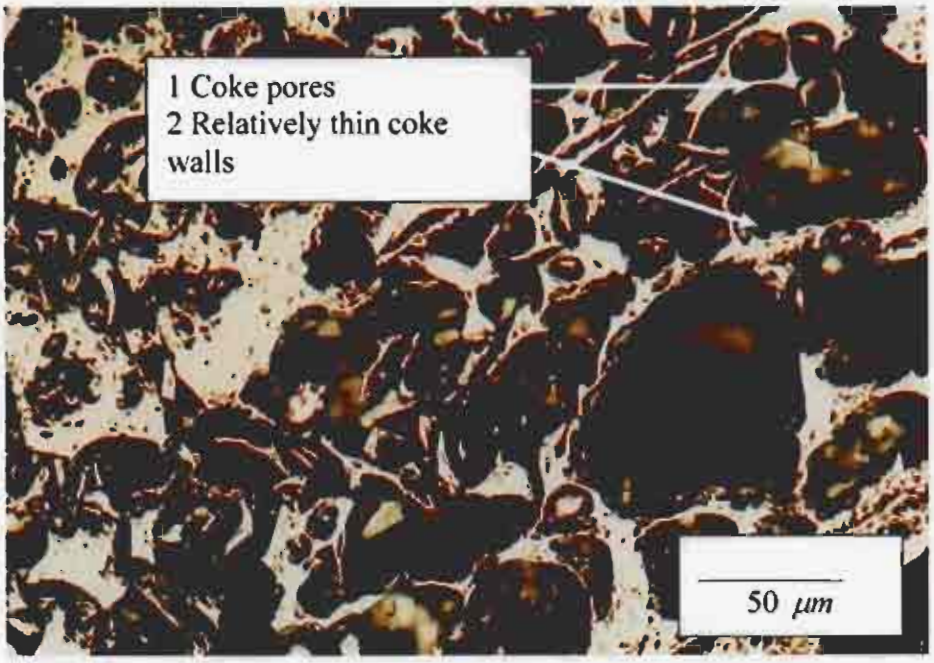

Figure 4.12: Char900 - Thin-walled highly porous isotropic "coke"

On comparing the effect of charring temperature on the properties of the chars, the following was found: The heat treatment of the parent coal to 700°C resulted in relatively little change in overall reflectance levels and maceral structure. The presence of non-reacted and partially reacted vitrinites in this char is a function of the heating process (e.g. coal size used, temperature attained, residence time etc.). At 700°C, the charring process did not devolatilise the original coal completely. At 900°C, marked devolatilisation and char formation occurred. However, the majority of the char carbon forms had not increased in porosity.

4.4.2.5 General condition analysis of parent coal and chars

The results from this analysis are shown in Tables 4.8 and 4.9. A significant portion of the particles examined displayed extensive cracks and micro-fissures. Some cracking probably occurred during handling and preparation due to the somewhat brittle nature of coal (particularly vitrinite) of this level of maturity. The pyrite present appeared as a 'fresh" bright yellow colour throughout the coal. However, an approximately 10% portion of severely weathered particles was noted.

There was a 25% increase in the proportion of extensively cracked and fissured organic material because of charring (i.e. from 25% in the parent coal material to 50%

in both chars) this is attributed to thermal stress fracturing. This phenomenon may well be a positive factor in aiding the burning of this low-grade, high-ash, inertinite-rich coal.

Photomicrographs illustrating the fragmentation occurring during charring are shown in Figures 4.13 to 4.15 (du Cann, 2005b). The effects of charring temperature involving essentially inertinites is shown in Figures 4.13 and 4.14, which need to be compared to Figure 4.7 that shows a corresponding image for the parent coal. These photomicrographs show a widespread development of low temperature thermal stress fractures (i.e., "passive deflagration") in between and across compacted inertodetrinites. Such particles have increased surface areas and can easily disintegrate. No gas vesicles have developed in these inertodetrinites. The proportion of material that had undergone abnormal cracking and fissuring at 700°C remained approximately the same as for the 900°C charring, thereby indicating that all the material that was likely to thermally crack had done so early on in the temperature regimes. A photomicrograph showing the thermal cracking of the vitrinite maceral for a charring temperature of 700°C is given in Figure 4.15 (compare with Figure 4.4). Extensive micro-fissures attributed to low temperature thermal stress fracturing ("passive deflagration") are clearly visible. The vitrinite has increased slightly in reflectance, but has not devolatilised (for this particular particle) to form a porous char. The fine syngenetic grains of pyrite embedded in the vitrinite have also retained their "fresh" bright yellow colour.

Table 4.8: General condition analysis of parent coal sample AR

Fresh Coal Particles %	**Pyrite**		**Particles with extensive cracks or fissures %**	**Severely weathered Particles %**	**Particles with desiccation cracks %**	**Particles with thermally affected rims or zones %**
	Normal %	**Altered %**				
71	4	0	13	10	2	0
A significant portion of particles examined displayed extensive cracks and micro fissures. Some cracking probably occurred during handling and preparation due to the brittle nature of coal (particularly vitrinite) of this nature of maturity. The pyrite present appeared as a "fresh" bright yellow colour throughout the sample. However, approximately 10% of severely weathered coal was noted in coal AR.						

Table 4.9: Coal/Char Condition Analysis

	Fresh/Uncracked (%)	**Cracks and Fissures (%)**	**Severely weathered coal /thermally cracked char (%)**
Coal AR	75	15	10
Char700	50	22	28
Char900	50	24	26

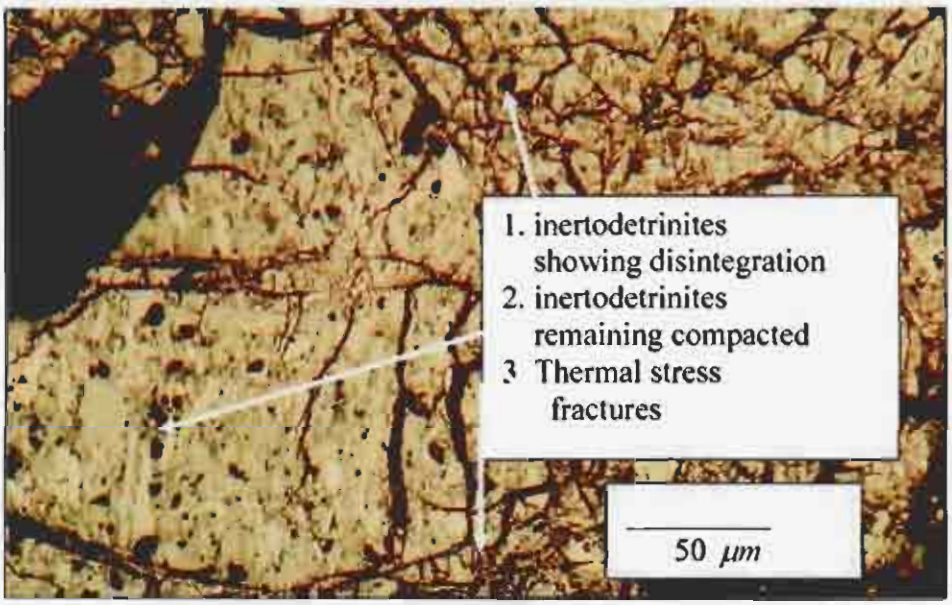

Figure 4.13: Char700 - Thermal cracking and disintegration of inertinites

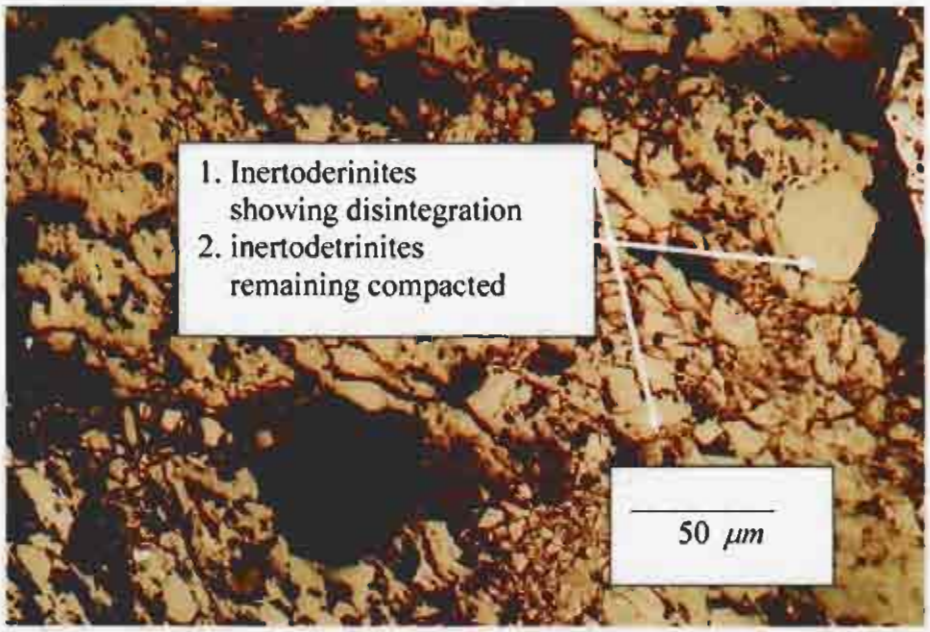

Figure 4.14: Char 900 - Advanced thermal cracking of inertodetritic

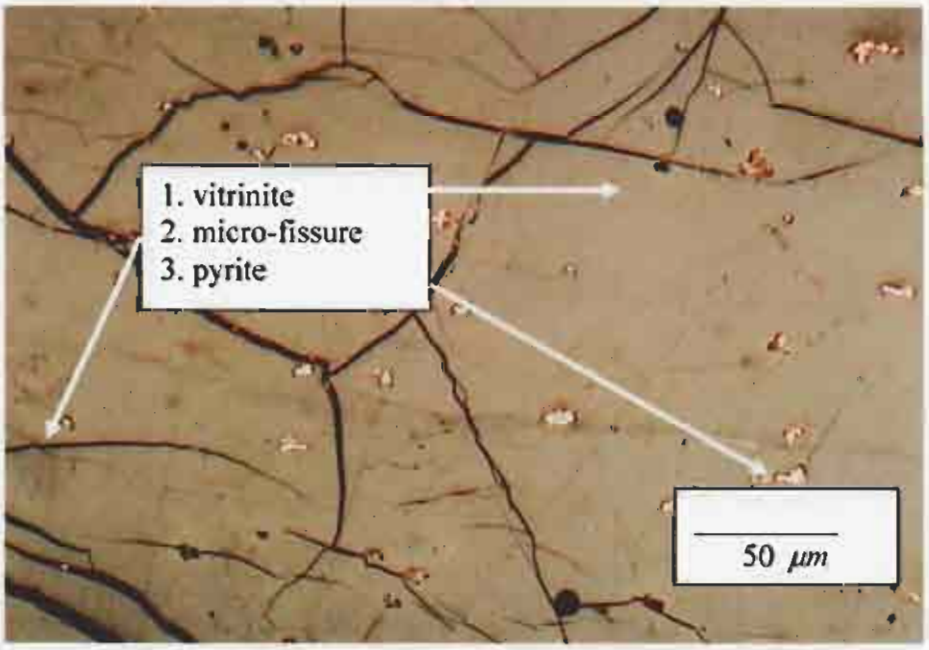

Figure 4.15: Char700 – Thermal cracking of vitrinite

4.4.3 Computer Controlled Scanning Electron Microscope analysis

4.4.3.1 Mineral analysis

The different minerals that are present in Char900 are summarised in Table 4.10. The presence of exceptionally-high concentrations of quartz, kaolinite and to a lesser

extent of pyrite, pyrrhotite and calcite constitutes a most usual feedstock, which can create operational problems when used in pulverised fuel combustion.

Table 4.10: Mass-% mineral abundance

Mineral	Char900 Mass-%	Mineral source in original coal
Pyrite/pyrrhotite	3.4	Partial transformation of pyrite (FeS_2)
Quartz	7.7	Quartz (SiO_2)
Feldspar	0.4	Microcline ($KAlSi_3O_8$) feldspar
Illite/muscovite	1.1	Illite/muscovite $(K_{1-1.5})Al_4[Si_{7-6.5}Al_{1-1.5}O_{20}](OH)_4$) ($KAl_3Si_3O_{10}(OH)_4$)
Kaolinite	22.9	Kaolinite ($Al_2Si_2O_5(OH)_4$) – clay
--Fe-oxide/siderite	1.4	Fe-hydroxides/Fe-oxide, $FeCO_3$
Calcite	3.4	$CaCO_3$
Dolomite	1.7	$CaMg(CO_3)_2$
Ankerite	0.3	$CaFe(CO_3)_2$/ $FeCO_3$
Apatite	0.5	$Ca_3(PO_4)_3(F,Cl,OH)$
Anatase/Rutile	0.2	TiO_2
Gypsum/Anhydrite	0.14	$CaSO_4 2H_2O/CaSO_4$
Other	0.03	Unidentified minerals
"Char/Coal"	56.9	Carbon-rich coal
Total	100.0	

4.4.3.2 CCSEM image analysis

An electron image of the carbon-mineral interactions was determined for Char900 and is shown in Figure 4.16 (Van Alphen, 2005a and 2005b). The high ash content of the coal-char is attributed to the higher proportion of extraneous rock fragments. Kaolinite rich siltstone/mudstone and to a lesser extent arkosic sandstone are the two common rock fragments.

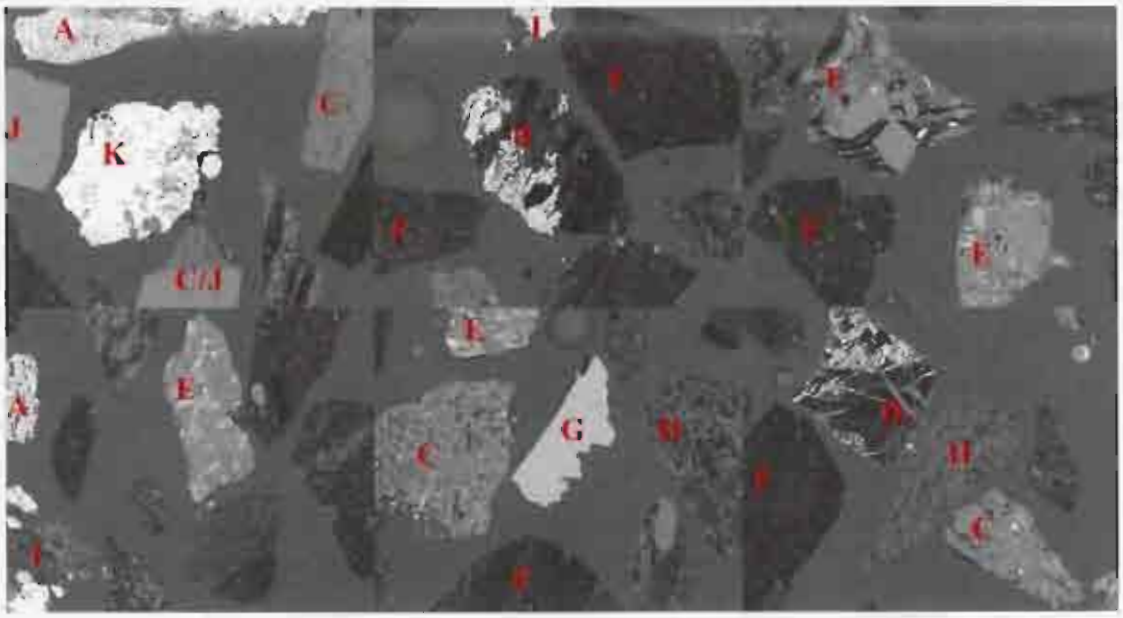

Carbon rich char is black, iodoform epoxy resin is dark grey and minerals are light grey to white. Width of the individual images is 2.1mm

Figure 4.16: Various backscattered electron images of Char900

The characteristics of the particles highlighted in Figure 4.16 are as follows:

Particle A – large extraneous pyrite cleat fragments

Particle B – large pyrite (white) inclusions in carbon-rich particles

Particle C – large extraneous kaolinite and quartz rich siltstone/mudstone rock fragments. Mica/illite, apatite, anatase are also present in these siltstone/mudstone rock fragments.

Particle D – fine pyrite (white) and calcite/dolomite (grey) cleats transecting carbon rich matrix (black). The fine pyrite cleats form a complex network.

Particle E – arkosic sandstone rock fragments consisting predominately of quartz grains (light grey) and kaolinite (dark grey), with minor feldspar (light grey) and anatase (white).

Particle F – fine kaolinite and quartz inclusions (grey) in carbon matrix (black).

Particle G – large calcite rich extraneous cleat fragment.

Particle H – kaolinite mixed with carbon in mudstone rock fragment.

Particle I – siderite/ankerite grain (white) attached to carbon matrix.

Particle J – large quartz grains remnant of coarse grained sandstone.

Particle K – large extraneous siderite/Fe-oxide grain

Kaolinite, quartz and muscovite/illite can occur as fine inclusions in carbon matrix or associated with siltstone/mudstone and sandstone rock fragments. Large angular included quartz grains can reach sizes of 280 μm whereas round quartz grains can exceed sizes of 1 mm (particle J). These large quartz grains are the milled products of coarse-grained sandstone. Pyrite occurs as large extraneous cleat fragments, fine to large inclusions in carbon matrix and infilling cleats. The extraneous pyrite cleat fragments exceed 1mm in size (Particle A).

The fine pyrite-rich cleats can form a complex network of cleats transecting the coal particle. The large pyrite inclusions can reach sizes of 410 μm. Pyrite is commonly associated with the carbonates, dolomite and calcite. Dolomite and calcite have similar association characteristics as pyrite. Dolomite cleats perpendicular to layers do occur, whereas calcite rich lenses parallel to the layers are common. Extraneous carbonate cleat fragments can be a complex association of fine calcite and dolomite or consisting entirely of calcite (Particle G).

Pure dolomite extraneous cleat fragments were not detected. These extraneous carbonate cleat fragments exceed 1mm in size. Large apatite rich extraneous particles associated with calcite, kaolinite and "char/coal" were evident. Apatite can also occur as fine inclusions in siltstone rock fragments or in carbon-rich particles. Siderite is commonly associated with ankerite and occurs as large grains attached to carbon rich particles (particle I) or as large extraneous particles (particle K).

4.4.3.3 Association characteristics

From the CCSEM results, the area proportion of the individual mineral species and the carbon matrix ("char/coal") for each particle can be obtained. The total mineral area proportion is used to classify each particle into 12 association classes. These classes range from mineral rich particles (0-class) to carbon-rich, mineral-free particles (100-class). The total particle area for each association class is quantified and percent area distribution is determined. The association characteristics of the Char900 examined are summarised in Figure 4.17. In this figure, three distributions are described: (1) Particle – this is the total particle distribution per association class. It includes the mineral matter and carbon proportion in the particle. (2) Mineral – this is the total mineral matter distribution per association class. (3) Char – this is the total carbon ("char/coal") distribution per association class.

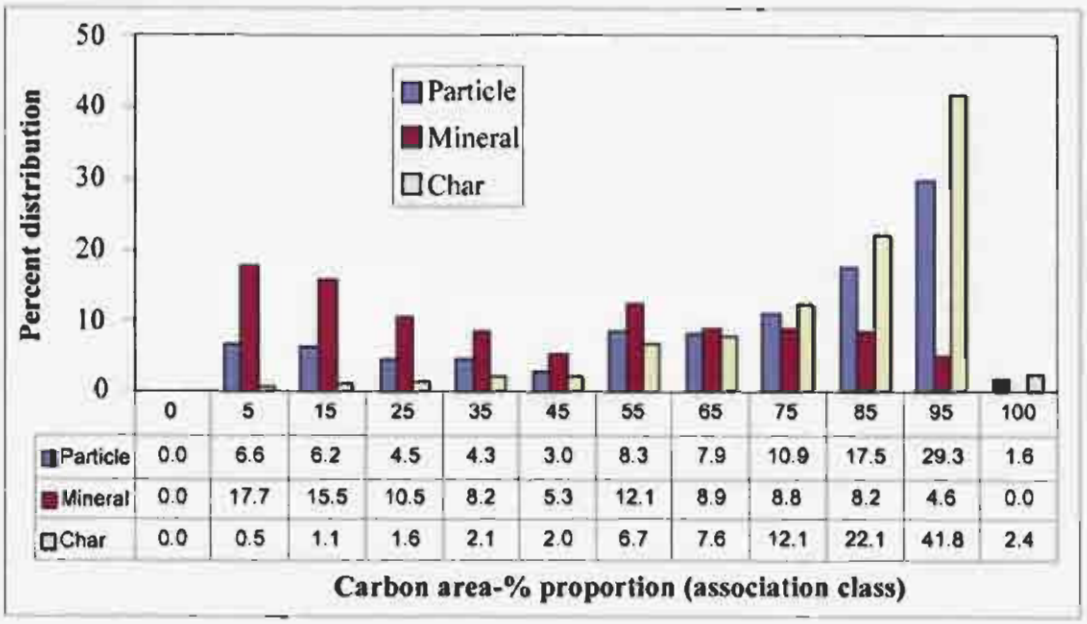

	0	5	15	25	35	45	55	65	75	85	95	100
Particle	0.0	6.6	6.2	4.5	4.3	3.0	8.3	7.9	10.9	17.5	29.3	1.6
Mineral	0.0	17.7	15.5	10.5	8.2	5.3	12.1	8.9	8.8	8.2	4.6	0.0
Char	0.0	0.5	1.1	1.6	2.1	2.0	6.7	7.6	12.1	22.1	41.8	2.4

Figure 4:17: Association characteristics of Char900 (1mm particles)

To simplify the classification further, the individual association classes are grouped into four classes as shown in Table 4.11 (Falcon and Snyman, 1986). The groups are: (1) extraneous particles – mineral matter proportion exceeds 60 area-percentage. This group includes the association classes ranging from 0 to 35. This group is analogous to a minerite microlithotype group (2) Middling particles – the mineral matter proportion varies from 20 to 60 area-percentage. It includes the association classes ranging from 45 to 75. This group is analogous to a carbominerite microlithotype group. (3) Included particles – the mineral matter proportion is less than 20% area. It includes the 85 and 95 association classes. (4) Free particles – these are carbon-rich particles with no measured mineral inclusions. It includes the 100-association class. It is seen that the coal-char has a significantly high proportion of mineral-rich char particles with a lower proportion of carbon-rich, mineral free particles. It should be noted that 52% of the minerals in the Char900 occur as extraneous siltstone/mudstone and sandstone rock fragments and as coarse calcite, dolomite and pyrite-rich cleat fragments.

Table 4.11: Particle classification

Association Class	Particle	Mineral	Char
Extraneous	21.6	52.0	5.2
Middling	30.0	35.1	28.4
Included	46.8	12.9	63.9
Free	1.6	0.0	2.4
Total	100	100	100

4.4.4 Structural analysis

Since the chars were very dense, thus consisting of a large proportion of micro pores, measurements of structural properties were confined to BET adsorption measurements. Many investigators have used both nitrogen and carbon dioxide adsorption and it is not clear from the literature which gas is the most desirable (Schobert, 2006). Nitrogen adsorption has been used for chars with micropores, but with a high overall porosity (Liu et al., 2000a) derived from vitrinite-rich coals.

Adsorption isotherms obtained from the BET measurements with nitrogen for Char700 and Char900 are shown in Figure 4.18. It was not possible to obtain repeatable results for the raw coal, as it could not be degassed to a constant vacuum during the preparation period, which indicated a very slow release of volatiles associated with the coal. Degassing over a number of days was tried without success.

The isotherms in Figure 4.18 are characteristic of a combination of isotherms Class I (plateau behaviour) and IV (hysteresis behaviour) according to a classification given by Gregg and Sing (1982) and Brunauer *et al.* (1940), which indicates that the chars consist of micro- and mesopores. A pore size distribution calculated (BJH) from this measurement is non-uniform and repeatable results could not be obtained (because of the heterogeneous nature and mass of sample used), consequently it was difficult to quantify this characterisation for modeling purposes as done by other investigators (Liu *et al.*, 2000a). Results for Char900 have a slightly higher adsorption capacity, which could be attributed to slightly more thermal cracking at the higher charring temperature. This difference was, however, difficult to deduce from the photomicrographs shown in Section 4.4.2.5.

A complete summary of the BET analysis based on average properties is shown in Table 4.11. The results are most unusual with both chars having very low BET surface areas and porosities when compared to results obtained from vitrinite-rich coals which have typical values of 250 m^2/g and 82% respectively (Liu *et al.* 2000a).

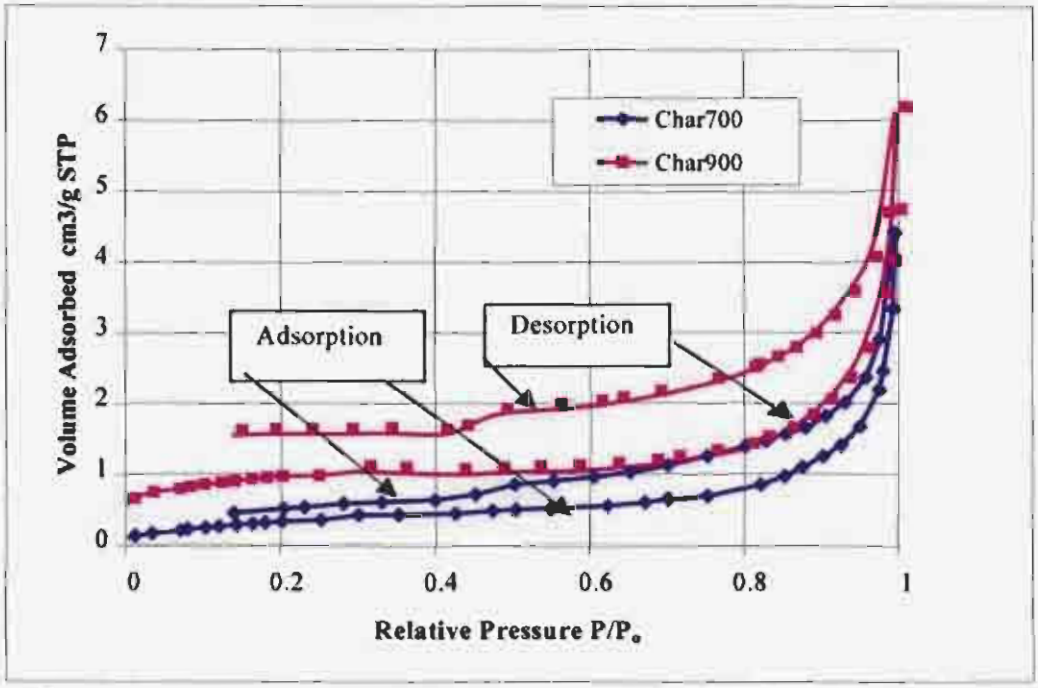

Figure 4.18: Adsorption isotherms for chars

Table 4.12: Adsorption results

Property	Char700	Char900
BET surface area (m^2g^{-1})	1.39	3.46
BJH Adsorption surface area (17< d_p <3000 Å) (m^2g^{-1})	1.41	1.51
BJH Desorption surface area (17< d_p <3000 Å) (m^2g^{-1})	2.13	2.25
Pore volume (cm^3g^{-1}) dp < 810	0.0034	0.0053
BJH Adsorption pore volume (17< d_p <3000 Å) (cm^3g^{-1})	0.0051	0.0087
BJH Desorption pore volume (17< d_p <3000 Å)(cm^3g^{-1})	0.0069	0.0080
Average pore diameter (Å) by BET	97.70	62.12
BJH Adsorption pore diameter (Å)	146.28	231.20
BJH Desorption pore diameter (Å)	129.52	142.54
*Total porosity, ε_o, (d_p< 810 Å)	0.007	0.0104

**Calculated from density (1.94g/cm³) measured by mercury porosimetry*

4.5 Summary of Results

The original coal possessed an ash content of 33.8%, a volatile matter content of 21.4% and total sulphur content of 1.67%, all on an air dried basis. The average vitrinite reflectance (rank) was 0.70%, which is not much different to results reported for different coal samples in the literature.

Petrographically, the mean vitrinite reflectance value of the parent coal was 0.70% of random reflectance (Medium Rank C).

The coal was high in total inertinite content (59% on a mineral matter included basis, mmb), and low in vitrinite (15% mmb).

In terms of the microlithotypes, the monomaceral vitrinite accounted for 7% of the coal, inertinite for 32%, while intermediate maceral/maceral mixtures accounted for 13%. Maceral/mineral associations represented 30% of the whole coal and mineral-rich particles 18%.

Charring at 700°C with nitrogen for one hour showed a modest reduction in volatile matter from 21.4 to 17.7%, no significant change in ash content and maceral proportion, and only a minor increase in the mean random reflectance of vitrinite (0.70 to 1.27%RoV).

In terms of char development, more than half of the pure vitrinite material and all the inertinite material remained the same in structure, colour and form as the parent coal. Thereby indicating that, with the exception of some incipient vitrinite-sourced "heated coal", no true chars developed and very little change took place during the charring process at 700°C for one hour. The one significant observation, however, was the increase in the abnormal condition of the coal, namely, there was a 25% increase in the proportion of extensively cracked and fissured coally particles (i.e. from 25% in the raw coal material to 50% in the char product), this condition being found predominantly in the inertodetritic association of macerals. Based upon previous experience, this notable structural change was attributed to thermal stress fracturing in specific association of macerals, with the low temperature forms being known as "passive deflagration" as opposed to the better known forms of high temperature thermal shattering, which has been described as "active deflagration".

Charring at 900°C for one hour, showed a dramatic series of changes relative to the 700°C charring, the volatile content was reduced from 17.7% to 7.2%. There was also a proportional rise in ash and carbon contents, the reflectance of vitrinite increased from 1.27% to 4.47% RoV. The bulk of the vitrinitic and related semi-reactive material had been transformed from normal raw coal forms into isotropic cokes and fine char networks and all the inertinitic-coally materials had increased in reflectance (but not in porosity) thus producing a product comprised predominantly of [mineral-free] dense and thick-walled chars (52%) and mineral-rich dense chars (31%). The reflectance scan of the entire sample (including both porous and dense chars) was found to be 4.49% RoV, i.e. virtually identical to that of the porous vitrinite-sourced materials.

The difference between the two chars prepared at the different temperatures was further noted in the shift in the ranges of reflectance classes for the whole sample scans. These moved from a range of 0.2-3.9% in the 700°C char to 2.3 to 6.9% in the 900°C char, with mean random values of 1.64 to 4.49%, respectively. The proportion of material that had undergone abnormal cracking and fissuring in the 700°C char remained the same in the 900°C char thereby indicating that all the material that was likely to thermally crack had done so early on in the temperature regimes.

Based upon the above, the conclusion was reached that little or no significant change took place in the coal during the 700°C charring preparation, even over a period of one hour, with the exception of an apparent increase in passive deflagration noted in one suite of maceral associations (inertodetrite). A far more significant change was noted when the coal was exposed to 900°C with notable devolatilisation and char formation. However, the char form was predominantly of a dense nature with extremely low porosity (possibly poor burn-out characteristics). The presence of deflagrating particles is, however, encouraging in that this condition will undoubtedly result in increased fines production and therefore far higher surface areas on which combustion can take place.

A high proportion (52%) of the minerals in the char sample prepared at 900°C occurs as extraneous siltstone/mudstone and as coarse to fine grained sandstone rock

fragments and as extraneous carbonate (calcite and dolomite) and pyrite cleat fragments. Only 12.9% of the minerals occur as fine intrusions in the carbon-rich matrix. Coarse quartz grains and cleat fragments can exceed sizes of 1mm. Pyrite rich inclusions can reach sizes of 410 microns. Carbon-rich mineral poor char particles with prominent coarse pores are not common and can be attributed to the presence of a high proportion of non-reactive inertinite macerals. Particles with varying proportions of included minerals can have a lower activity as a result of the included minerals acting as a heat sink. The presence of minerals in a particle could also be such as to ensure the retention of the particle shape and size during gasification and combustion.

The surface areas (1.4 to 3.5 m^2/g) and porosities (0.07 to 0 0.01) of the chars formed were exceedingly low, which indicated that the chars would have a very low initial reactivity and reaction rate. The structural parameter as defined for the random pore model (Bhatia and Perlmutter, 1980) calculated with the BET results, were found to be exceedingly large (close to 100), which was inconsistent with experimental results and much greater than values reported by other investigators for reaction controlled reactions.

CHAPTER 5 EXPERIMENTAL: GASIFICATION AND COMBUSTION

5.1 Introduction

In this Chapter a description of the experimental apparatus, methods and techniques is given. The experimental apparatus is described in detail in Section 5.2, while the specifications of the chemicals used are given in Section 5.3. The experimental procedures are given in Section 5.4 and the experimental programme is discussed in Section 5.5.

5.2 Experimental apparatus

A thermogravimetric analyser (TGA) was used for the determination of the reaction reactivity of the chars with respect to carbon dioxide-nitrogen and oxygen-nitrogen mixtures. The main advantages of the TGA are that:

(1) the mass of the char sample is continuously recorded during the reaction period, which enables instantaneous conversion levels and reaction rates to be calculated, which is most suitable for reaction rate modeling.

(2) Since the operation is differential, the concentration of the reacting gas at the gas-solid surface is very close to that of the feed gas composition and can be easily manipulated.

However, it is not possible to measure accurately the products formed as a result of the low conversion per pass. This apparatus has also been used with success by many other investigators for coal/char conversion studies (Johnson J.L., 1981&1979b, Schumacher *et al.*, 1986, Mühlen, H.J. and Sulima, 1986; Calo and Suuberg, 1999; Kajitani, 2006).

A schematic presentation of the apparatus is shown in Figure 5.1 and a photograph is also shown in Figure 5.2. The apparatus shown consists of a gas supply system, the TGA (reactor and microbalance), a pressure control system and a data acquisition interface.

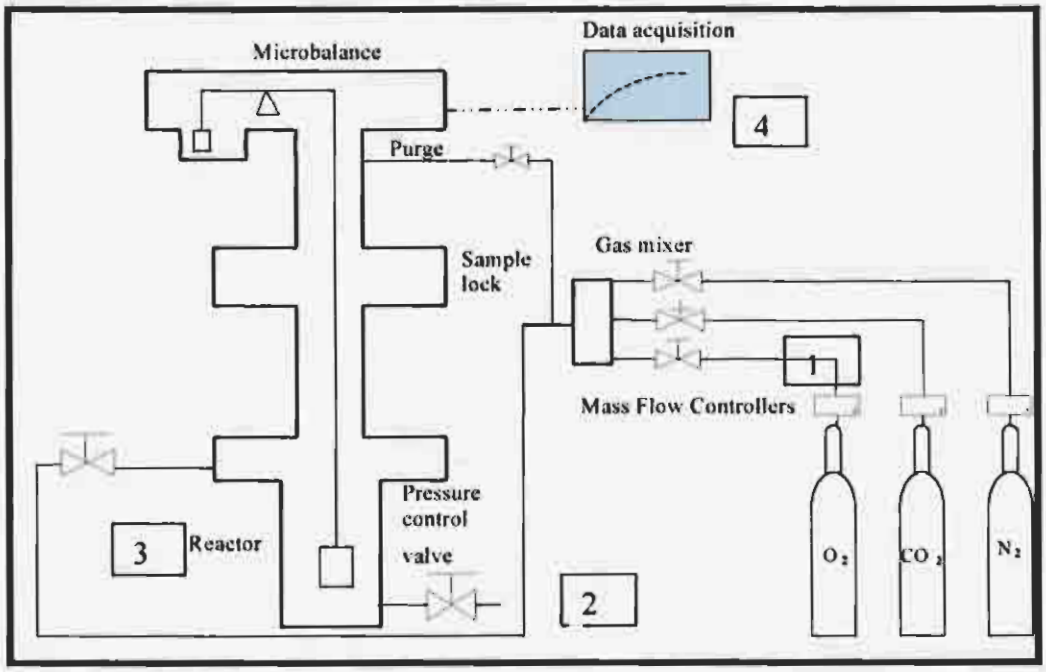

Figure 5.1 A Schematic representation of the apparatus

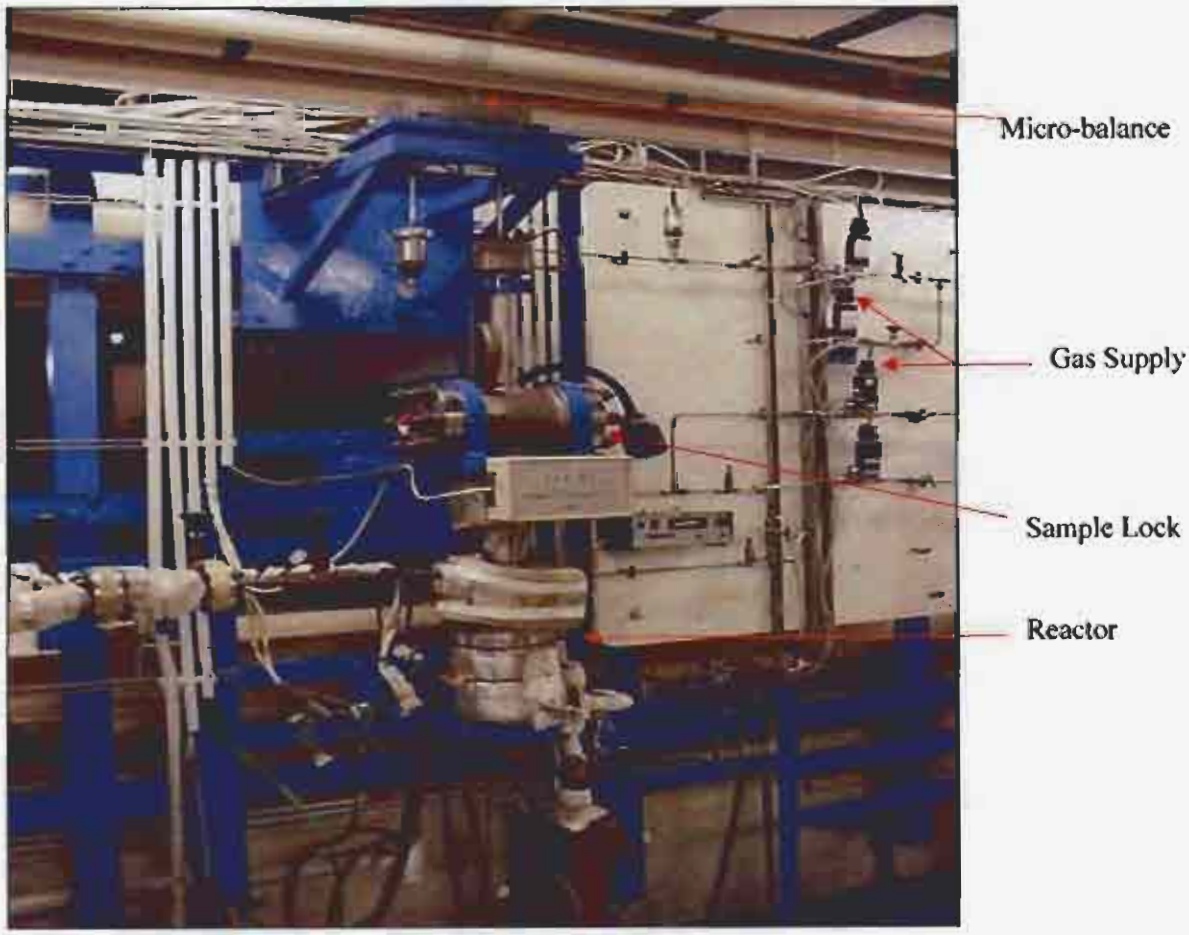

Figure 5.2: A photograph of the Thermogravimetric Analyse

5.2.1 Gas supply

The reaction gas is supplied through a series of interconnected stainless tubes. The gas supply unit allows the gas to be mixed to the desired compositions, which is achieved by setting the appropriate flow rates (with an error of ±0.35%) using three Brooks-5850 mass flow controller units.

5.2.2 Thermogravimetric Analyser -TGA

The TGA used is a Bergbau-Forshung GMBH7 model supplied by Deutsche Montan Technologie (DMT), Germany. This TGA can handle solid granules with diameters between 1 and 5mm and sample masses up to 2 grams at temperatures up to 1000°C and pressures up to 10 MPa. The apparatus was specially designed for the determination of the reactivity of solid fuels such as coal and char under varied oxidation and gasification conditions. The instrument can be operated isothermally or the temperature can be increased linearly at a desired heating rate varying between 1 and 100°C min^{-1}. The thermogravimetric analyser consists of two main parts, the reactor and the microbalance, which is shown in Figure 5.1.

The principle behind the operation of this apparatus is the same as that for any type of TGA and consists of the continuous measurement of the change of the loss of mass under isothermal or non-isothermal conditions. This reactor operates as a differential reactor with a low gas conversion, thus ensuring that there is a constant gas atmosphere and overcoming the effect of combustion products on conversion rate. A miniature basket made of platinum gauze is suspended inside a heated tube reactor the temperature of which is accurately controlled (±2°C). The sample basket is suspended with a silver and inco-alloy 800 chain from a highly accurate microbalance linked to the electronic data logging and video display. The basket is lowered by a winch system designed in such a way that there is no swinging of the basket and potential effects of thermal radiation are minimised. For the temperature measurement, a K-type thermocouple is used. For accurate temperature measurement, it is located three millimetres below the sample holder in such a way that it does not disturb the balance signal.

The balance system consists of a highly accurate (error of ≤ 1%) Sartorius® micro-balance model M25D. It is enclosed in steel casing to avoid disturbance from the

external environment. A digital balance electronics system provides for adjustable damping of the signal and allows sampling rates of up to 10 readings per second. This allows accurate measurement of fast weight changes in flowing gas. To avoid damage of the balance from corrosive reaction gases and products, a cold nitrogen/oxygen gas mixture in the case of combustion and carbon dioxide/nitrogen mixture for gasification continuously purges the balance during the reaction zone.

5.2.3 Pressure control unit

The pressure is electronically controlled by two electric motor actuators (Kämmer Ventile Valves, Type 20157, 50 Series). Initially, the –Kv 0.025 valve is used for high flow control, and the pressure is finally fine-tuned with the –Kv 0.00004 valve. The pressure can be varied between ambient and 100 bar with a precision of ±2%.

5.2.4 Data acquisition interface

A computerised data acquisition and process control system allows for real time recording of time, temperature, pressure, gas flow rates and sample mass. All relevant test parameters are presented on the monitor and recorded into an electronic file during the course of the experiment.

5.3. Chemicals

The gasses used in the combustion and gasification experiments were supplied by African Oxygen (Afrox) South Africa, while the coal was supplied by Eskom. Specifications of the gases are given in Table 5.1, and a detailed characterisation of the coal is given in Chapter 4. The char was prepared as given in Section 4.3.1, and a final charring temperature of 700 or 900°C was used.

Table 5.1: Specifications of gasses used in experimental work

Gas	Grade	Purity
Carbon dioxide	Industrial Purity Grade	>99.99%
Nitrogen	Ultra High Purity Grade	>99.999%
Oxygen	Industrial Purity Grade	>99.99%

5.4 Experimental procedures

From the char batches prepared as described in Section 4.3.1, 40-200mg of 1 or 3mm char particles were loaded into the basket. After insertion of the basket in the reaction chamber the system was sealed and a cold purge gas (nitrogen) allowed to flow through the apparatus to flushed out remaining oxygen

The sample-loaded basket was kept out of the reaction zone (upper section) while the reactor (lower section) was being heated to reaction temperature under the flow of nitrogen. On attaining the reaction temperature, the data logging computer programme was started and the basket was lowered into the reactor and kept under nitrogen (till constant mass attained) to passivate the char. There was then a switch over to the reactant gas which was preset at a total flow rate of 1800ml min^{-1}(STP), which was the setting used for all experiments.

For the elevated pressure experiments the sample-loaded basket was raised after passivation with nitrogen. The reactor was then pressurised by closing the outlet valve. On attaining the required pressure, the computer pressure control system was activated and the sample-loaded basket lowered into the high temperature reactor region and the experiment continued as described above. The reaction data, temperature, mass; pressure and time were logged (on-line) by the data acquisition system and at the end of each experiment the data was retrieved into an Excel® file for data processing.

The three main parameters; temperature, pressure and reaction gas concentration under which investigations were carried out were varied as shown in Table 5.2. The results were processed as presented in Chapters 6 and 7 involving the gasification and combustion experimental results respectively. Experiments were also carried out to determine the reproducibility of the final result and an error of ±5% associated with the final mass was estimated.

5.5 Experimental programme

Experiments with the thermogravimetric analyser were carried out in order to achieve the objectives (items 2 and 3) of the investigation as listed in Section 1.2 and consisted of gasification and combustion experiments.

Gasification: This involved experiments with carbon dioxide/nitrogen mixture in order to (1) assess the effect of operating conditions on char activity, and (2) evaluate a suitable model to establish the controlling reaction regime. For this purpose, a suitable char preparation was chosen based on a detailed characterisation.

Combustion: This involved experiments with oxygen/nitrogen mixtures in order to: (1) determine the effect of charring temperature on char activity to illustrate the importance of char properties for an overall reaction kinetics study; (2) assess the effect of operating conditions and particle size on char activity; (3) evaluate a suitable reaction rate model in order to establish the reaction rate controlling regime (s). A suitable char preparation based on char characteristics was also necessary.

In order to achieve the above, the experiments listed in Table 5.2 were carried out and are motivated in more detail in the relevant chapters describing gasification (Chapter 6) and combustion (Chapter 7) with the accompanying results.

Table 5.2: Reaction Conditions for char gasification and combustion experiments

Char Type	**Reaction**	**Pressure kPa**	**Particle Size mm**	**CO_2 or O_2 Composition mole %**	**Temperatures °C**
Char900	Gasification	87.5	1	40	900
	Gasification		1	60	875, 900
	Gasification		1	80, 100	850,863,875,888,900
	Gasification	287.5	1	20,40,60,80,100	850,875,900
Char900	Combustion	87.5, 287.5	1, 3	5,10,15,20,40	700,750,800,850,900
	Combustion	87.5, 287.5	1, 3	20	450,500,600,
Char700	Combustion	87.5	1, 3	20	900

CHAPTER 6 RESULTS AND DISCUSSION: GASIFICATION

6.1 Introduction

The experimental results and the modelling of the overall reaction rate involving the gasification of chars with carbon dioxide-nitrogen mixtures are presented, (also in Appendix D). The experiments were all carried out in a thermogravimetric analyser (Section 5.2 using the 1mm char prepared at 900°C (Section 4.3.1).

The objective of this chapter is to show: (1) the relative effect and order of magnitude of the operating conditions such as gas composition (carbon dioxide concentration), temperature and pressure on the conversion of carbon; (2) to demonstrate the validity and applicability of a suitable model; and (3) to provide quantitative information (parameters) concerning the reactivity behaviour of the char in the presence of a very slow intrinsic reaction, which was required for the development of combustion kinetics (fast intrinsic reaction).

A summary of the properties of the char prepared at 900°C and the normalisation of experimental results is presented in Section 6.2, with the effect of the operating variables given in Section 6.3, which includes carbon dioxide composition, temperature and pressure. The carbon conversion results are modelled with the random pore model (as described in Section 3.3.1) in Section 6.4 and the conclusions are given in Section 6.5.

6.2 Properties of char and normalisation of experimental results

Properties: The different petrographic properties of chars prepared at 900°C (Char900) are discussed in Section 4.4, which include mainly reflectance (vitrinite and total macerals) and carbon form compositions. Char900 contained a large fraction of dense char with a higher reflectance and had a very low pore volume and consequently a low porosity, which could be attributed mainly to the devolatilisation of the vitrinite-containing maceral intermediates, present in small quantities and to thermal cracking. The combustion properties of Char900 are lower than that of Char700 as shown and discussed in Section 7.2. Since the gasification experiments were carried out at temperatures less than 900°C, the char prepared at 900°C was used

for all gasification experiments, similar to the combustion experiments described in Section 7.3.

Normalisation of experimental results: A typical experimental result obtained from the Thermogravimetric analyser at 900 °C, 87.5 kPa and 100% carbon dioxide is given in Figure 6.1, where both the mass of the char sample and the reaction temperature are given as a function of time. The mass initially decreases rapidly, until about 50% of the carbon is consumed. After this period, the mass decrease is slightly retarded. Finally, an equilibrium stage is reached where no significant change of mass is observed, which indicates that the reactive material (carbon compounds) in the char sample is depleted. The final mass value, for all experiments, was found to be 50(±3)% of the initial char mass, which is in agreement with the ash percentage (proximate analysis) of the char (Section 4.2.1), showing that all the reactive carbon is converted. The reaction times are in the order of hours, which are much slower (factor of 100) than the combustion experiments that are presented in Section 7.3.

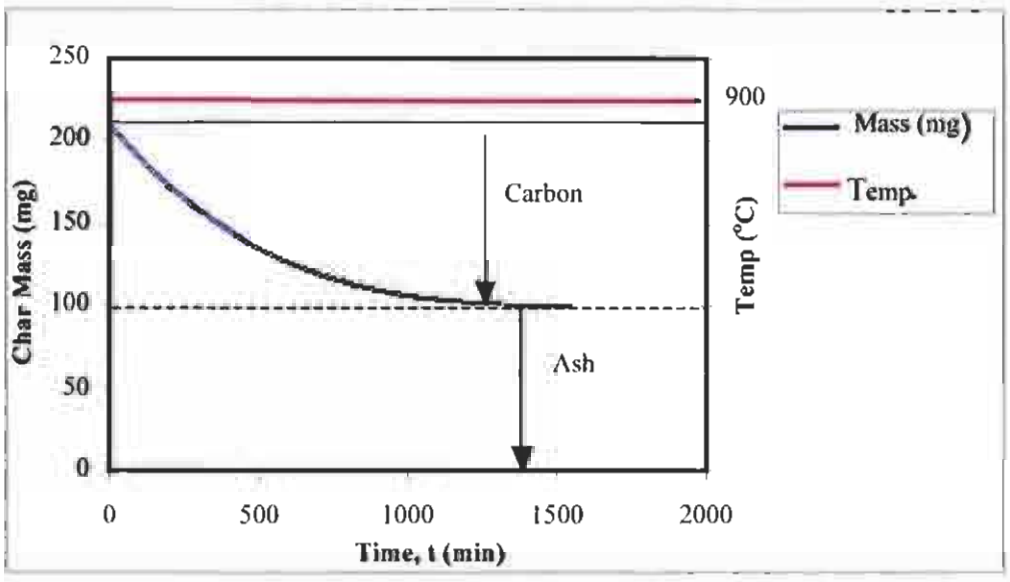

Figure 6.1: Isothermal gasification of coal char at 900°C in 100% CO_2 at 87.5kPa

It is convenient to express the carbon conversion variation with time on an ash free basis so that the mass loss is due to conversion of only carbon compounds. This approach has been used successfully by nearly all research concerning investigations involving char kinetics. Results from this calculation enable meaningful, quantitative comparisons of the conversion rates of the carbon containing compounds and the

modelling thereof. The effect of the ash is considered to contribute to structural properties (porosity and surface area) and catalytic activity as a result of included minerals in carbon/mineral associations, which can vary with particle size (Section 2.2.2.1).

The experimental results involving gasification (and combustion) were normalised according to:

$$X = \frac{m_0 - m_t}{m_0 - m_{ASH}} \qquad (6.1)$$

A typical normalised result derived from the experimental results is given in Figure 6.2. Throughout this investigation, 20-40 experimental points were used, which was considered accurate enough for all interpretations and modelling. It should be noted that the mass of ash, m_{ASH} was determined for each experiment.

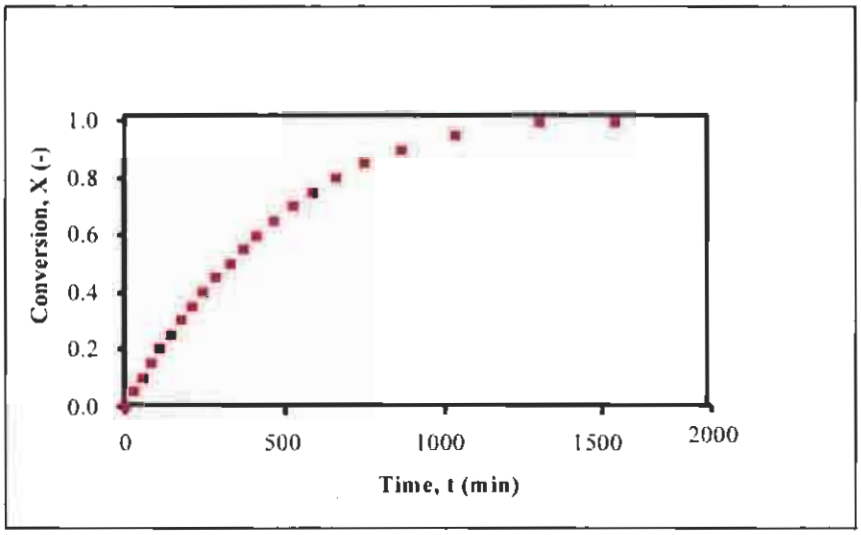

Figure 6.2: Conversion of char at 900°C, 87.5kPa and 100% CO_2

6.3 Effect of operating conditions on char gasification reactivity

Carbon dioxide composition: The effect of carbon dioxide concentration (20-100% mole) on the gasification conversion is given in Figures 6.3 and 6.4 for a total pressure of 87.5 and 287.5 kPa, respectively. From these Figures, it can be seen that the carbon conversion rate increases with increasing carbon dioxide composition as expected. The results at 287.5 kPa, however, appear to be much closer at the high concentrations. Results at different temperatures and pressures showed similar trends

and are given in Appendix D1 and D2. The results obtained are in agreement with other published results (Ye *et al.*, 1998; Ahn *et al.*, 2001 and Murillo *et al.*, 2006).

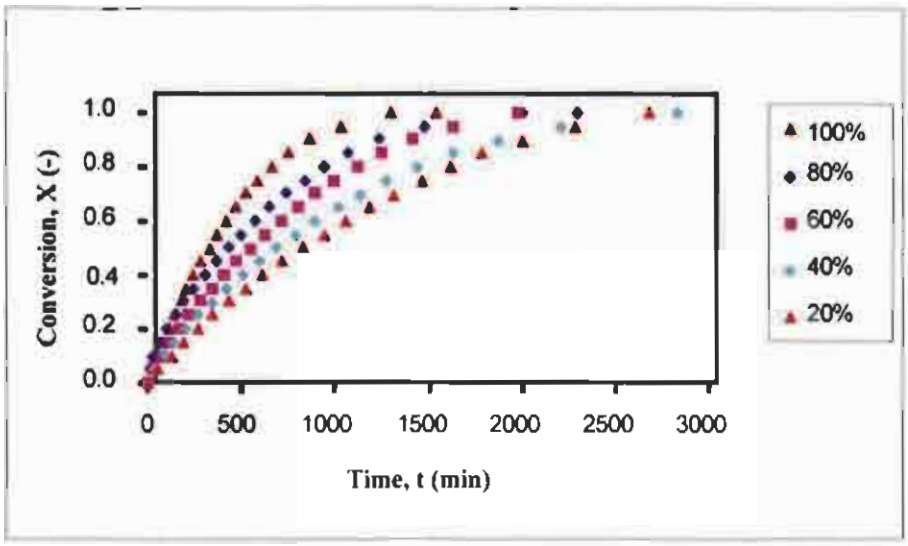

Figure 6.3: Effect of CO_2 concentration on gasification rate at 900°C at 87.5kPa

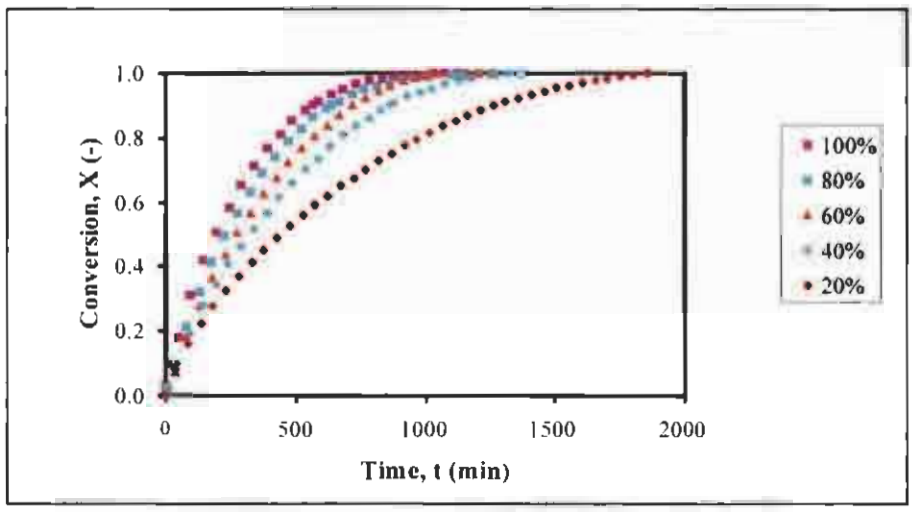

Figure 6.4: Effect of CO_2 concentration on gasification rate at 900°C at 287.5kPa

Temperature: In Figures 6.5 and 6.6, the effect of temperature on the gasification conversion is given at 87.5 and 287.5 kPa, respectively. In both cases, the rate of reaction was found to increase with temperature. The relative increase in carbon conversion (reaction rate) with increasing temperature according to Arrhenius type kinetics is evident which is different to combustion behaviour with the same char over the same temperature range (Section 7.3). Similar reaction behaviour was observed in

all results for different carbon dioxide concentration and the results are shown in Appendices D3 and D4. Other researchers, including Ye *et al.* (1998), Moors (1998), Shufen and Ruizheng (1994) and Lu and Do (1992), also reported similar results.

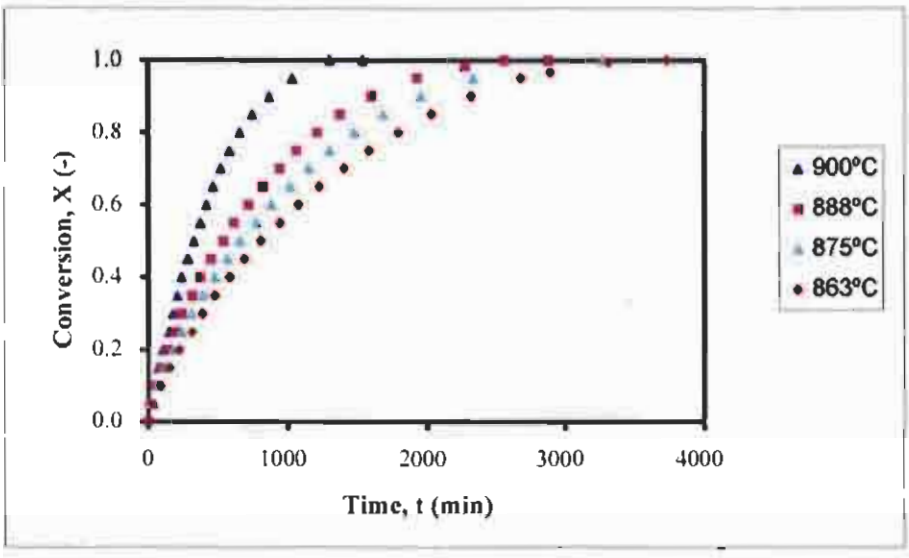

Figure 6.5: Effect of Temperature on gasification rate at 87.5kPa and 100% CO_2

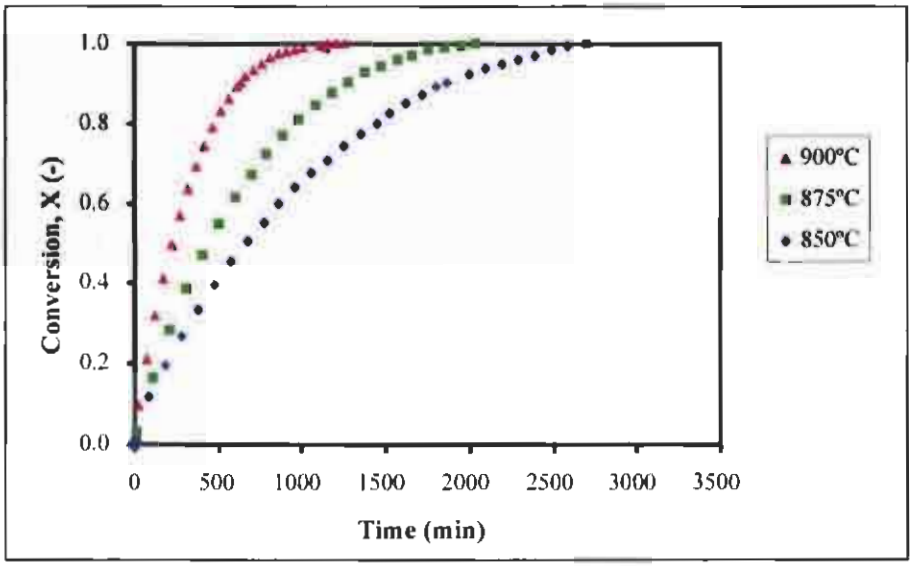

Figure 6.6: Effect of Temperature on gasification rate at 287.5kPa and 100% CO_2

Pressure: Gasification experiments at different pressures were conducted at different temperatures and carbon dioxide partial pressures. Results of comparative experiments of gasification activity of coal chars are shown in Figures 6.7 and 6.8. In both cases, there is a significant decrease in reaction time with an increase in pressure. These results inidicate that an increase in pressure results in an increase in the

conversion rate of the char, which is also in agreement with results reported by Moors (1998), Messenbock *et al.* (1999) and Ahn *et al.* (2001).

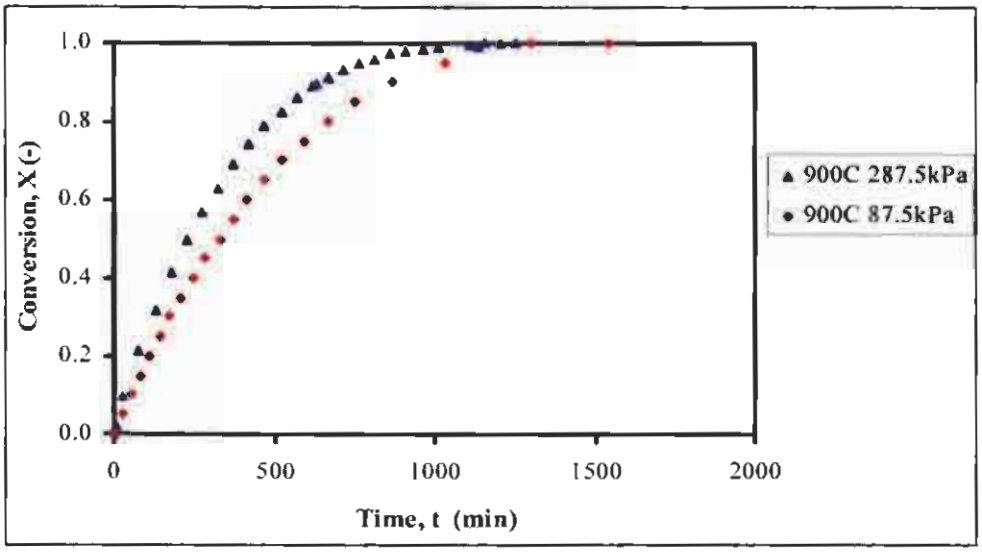

Figure 6.7: Effect of Pressure on Gasification at 900°C and 100% CO_2

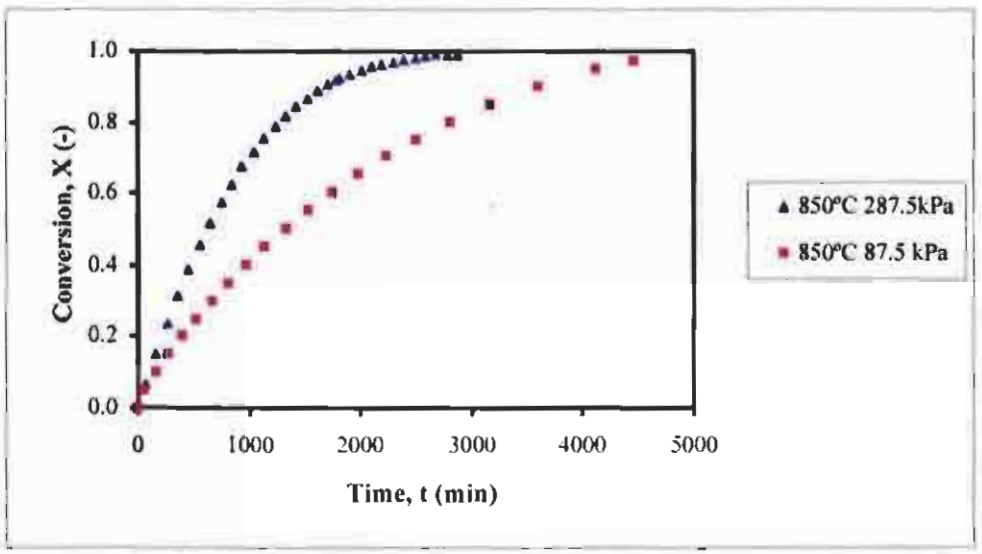

Figure 6.8: Effect of Pressure on Gasification at 850°C and 80% CO_2

The results for different reaction conditions to show the effect of total pressure, are given in Appendix D5, and show similar trends displayed in Figures 6.7 and 6.8

6.4 Modeling

6.4.1 Experimental results

The experimental results used for the evaluation of the model and subsequent determination of the parameters were done under reaction conditions given in Table 6.1. These conditions were chosen to correspond to an intermediate temperature range (< 900°C) and at atmospheric and an elevated pressure suitable for fluidised bed gasification.

Table 6.1: Details of experiments used for model evaluation for gasification

Reaction variable	Conditions
Temperatures (°C)	850, 863, 875, 888 and 900
Pressures (kPa)	87.5 and 287.5
Gas composition mole % Carbon dioxide	20, 40, 60, 80 and 100
Coal chars	Prepared at 900°C
Particle diameter (mm)	1
Volumetric gas flow rate (m^3min^{-1})	$1.8 \cdot 10^{-3}$
Mass of char sample (mg)	200(±2)

6.4.2 Validity of chemical reaction controlled regime using reduced time result

The models described in Sections 3.3.1 and 3.3.2 were evaluated against experimental results according to the relevant procedures and it was found that the random pore model without pore diffusion was applicable. This was shown to be valid for experimental results consisting of plots of (1) carbon conversion versus the reduced time parameter, which is discussed in this section. This evaluation is actually the validation of the structural model; (2) carbon conversion versus real time discussed in Section 6.4.4.3. Both these calculations involved a regression procedure with the relevant parameters as a variable parameter.

Structural model validation and determination of structural parameter: For the procedure using the reduced time plot, that is $t/t_{0.9}$ Equation (3.9), the structural parameter together with the evaluation of the random pore model was calculated by regression with the use of experimental results at different operating conditions. The

comparison of the final model result and the experimental results are shown in Figures 6.9 and 6.10 at 87.5 kPa and 287.5 kPa, respectively. The agreement between the results is considered good within the limits of the errors associated with the experiments. The structural parameter (ψ) was found to be 1.04 ($\pm$ 0.34) and is independent of pressure, gas composition or temperature as expected. This value corresponds to a gasification reaction during which there is a decreasing surface area, which is attributed to essentially pore coalescence (Bhatia and Perlmutter, 1980). Thus, the carbon dioxide reaction is kinetically controlled, even at 900°C, according to the random pore model despite the low porosity of the char.

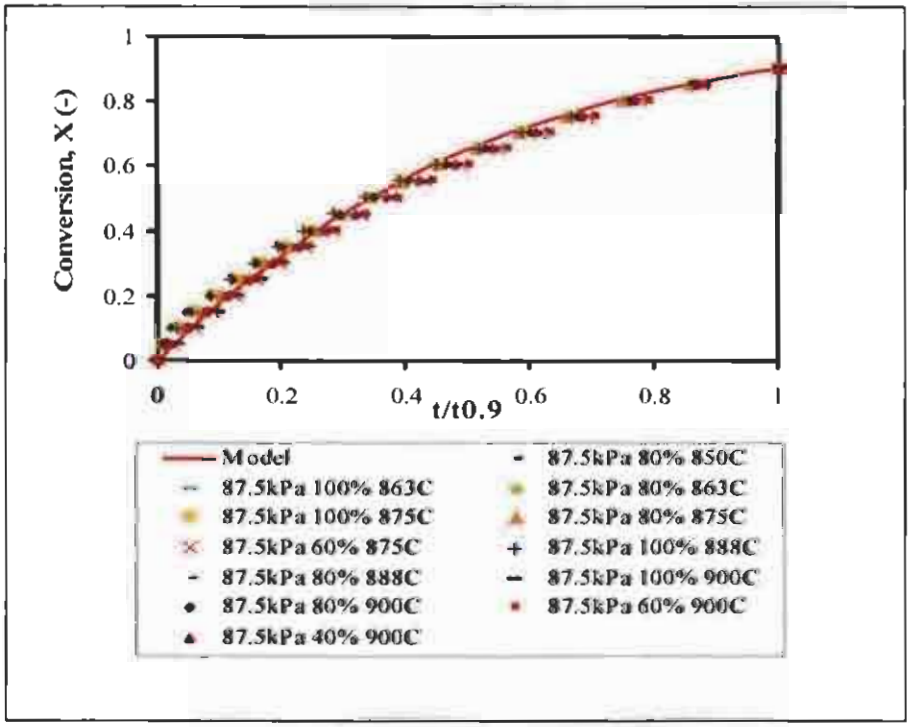

Figure 6.9: Comparison of gasification experimental and model results at 87.5 kPa.

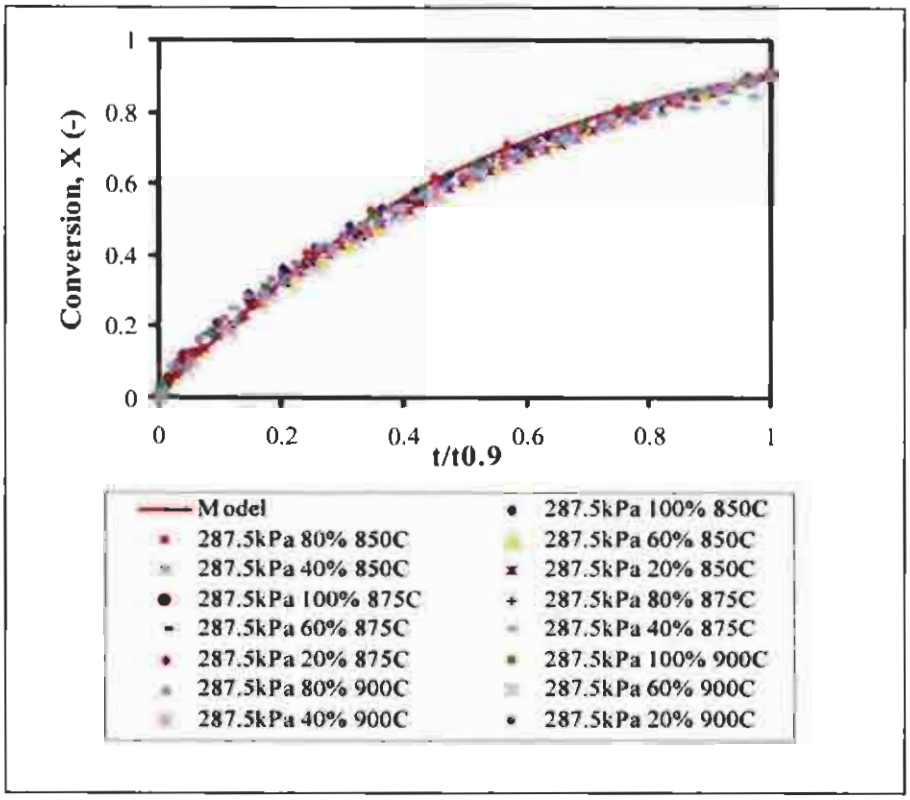

Figure 6.10: Comparison of gasification experimental and model results at 287.5 kPa.

6.4.3. Determination of intrinsic reaction rate constants

The intrinsic kinetic parameters were determined and were also to be used to validate the model (Section 6.4.4). This consisted of the determination of the time factor parameter, t_f, for each experiment, followed by the calculation of the relevant intrinsic parameters, consisting of the order of reaction with respect to carbon dioxide partial pressure (n), the activation energy (E) and the pre-exponential factor (k'_{so}), using the nth order power rate law and the Arrhenius equation (Section 3.3.1.2)

Time factor (t_f): Using Equation (3.8), the time scale parameter (t_f) was evaluated by regression for each experiment, with the structural parameter $\psi = 1.04$ as determined in Section 6.4.2. The calculated values are reported in Table 6.2 with final comparisons (experimental and model) having a correlation coefficient of the order of 0.99.

Table 6.2: Values for time factor (t_f) at 87.5kPa and 287.5kPa

	87.5 kPa		**287.5 kPa**	
Temp.	**%CO_2**	**t_f min^{-1}**	**%CO_2**	**t_f min^{-1}**
850°C	20		20	$5.37 \cdot 10^{-4}$
	40		40	$6.18 \cdot 10^{-4}$
	60		60	$7.83 \cdot 10^{-4}$
	80	$4.53 \cdot 10^{-4}$	80	$8.79 \cdot 10^{-4}$
	100		100	$9.59 \cdot 10^{-4}$
863°C	80	$5.95 \cdot 10^{-4}$		
	100	$7.26 \cdot 10^{-4}$		
875°C	20	$4.20 \cdot 10^{-4}$	20	$6.28 \cdot 10^{-4}$
	40	$5.09 \cdot 10^{-4}$	40	$8.31 \cdot 10^{-4}$
	60	$6.57 \cdot 10^{-4}$	60	$1.21 \cdot 10^{-3}$
	80	$8.18 \cdot 10^{-4}$	80	$1.31 \cdot 10^{-3}$
	100	$8.86 \cdot 10^{-4}$	100	$1.49 \cdot 10^{-3}$
888°C	80	$9.34 \cdot 10^{-4}$		
	100	$1.09 \cdot 10^{-3}$		
900°C	20	$7.43 \cdot 10^{-4}$	20	$1.30 \cdot 10^{-3}$
	40	$8.72 \cdot 10^{-4}$	40	$1.83 \cdot 10^{-3}$
	60	$1.10 \cdot 10^{-3}$	60	$2.17 \cdot 10^{-3}$
	80	$1.38 \cdot 10^{-3}$	80	$2.75 \cdot 10^{-3}$
	100	$1.84 \cdot 10^{-3}$	100	$2.97 \cdot 10^{-3}$

From this Table it can be seen that the time factor increased with an increase in temperature, partial pressure and total pressure as expected.

Partial pressure dependency (n): The reaction order with respect to carbon dioxide partial pressure was obtained with Equation (3.11), by plotting $\ln(t_f)$ as a function of $\ln(P_{CO2})$ for different temperatures and pressures. These results for total pressures of 87.5 and 287.5 are given in Figure 6.11 (more figures given in Appendix D6). It is clear that the order is independent of total pressure.

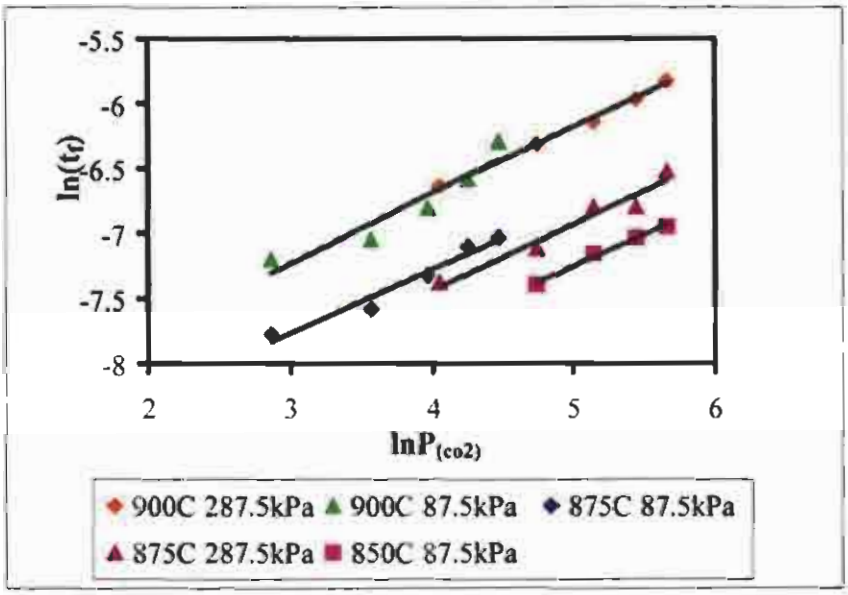

Figure 6.11: Determination of CO_2 gasification reaction order

The partial pressure dependence was obtained directly from the slope of the lines and the results are given in Table 6.3. From this table, it can be seen that the order with respect to carbon dioxide partial pressure is 0.50 (±0.05) and that correlation coefficients greater than 0.95 were obtained. The value is in agreement with Kajitani *et al.* (2006), who found values between 0.43 and 0.56 and Kasoka *et al.* (1985), with a reaction order of 0.5 from a modified volume reaction model. However, Dutta *et al.* (1977) found that the reaction order converges to zero at high pressure (1.5 MPa) and that at atmospheric pressures n was equal to 1.0, which does not agree with results obtained in this investigation. The effect of pressure on the reaction order is seen to be insignificant over the relatively low pressure range used.

Table 6.3: Order of reaction values at different temperatures and pressures

Temperature °C	Pressure kPa	Order of reaction	Correlation Co-efficient
875	87.5	0.46	0.9628
900	87.5	0.54	0.8982
850	287.5	0.48	0.9889
875	287.5	0.51	0.9532
900	287.5	0.50	0.9957

Activation Energy: The activation energy was determined by using Equation (3.11), which consisted of plotting $\ln(t_r)$ against the reciprocal temperature, at constant partial pressures of carbon dioxide. These results are given in Figures 6.12 and 6.13 for total pressures of 87.5 and 287.5 kPa respectively (see also Appendix D7). The activation energy was subsequently determined from the slope of these lines and the results are presented in Table 6.4 with correlation coefficients greater than 0.87.

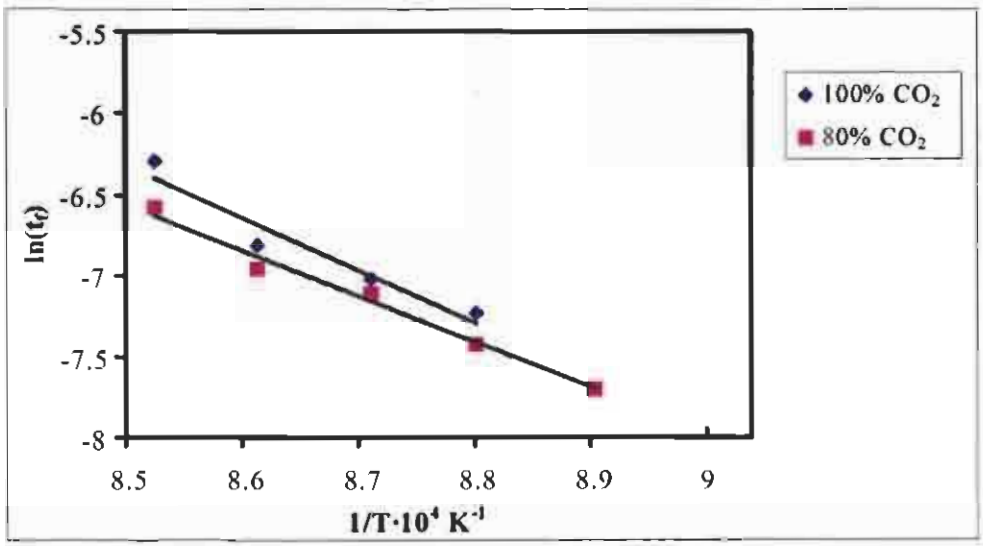

Figure 6.12: Apparent activation energy of CO_2 gasification at 87.5kPa

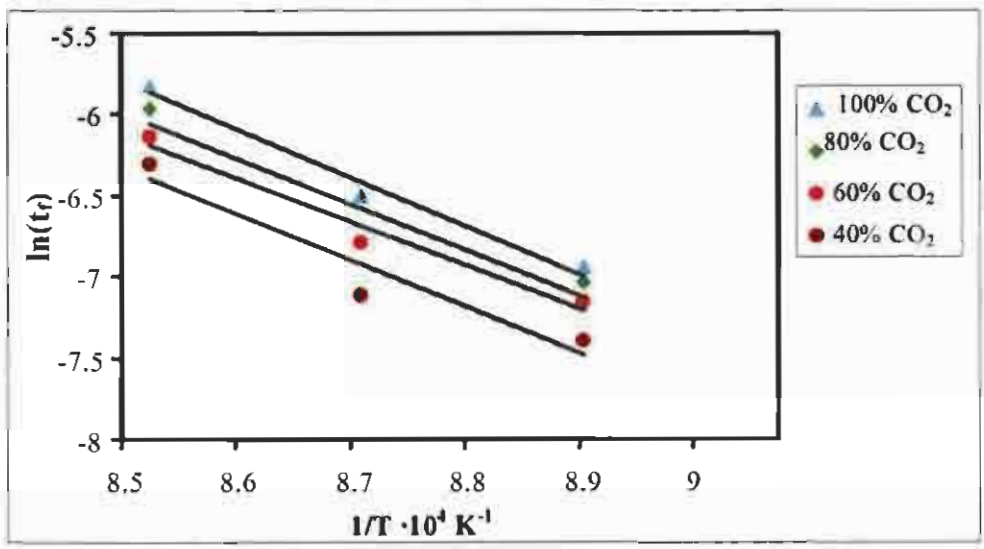

Figure 6.13: Apparent activation energy of CO_2 gasification at 287.5kPa

Table 6.4: Activation energy values obtained at 87.5 and 287.5kPa

$[CO_2]$%	Pressure kPa	E $kJmol^{-1}$	Correlation Co-efficient
100	87.5	266	0.9277
80	87.5	236	0.9862
100	287.5	247	0.9808
80	287.5	234	0.9067
60	287.5	223	0.9670
40	287.5	237	0.9178
20	287.5	192	0.8696

From Table 6.4 it can be seen that the activation energy does not vary significantly with the carbon dioxide concentration and an average value of 229(±37) $kJmol^{-1}$ is obtained. The pre-exponential factor can be obtained from the intercept of Figures 6.11 and 6.12 and an average value of 9.6 $(\pm 2)\cdot 10^{8}$ $s^{-1}kPa^{-1}$ was determined. A comparison with other intrinsic kinetic parameters for the gasification of coal/char is given in Table 6.5 and it can be seen that the determined activation energy is in the range of values obtained from literature. It can also be seen that the activation energy is relatively high, which could be explained by the relatively high inertinite content of the coal, this however needs to be examined further with chars derived from different inertinite rich coal sample. Due to the relatively high activation energy, a catalytic effect of the high ash content could not be observed.

Table 6.5: Comparison of reaction kinetics constants with values reported from literature

Reference	Char Origin	E kJmol^{-1}	Pre-exponential factor/ s^{-1}	n
This Investigation	Coal AR	192-266	$9.60 \cdot 10^{8}$	0.5
Kajitani *et al.* (2006)	Coal	240-280	$6.59 \cdot 10^{8}$	0.43
Sinag *et. al.* (2003)	Coal	128-146		-
Marquez *et al.* (2002)	Coal	176-248		-
Fu, W.B. Wang (2001)	Coal	245	$1.18 \cdot 10^{7}$	0.85
Lu and Do (1992)	Coal	199		-
Murillo *et al.* (2006)	Coal	204-212	$6.17 \cdot 10^{6}$	0.86
Kwon *et al.* (1988)	Coal	151	-	1
Kasaoka *et. al.* (1985)	Coal	196	-	0.5
Njapha (2003)	Coal	136	$8.2 \cdot 10^{2}$	

6.4.4 Validity of Model and Associated Parameters

The determined intrinsic kinetic parameters for the carbon dioxide gasification of the char are summarised in Table 6.6 and are used to predict the experimental results with the random pore model,(Equation(3.8)).

Table 6.6: Intrinsic reaction rate parameters of carbon dioxide gasification

Kinetic Parameter	Calculated Value
Activation energy, E	229 (±37) kJ mol^{-1}
Pre-exponential factor (lumped), k_{so}	$9.6 \cdot 10^{8}$(±2) s^{-1}kPa^{-1}
Partial pressure dependency, n	0.50(±0.05)
Structural parameter, ψ	1.04(±0.39)

The model and experimental results at 850°C and 20-mole % carbon dioxide for a pressure of 87.5 and 287.5 kPa are given in Figure 6.14, which clearly illustrates the validity of the random pore model and the associated parameters.

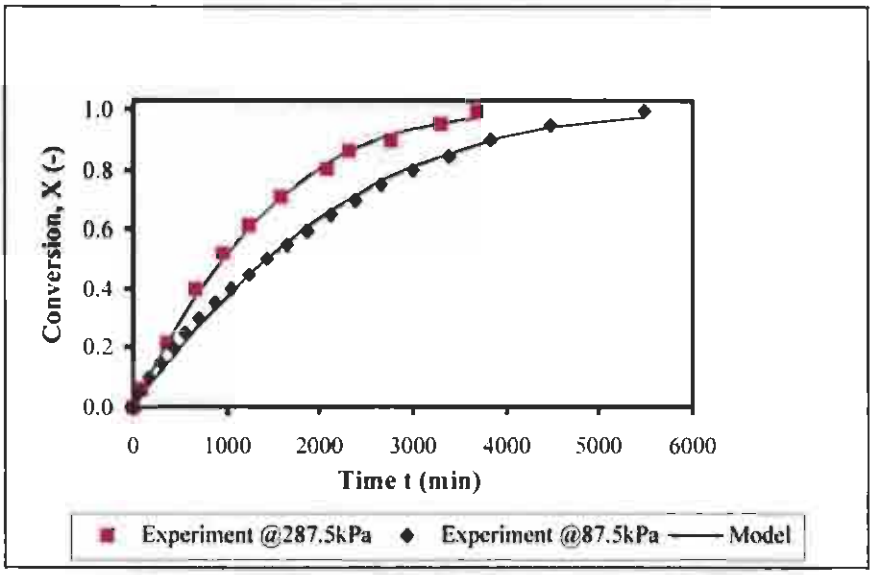

Figure 6.14: Random pore model for char gasification in 20-mole% CO_2 at 850°C

The model was also tested with results at 87.5 and 287.5kPa under various temperature conditions and results are shown in Figures 6.15 and 6.16 at the two respective pressures at a carbon dioxide partial pressure of 80%. Results for different carbon dioxide concentrations are also given in Appendix D8.

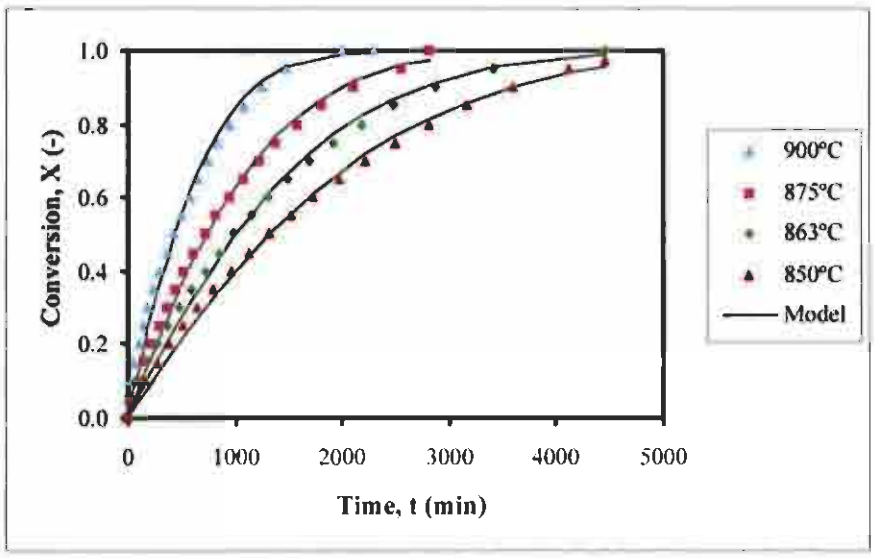

Figure 6.15: Random pore model for char at 87.5kPa and 80-mole % CO_2

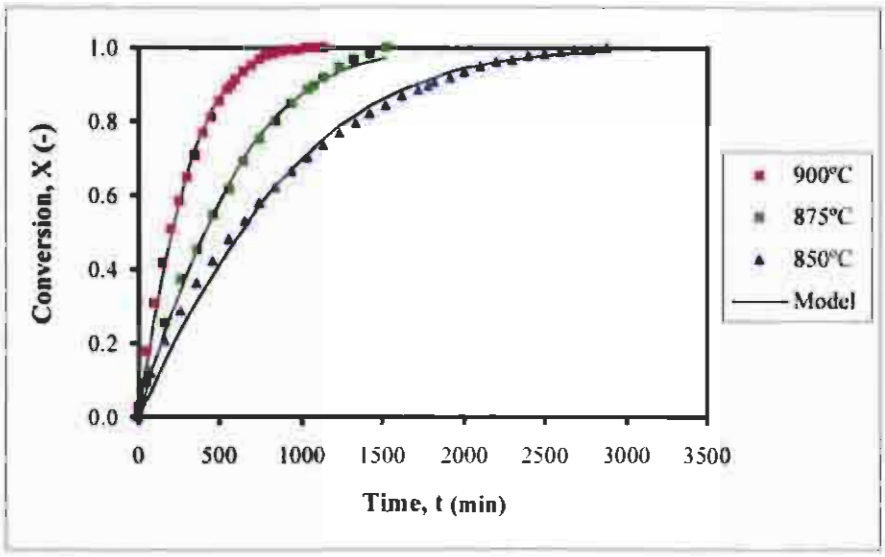

Figure 6.16: Random pore model for char at 287.5kPa and 80-mole% CO_2

Another illustration of the accuracy of the model and the determined kinetic parameters is shown on a parity plot of all the results as shown in Figure 6.17. The agreement is indeed satisfactory.

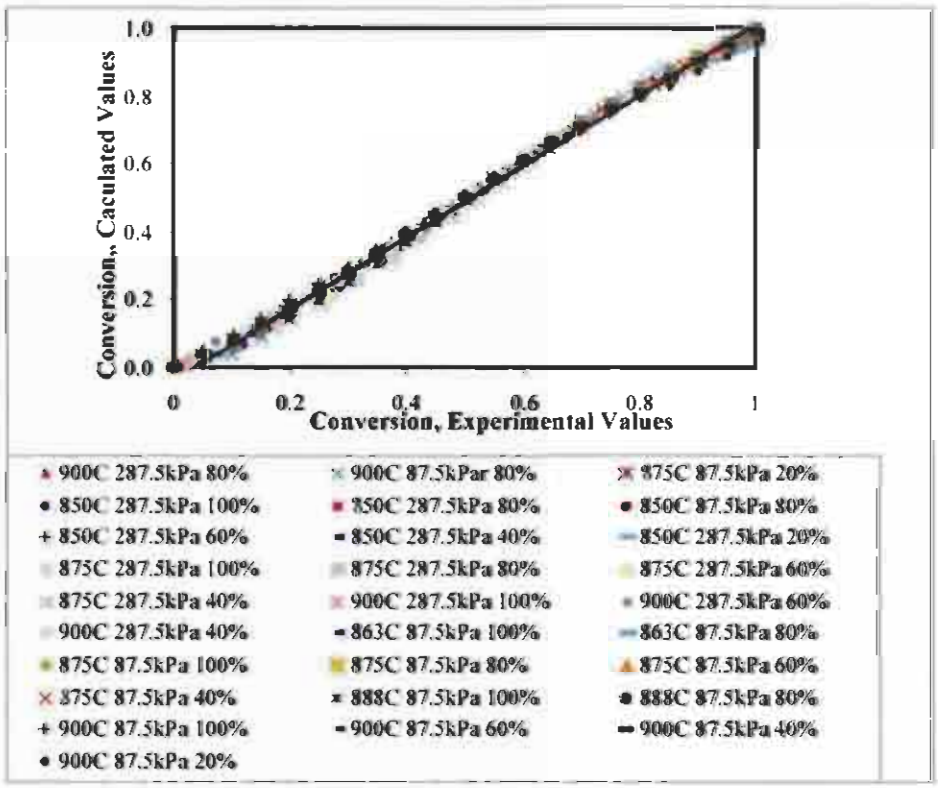

Figure 6.17: Comparison between experimental and model gasification results

6.5 Conclusions

The carbon dioxide gasification of a high-ash and high inertinite char was studied in the temperatures range between 850 and 900°C, carbon dioxide concentration between 20 and 100-mole % at an absolute pressure of 87.5 and 287.5 kPa with 1mm diameter char particles. Within this experimental range, it was found that the reaction rate increases with increasing temperature, increasing pressure and increasing carbon dioxide concentration. The results are consistent with carbon dioxide gasification literature.

The char conversion kinetics could well be described with the random pore model in the absence of diffusion limitation with a structural parameter, ψ, and equal to 1.04. The structural parameter was determined by a regression technique using a reduced time parameter, which eliminates the effect of intrinsic reaction rate kinetics.

The intrinsic kinetics could be accurately described with a nth order power law in combination with the Arrhenius equation and an order in carbon dioxide of 0.5, an activation energy of 229 $kJmol^{-1}$, and a pre-exponential factor of $9.6 \cdot 10^8$ $s^{-1}kPa^{-1}$ were determined. The activation energy is relatively high which could be attributed to the high inertinite content of the coal. Although the ash content was high, no significant catalytic effect of the ash could be observed.

CHAPTER 7: RESULTS AND DISCUSSION: COMBUSTION

7.1 Introduction

The experimental results and the modeling of the overall reaction rate involving the combustion of chars with oxygen-nitrogen mixtures are presented (also in Appendix E). The experiments were all carried out in a thermogravimetric analyser, (Section 5.2) using char prepared according to a procedure described in Section 4.3.1.

The objective of this chapter is to show: (1) the effect of coal charring temperature on the carbon conversion rate; (2) the relative effects and order of magnitude of operating variables, such as gas composition, (oxygen concentration), temperature, pressure, and initial particle size on the conversion rate of the carbon and the effect of combustion (complete combustion) on the particle size; and (3) to demonstrate the validity and applicability of a suitable reaction rate model with respect to carbon conversion.

The reactivity of chars prepared at 700 and 900°C (Char700 and Char900) is compared in Section 7.2. The effect of the operating variables using Char900 only is presented in Section 7.3. An account of the development, properties and validity of the chemical reaction pore diffusion model is given in Section 7.4 with the evaluation confined to experimental results obtained with Char900. The experimental results reported and used for the modelling were derived by normalising the results obtained from the thermogravimetric analyser in similar manner as for the gasification results shown in Chapter 6 (Section 6.2), which consisted essentially of expressing the carbon conversion on an ash free basis.

7.2 Properties of char prepared at 900°C

The different petrographic properties of chars prepared at 700 and 900°C are discussed in Section 4.4, which include mainly reflectance (vitrinite and total macerals) and carbon form compositions. Char700 consists of a larger fraction of non-reacted vitrinite with a low reflectance while Char900 contained a large fraction of dense char with a higher reflectance.

The chars both have a very low pore volume and consequently a low porosity, which could be attributed mainly to the devolatilisation of the vitrinite containing maceral

intermediates, present in small quantities and to thermal cracking. The gasification reaction rate of Char900 with carbon dioxide-nitrogen mixtures was found to be chemical reaction controlled up to temperatures of 900°C (Chapter 6).

It is well known that char reactivity decreases with increasing rank (reflectance) due to maturity of the coal because of graphitisation (ordering of carbon structure) especially for inertinite rich coals. Based on these arguments, the reactivity of Char900 should be less than that of Char700. However, using a char prepared at a lower temperature (say 700°C) than the combustion temperature (larger than 700°C), results would be characterised by an initial period involving devolatilisation, which would require complex calculation in order to evaluate a model for char combustion alone. Thus, all experimentation undertaken for the assessment of combustion (gasification) reactivity and modelling in this investigation was confined to a char prepared at the maximum reaction temperature used, namely 900°C. The decreasing reactivity with charring temperature was observed in this investigation, which is shown in Figure 7.1 for an experiment carried out at 87.5 kPa using 3mm diameter particles at a reaction temperature of 900°C with 20 % oxygen (also Appendix E1). A detailed evaluation of this property was considered beyond the scope of this investigation and consequently was not undertaken.

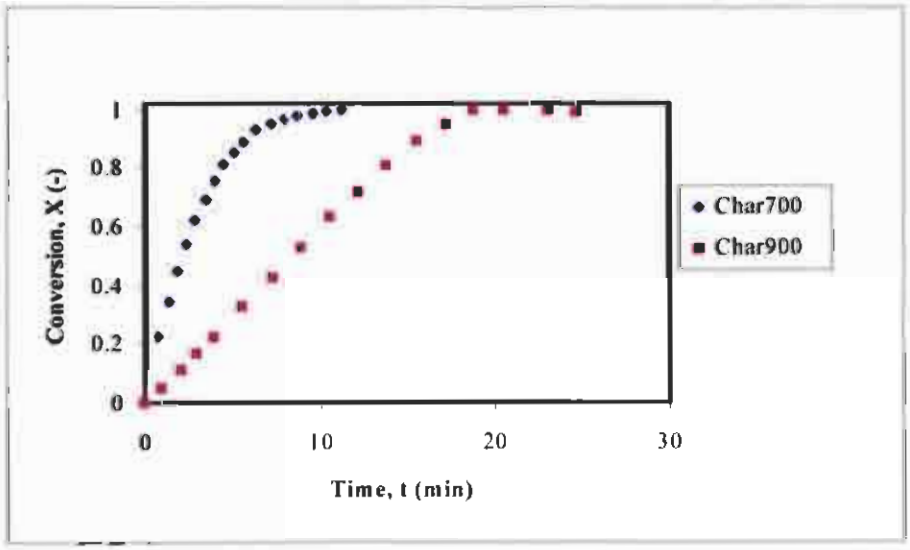

Figure 7.1: Effect of charring temperature on reactivity at 900°C, 87.5 kPa, 20 % oxygen)

7.3 Effect of operating conditions on combustion reactivity

Experiments were carried out to confirm established trends concerning the effect of operating variables and particle size on carbon conversion, and to generate results for the evaluation of a suitable reaction rate model. Results from relevant experiments to demonstrate the different effects were chosen from the list of experiments given in Table 5.2.

Oxygen Composition: The effect of oxygen concentration was investigated by varying the oxygen composition between 5 and 40 %, at pressures of 87.5 and 287.5kPa with typical results shown in Figures 7.2 and 7.3 (also in Appendix E2). As expected, the reactivity increases with an increase in oxygen composition for a constant gas velocity. It should be noted that the reaction rates are controlled by varying combinations of chemical reaction, and pore diffusion rates that can also vary as a result of pores being generated as carbon is converted during the duration of the experiment.

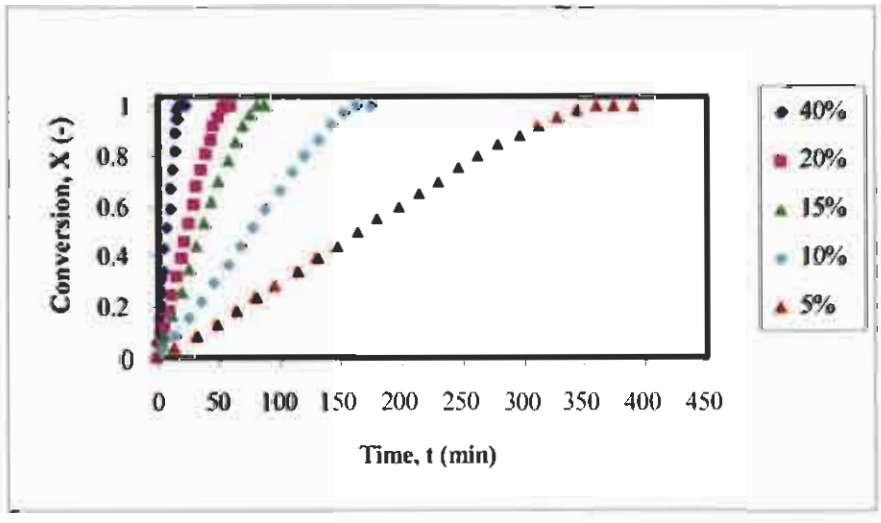

Figure 7.2: Effect of oxygen concentration on reactivity (1mm diameter particles at 87.5 kPa and 900°C)

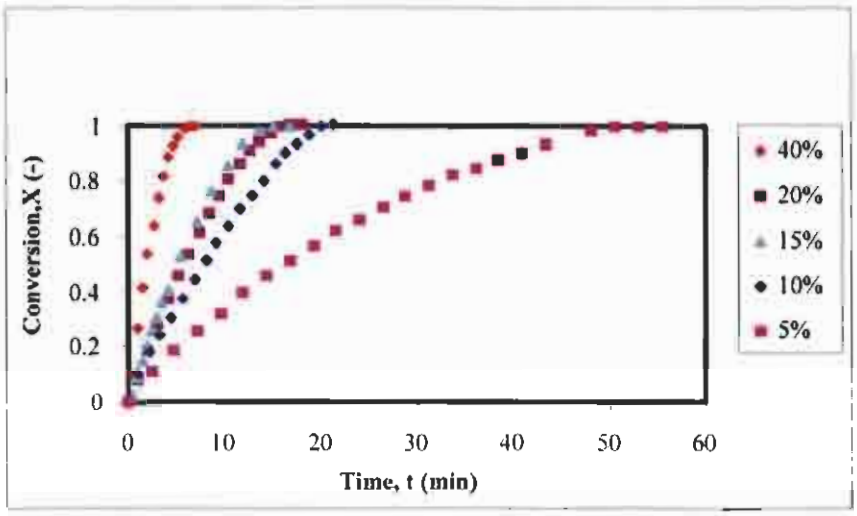

Figure 7.3: Effect of oxygen concentration on reactivity (1mm diameter particles at 287.5 kPa and 900°C)

Temperature: Typical results from experiments in the temperature range 450 to 900°C carried out at 287.5 kPa with 20 % oxygen are shown in Figures 7.4 and 7.5. The distinct variation of carbon conversion with time over the low temperature range (450 to 600°C) shown in Figure 7.4 can be attributed to the dominance of the intrinsic reaction rate with the effect of pore diffusion increasing with temperature. Over the higher temperature, range (700 to 950°C) shown in Figure 7.5, pore and external diffusion effects are controlling with film diffusion being dominant at the very high temperatures when the results are closer to one another.

Since reaction rates and diffusion coefficients and especially reaction kinetic constant for combustion are sensitive to temperature, reaction regimes have been defined primarily for different temperature intervals (Walker, *et al.*, 1959). This is considered the most important variable for any coal combustion kinetic study. The presence of different reaction regimes needs to be quantified with the aid of a mathematical model in order to obtain a satisfactory explanation. This was undertaken and explained in Section 7.4.3. It was also found that the ignition temperature at 87.5 kPa was very close to 450°C and was even lower for experiments preformed at 287.5 kPa. Appendix E3 gives more results on the temperature effect on combustion.

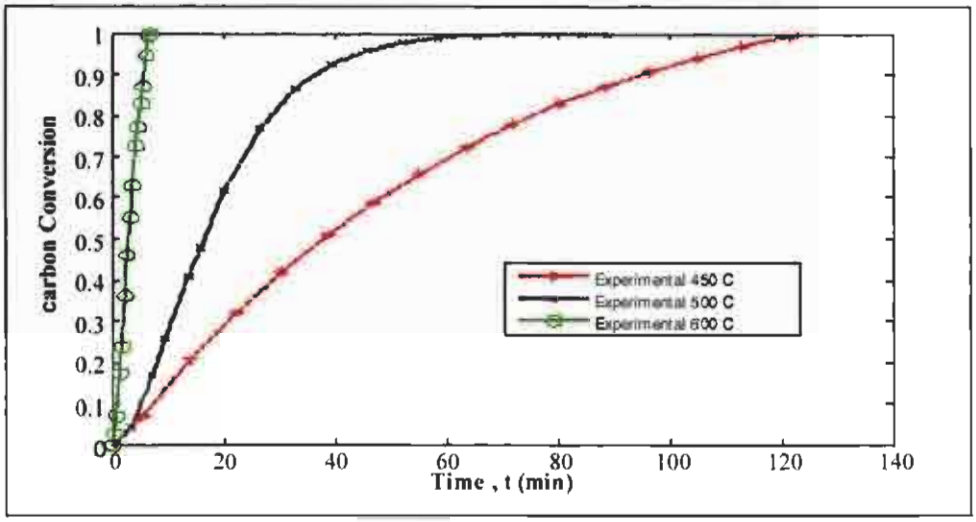

Figure 7.4: Effect of temperature on reactivity (3mm diameter particles at 287.5kPa and 450 to 600°C with 20 % oxygen)

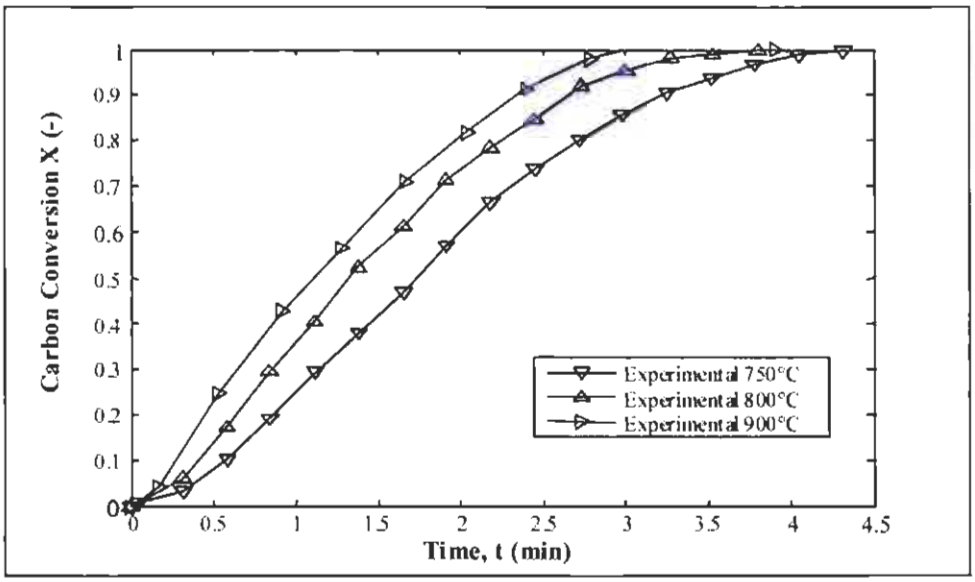

Figure 7.5: Effect of temperature on reactivity (3mm diameter particles at 287.5KPa and 750 to 900°C with 20 % oxygen)

Pressure: The effect of pressure on the carbon conversion is shown in Figures 7.6 and 7.7 for 87.5 and 287.5 kPa at low and high temperatures, respectively, with 20 % oxygen. The increase in reactivity is most significant, which is attributed mainly due to the increased intrinsic reaction rate. Also here, the effect of external diffusion appears to be important at the high temperature. More results involving the pressure effect are shown in Appendix E4.

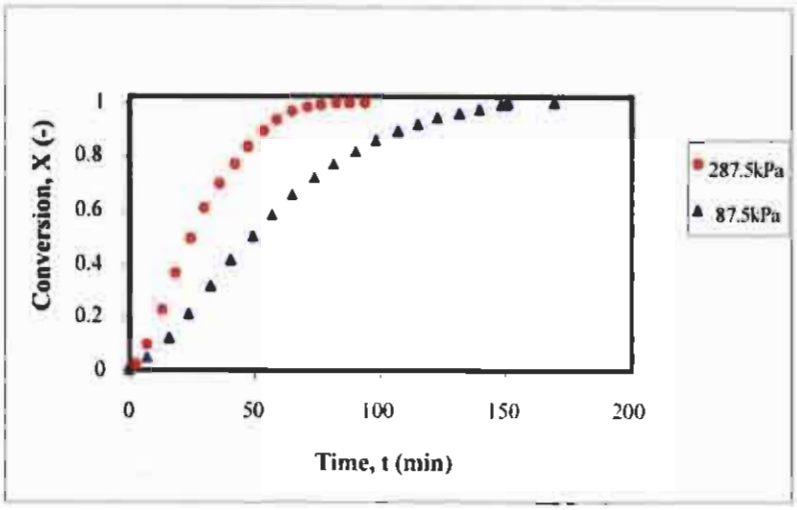

Figure 7.6: Effect of pressure on reactivity (1mm diameter particles at 500°C with 20 % Oxygen

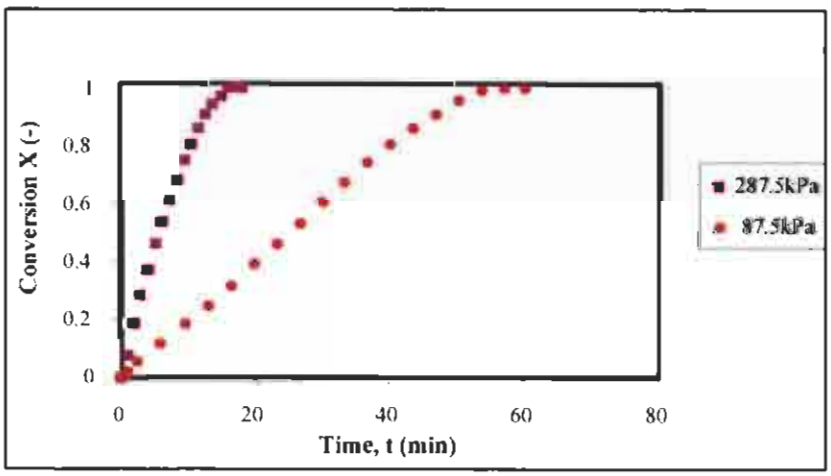

Figure 7.7: Effect of pressure on reactivity (1mm diameter particles at 900°C with 20 % Oxygen.

Particle Size: The results presented in Figures 7.8 and 7.9 and also in Appendix E5, show the effect of particle size for 1 and 3mm at 450 and 700°C, respectively at 87.5 kPa with 20 % oxygen. The particle diameter also does not change significantly during the reaction period as shown in Figure 7.10, which indicates that the inert material (ash and residual char) remaining during reaction does not collapse even after complete combustion. The difference in reactivity can be ascribed to an increased pore diffusional effect with bigger particles, which lowers the overall reactivity (Tsai, 1982).

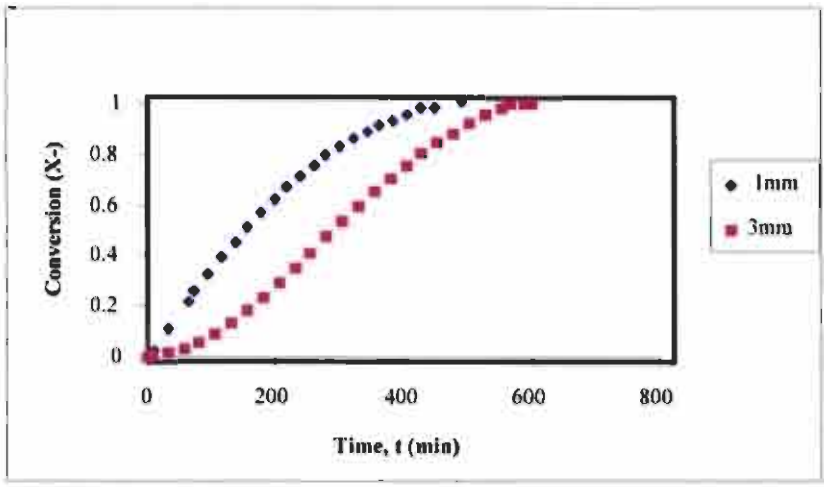

Figure 7.8: Effect of particle size on reactivity (287.5 kPa and 450°C with 20 % Oxygen).

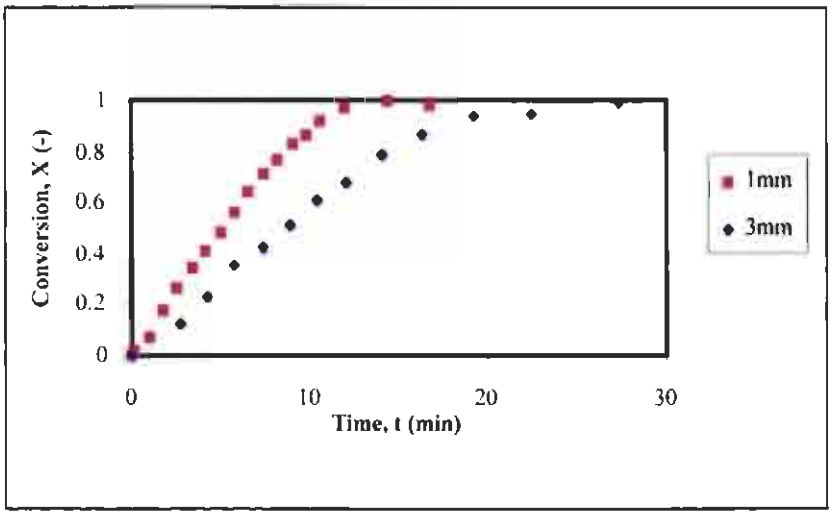

Figure 7.9: Effect of particle size on reactivity (287.5 kPa and 700°C with 20 % Oxygen).

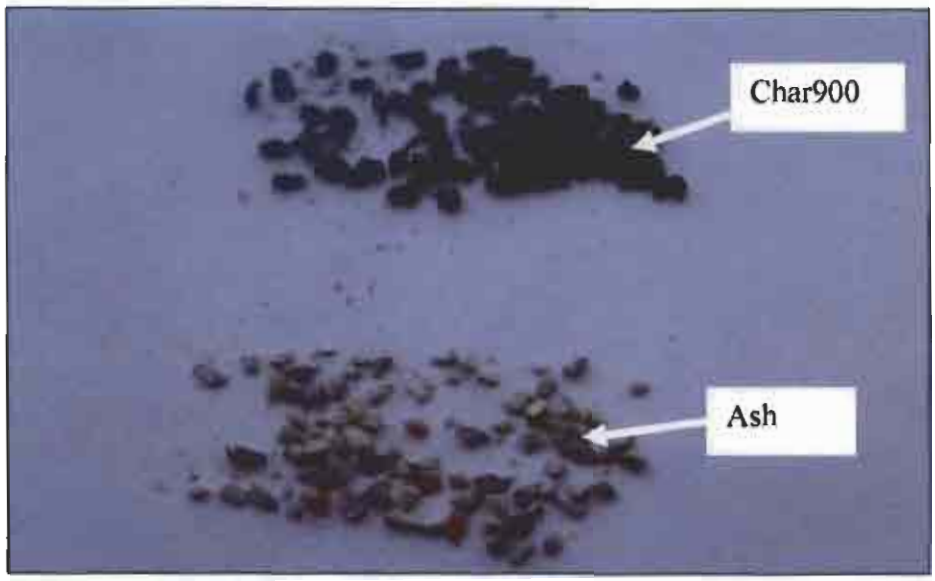

Figure 7.10: Photograph of Char900 and ash particles. (1mm diameter particles completely combusted at 87.5kPa and 900°C with 20 % Oxygen)

7.4 Modeling

The mathematical modeling of the combustion process consisting of the chemical reaction- pore diffusion model is presented in this section, which consists of (1) the validation of the numerical technique developed and used for solving the equations describing the model; (2) examination of the solutions of the reaction diffusion model with features characteristic of combustion; (3) description of a procedure to evaluate structural parameters and diffusion parameters (Thiele modulus) irrespective of the reaction kinetics; (4) evaluation of the reaction diffusion model against experimental results; and (5) determination of intrinsic reaction rate parameters in the presence of pore diffusion and the determination of diffusion coefficients.

A detailed description of the chemical reaction-pore diffusion model is given in Section 3.3.2.1 consisting of Equations (3.13) to (3.17). The initial porosity required for the determination of the effective diffusivity, Equations (3.26) and (3.28) for the solution of the equations was calculated from the BET results reported in Table 4.12. It should be noted that the results are confined to pores greater than 10Å, which is considered the lower limit measured by BET with nitrogen (Zhu 2007).

7.4.1 Numerical solution of model equations

A numerical method (MATLAB© routine) was used for solving the model equations consisted initially of determining the concentration profile of oxygen at different radial positions in the particle for different values of the Thiele modulus. Dimensionless times (iteration procedure) were used, followed by the calculation of the local reaction rates and carbon conversions at different mesh points and finally a calculation of the average carbon conversion at different time intervals. The solution of the equations were validated against analytical results involving (1) a chemical reaction controlled case, that is for a Initial Thiele Modulus equal to zero; and (2) a chemical reaction-pore diffusion controlled case involving a model with volume-based rate equation as published by Ishida and Wen (1968). Numerical results for the chemically-controlled case from the model are shown in Figure 7.11 for different structural parameters and compared with the corresponding analytical solutions involving the random pore model, Equation (3.8), all plotted against a dimensionless time parameter.

A comparison of numerical results for the chemical reaction- pore diffusion case with analytical solutions involving a volume-based reaction rate, instead of Equation (3.14), according to Ishida and Wen (1968) and with different Thiele moduli shown in Figure 7.12.

The comparisons shown in Figures 7.11 and 7.12 confirm the correctness and validity of the numerical solution of the model. A set of typical concentration profiles obtained for chemical reaction-pore diffusion controlled cases is shown in Figure 7.13, which illustrates the diffusion effect characterised by the Thiele modulus very clearly.

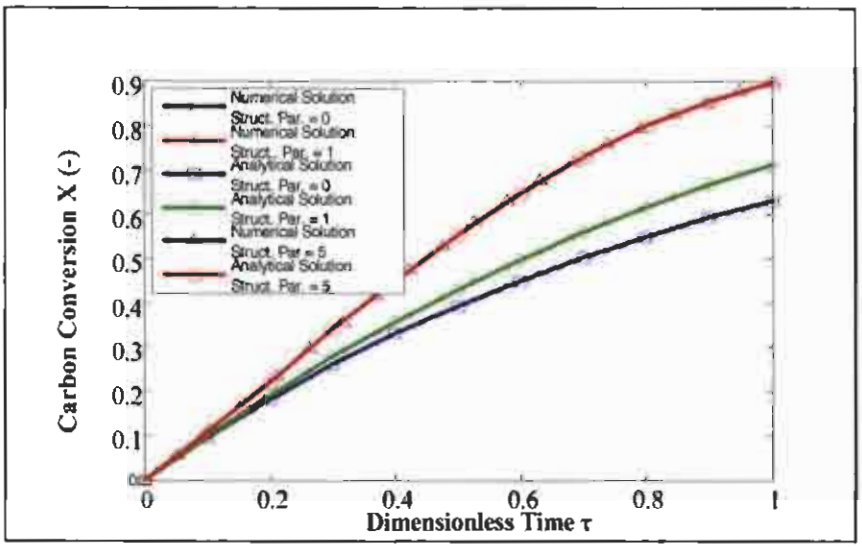

Figure 7.11: Comparison of numerical and analytical solutions for reaction controlled case (Initial Thiele Modulus = 0)

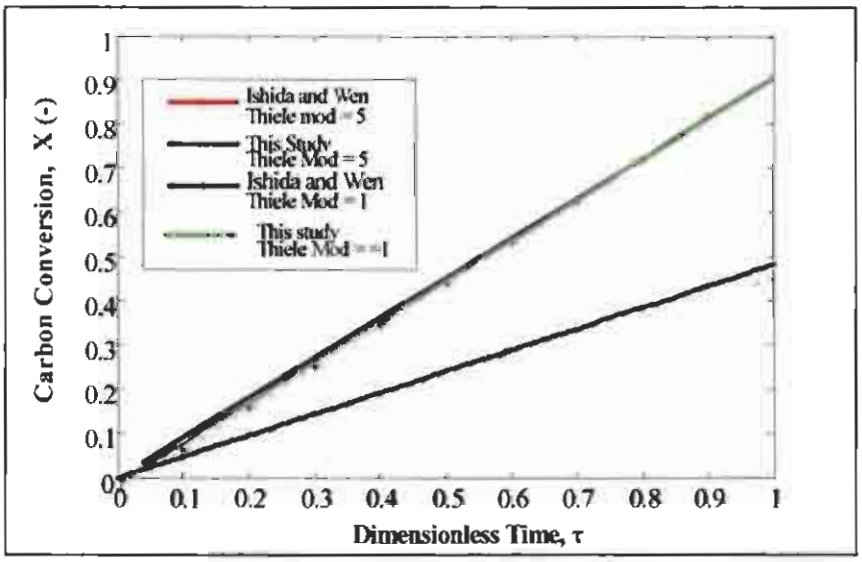

Figure 7.12: Comparison of numerical and analytical solutions of model used by Ishida and Wen (1968)

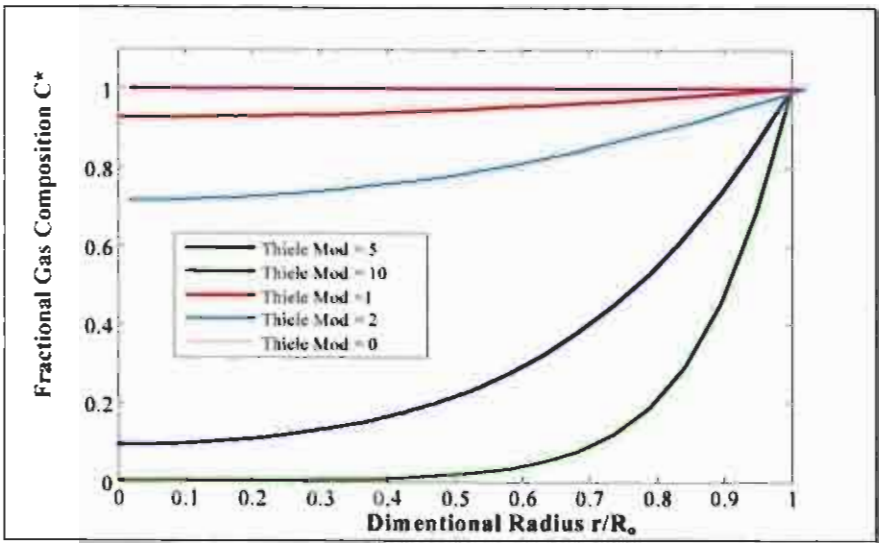

Figure 7.13: Numerically-calculated gas compositions for different Thiele Moduli according to the model of Ishida and Wen (1968)

7.4.2 Results from reaction-diffusion model applicable to coal char conversion

Theoretical model results are presented in this section involving different combination of parameters. The parameters involved are: (1) structural parameter, Equation (3.2); (2) Thiele modulus, Equation. (3.18), which is the initial value based on the properties of the char at the commencement of the reaction; (3) time factor, Equation (3.7) which consists of the intrinsic reaction parameters. (4) reduced time defined as $t/t_{0.9}$. The diffusion-porosity equation used is the quadratic relationship given by Equation (3.26).

7.4.2.1 Effect of porosity variation

In accordance with Section 3.3.2.1, Equations (3.26) and (3.28) equations for the variation of porosity, which affect the diffusion co-efficient, were introduced into the model. These equations account for the effect of porosity on the diffusivity co-efficient, and the mineral content on the porosity of the coal char for a fixed initial porosity, respectively.

The variation of the relative porosity $(\varepsilon/\varepsilon_0)$as the carbon conversion, Equation (3.28) increases is shown in Figure 7.14 as a function of the initial porosity and ash content of the char. It can be seen from Figure 7.14 that for coal chars with low initial porosities the relative variation is significant with the low ash coal char having the

largest variation. For high ash coal chars (46%) with very low initial porosities of 1% and 5%, the porosity increases to final values of 0.54 and 0.56, respectively. This is very different to low ash coal chars and has a marked effect on the effective diffusivity given by Equation (3.26). The effects on the dimensionless diffusivity coefficient and the Thiele modulus for initial values of 10, 50 and 100 are shown in Table 7.1, which were calculated from the definition of the Thiele modulus, Equation (3.18). The important characteristic worth noting is the strong decrease of the Thiele modulus with an increase in carbon conversion.

The decrease in Thiele modulus during the reaction is such that the diffusion effects become insignificant and that a transition from reaction-diffusion conditions to reaction controlled conditions occurs especially for lower values of the initial Thiele modulus. This feature is illustrated in Figure 7.15, which shows that the chemical reaction-diffusion model merges with the chemical reaction controlled model at higher carbon conversion levels. It should be noticed that the result has an S-shaped behaviour and that the transition to reaction-controlled conditions occurs at high carbon conversions as the Thiele moduli increase from its initial value. Very high values of the initial Thiele moduli are characteristic of combustion reactions involving very fast intrinsic reaction rates and low diffusivity in micro-porous structures (see Section 7.4.3.3).

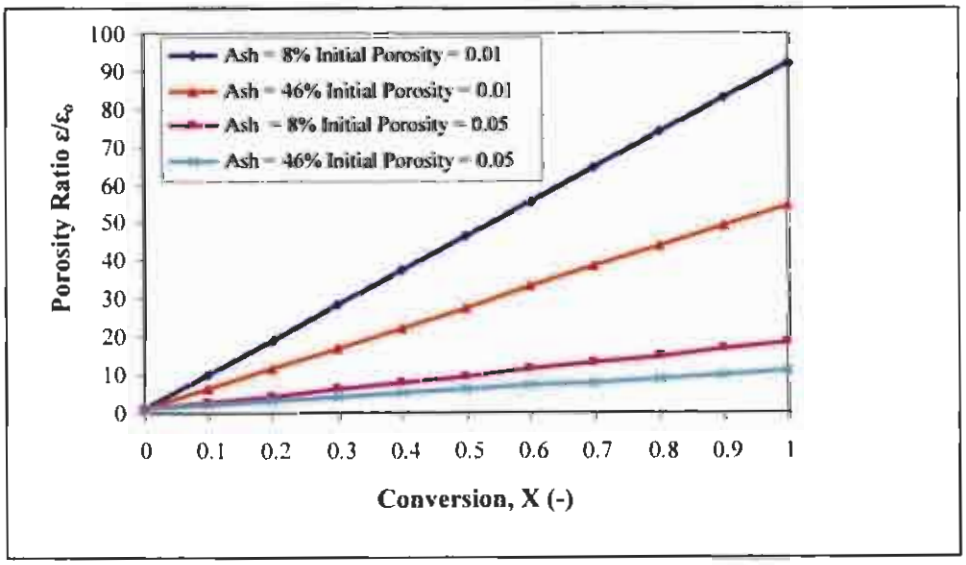

Figure 7.14: Variation of relative porosity with carbon conversion with effect of initial porosity and ash content.

Table 7.1: Effect of porosity variation on diffusivity and Thiele Modulus (Initial porosity 0.01 and ash content =46%)

Carbon Conversion	$D_{(\varepsilon)}/D_{(\varepsilon_0)}=(\varepsilon/\varepsilon_0)^2$	Thiele Modulus		
0.0	1	10	50	100
0.21	135	0.86	4.31	8.62
0.53	756	0.36	1.81	3.63
0.74	1451	0.26	1.31	2.62
1.00	2635	0.19	0.97	1.94

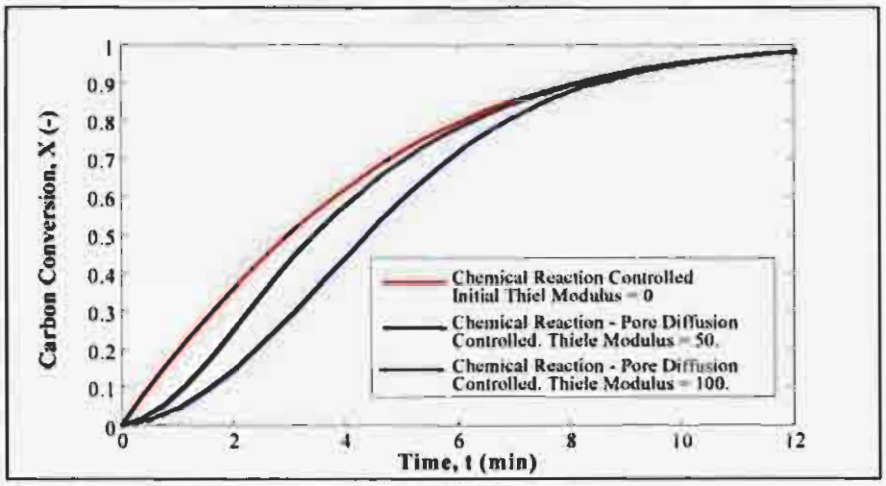

Figure 7.15: Comparison of chemical reaction controlled reaction with Chemical reaction –pore diffusion controlled reaction (ψ =1).

7.4.2.2 Carbon conversion versus reduced time plots

The advantage of using the reduced time parameter ($t/t_{0.9}$) is that the effect of the intrinsic chemical reaction can be eliminated and that parameters such as the structural parameter and/or the Thiele modulus can be evaluated. For the chemical controlled model the following was derived in Section 3.3.1.1, which can be seen to be independent of the intrinsic reaction rate parameters:

$$\frac{t}{t_{0.9}} = \frac{\sqrt{1-\psi\ln(1-X)}-1}{\sqrt{1-\ln(0.1)}-1} \qquad (3.9)$$

This property is also illustrated for the chemical reaction-pore diffusion model results from the numerical solution, shown in Figure 7.16, where results are plotted for different intrinsic reaction rate constants (contained in the time factor t_r) with a constant Thiele modulus. The identical results are evident, which also demonstrates the usefulness of using the reduced time parameter. It should be noted that the normalised time can be at any carbon conversion level.

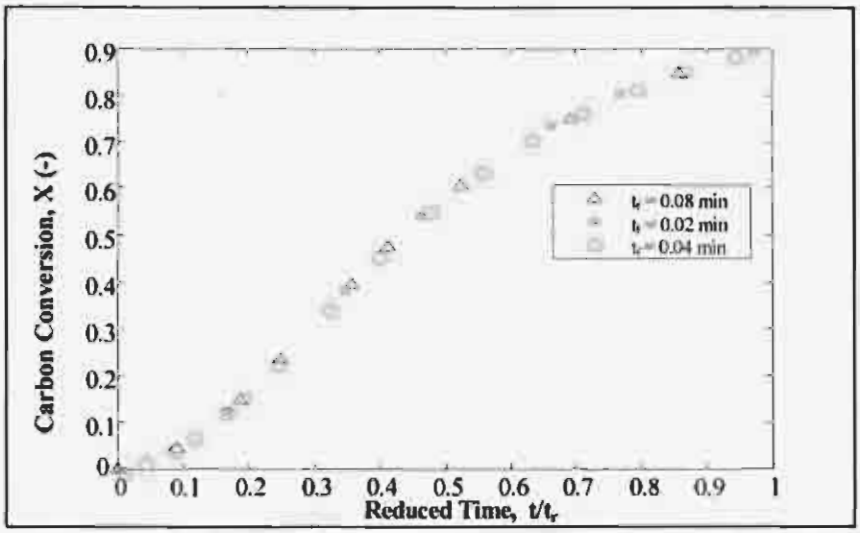

Figure 7.16: Plot of carbon conversion versus reduced time showing elimination of reaction rate effect (Thiele Modulus =60)

7.4.2.3. Effect of structural parameter

The effect of the structural parameter for chemical reaction-controlled systems is shown in Figure 7.17, which indicates that the carbon conversion decreases as the structural parameter increases. Also shown in Figure 7.17 is a comparison of a result derived from a chemical reaction-pore diffusion model to indicate the deviation from the reaction-controlled result with a combination of similar parameters. The merging at very high carbon conversions for similar structural parameters is again evident.

For both chemical reaction–and chemical reaction - pore diffusion-controlled systems, the structural parameter can be determined from the carbon conversion versus reduced time plots, which can be achieved as follows, (1) for the reaction controlled system this parameter is the only unknown and can be easily estimated by regression.

This occurs either for very slow reaction (rates), such as for the carbon dioxide reactions, reported in Chapter 6 or for combustion reactions at very low temperatures where chemical reaction controlling conditions could prevail; (2) for the chemical reaction-pore diffusion controlled system with an increasing porosity this parameter can be estimated, by regression, at high carbon conversions should the transition to reaction control occur. This calculation would depend on an accurate determination of a transition, which is asymptotic and would be difficult to assess. For systems where the transition is not present, regression involving both the structural parameter and the Thiele modulus needs to be done, which is undesirable. In this investigation results from the carbon dioxide experiments, which is a very slow reaction, using the same char were used for the determination of the structural parameter.

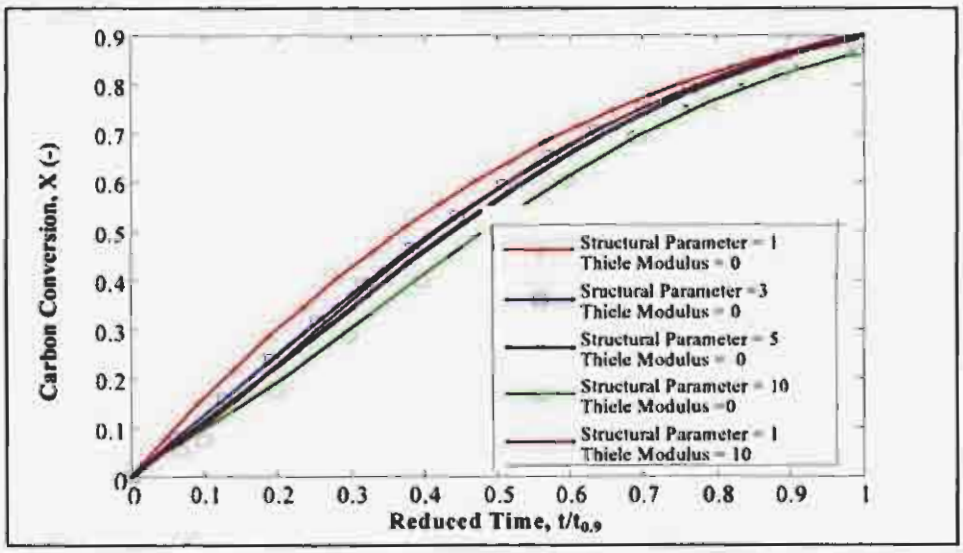

Figure 7.17: Effect of Structural parameter using carbon conversion versus reduced time

7.4.2.4 Effect of Initial Thiele modulus

The influence of the initial Thiele modulus on the carbon conversion for a constant structural parameter is shown in Figure 7.18. The effect is confined to the initial stages and that merging with chemical reaction-controlled systems for low Thiele moduli is evident. The results again show characteristic S-shape behaviour and the convergent behaviour.

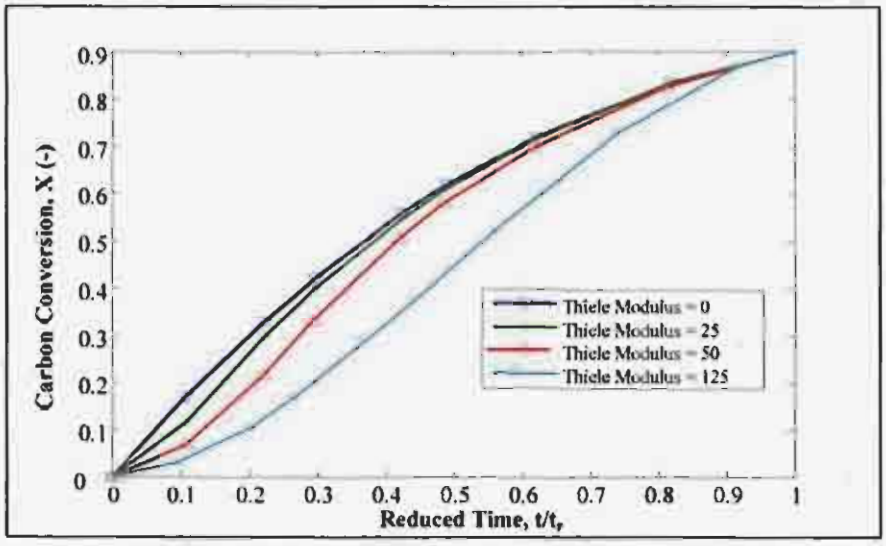

Figure 7.18: Effect of Thiele Modulus using carbon conversion versus reduced time transformation. (Structural Parameter = 1).

7.3.2.5 Conversion versus real time plots

For the determination of intrinsic reaction rate parameters it is necessary to generate carbon conversion versus real time plots in order to carry out a regression analysis involving the experimental results. Since the conversion varies along the radius of the particle when diffusional effects are present, it will be necessary to determine an overall conversion over the particle radius. Local conversions at the different mesh points are shown in Figure 7.19, which are derived from local oxygen concentrations shown in Figure 7.20 for typical values of the parameters. The effect of diffusion is seen to occur over a very short initial period when a decreasing oxygen profile exists in the particle and a lower carbon conversion at the centre of the particle. The final average carbon conversion at different times is shown in Figure 7.21.

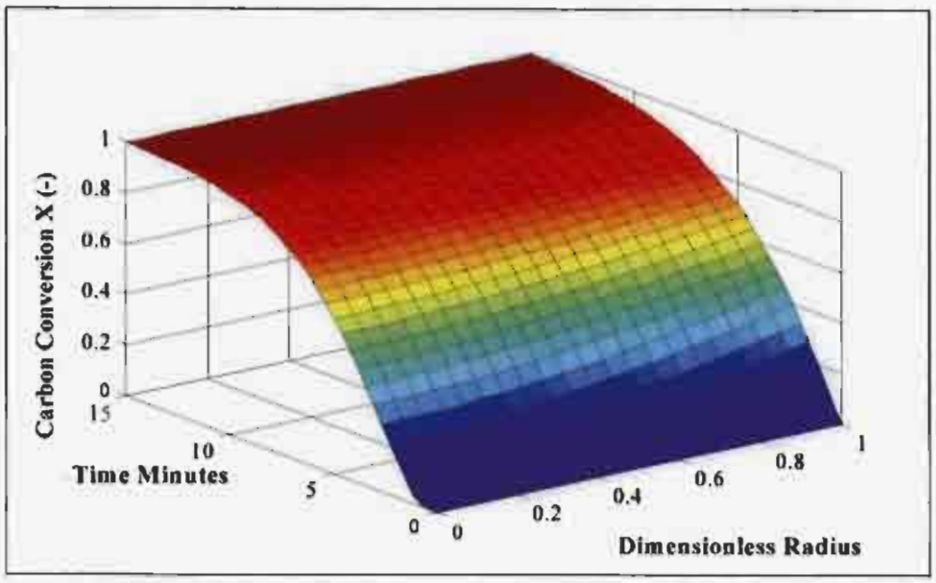

Figure 7.19: Local carbon conversion on (Thiele Modulus = 50, t_f = 0.05 min^{-1}, Structural parameter = 1).

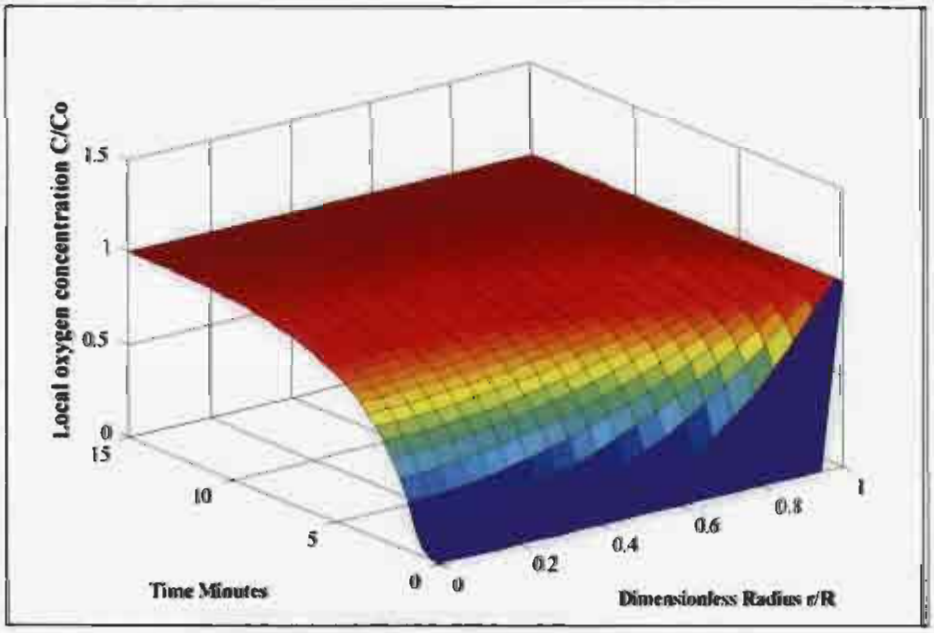

Figure 7.20: Local oxygen concentration on (Thiele Modulus = 50, t_f = 0.05 min^{-1}, Structural parameter = 1)

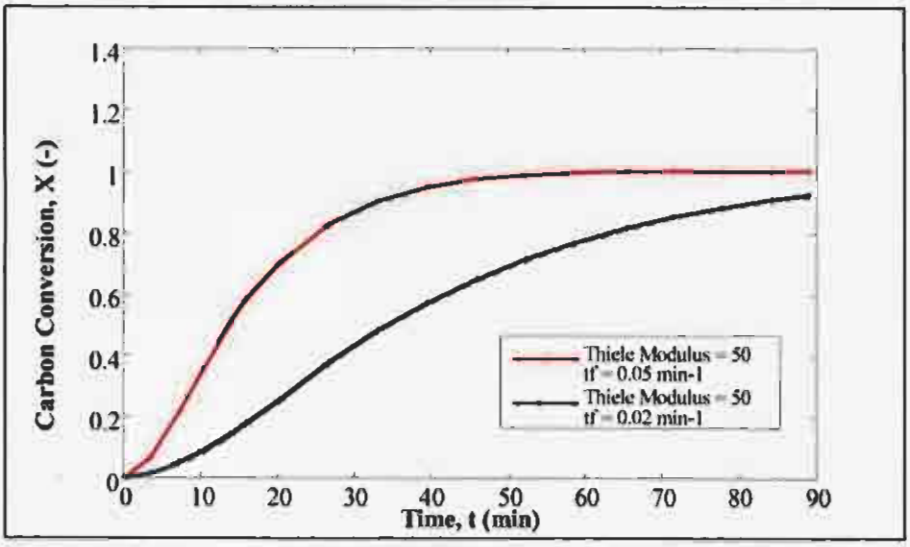

Figure 7.21: Average carbon conversion in particle (Initial Thiele Modulus = 50, Structural parameter = 1)

7.4.3 Evaluation of Chemical reaction–pore diffusion model with experimental results.

7.4.3.1 Experimental results

The experimental results used for the evaluation of the reaction diffusion model and subsequent determination of the parameters were done under reaction conditions given in Table 7.2. These conditions were chosen to correspond to low and intermediate temperatures (<900°C) and at an elevated pressure under which the char has an acceptable reactivity for practical application. The thermogravimetric analyser volumetric flow rate was maintained at a high value and the mass of the sample was small in order to minimise external diffusional effects. The results obtained under these conditions are shown in Figures 7.4 and 7.5.

Table 7.2: Details of experiments used for combustion model evaluation

Reaction variable	**Conditions**
Temperatures (°C)	450, 500, 600 750, 800, 850 and 900
Pressures kPa	287.5
Gas composition mole% Oxygen	20%
Coal char-Char900 for gasification experiments	Prepared at 900°C
Particle diameter (mm)	1
Volumetric gas flow rate (m^3 min^{-1})	$1.8 \cdot 10^{-3}$
Mass of char sample (mg)	200(±2)

7.4.3.2 Confirmation of deviation from chemical reaction controlled regime

A comparison of low and high temperature experimental results with a prediction from the random pore model without diffusional effects for a structural parameter equal to the value determined with carbon dioxide mixtures (ψ = 1.04) is shown in Figures 7.22 and 7.23 with a carbon conversion plot against the reduced time co-ordinate. It is clear that all the experimental results deviate from the chemical reaction controlled result with the low temperature results showing a consistent trend similar to results shown in Figure 7.18 for different values of the Thiele modulus. It should, however, be noted that the result obtained at 450°C is close to the chemical reaction controlled result but still consistently lower and different to results obtained with the carbon dioxide mixtures (Figure 6.10).

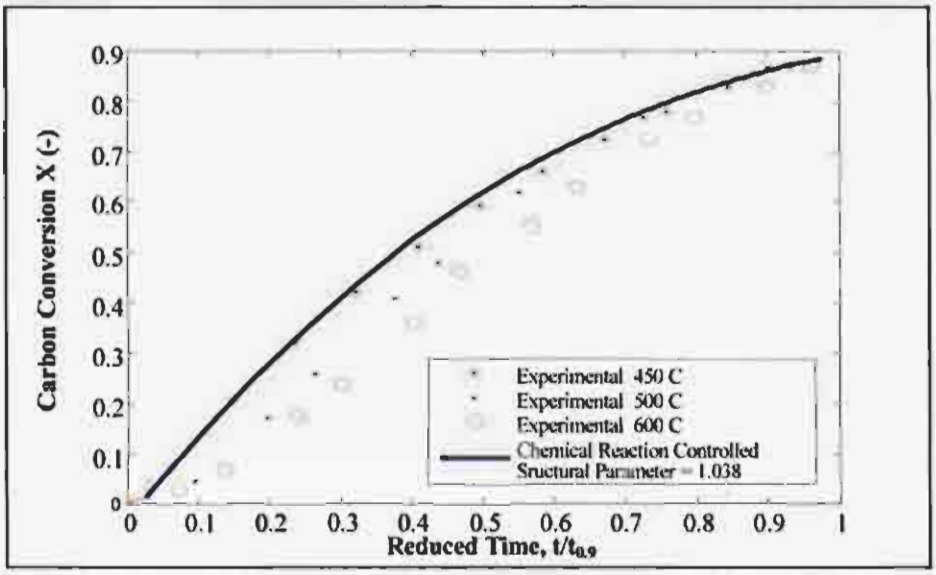

Figure 7.22: Deviation of experimental results at low temperatures from chemical reaction controlled reaction. (Pressure = 287.5 kPa, Oxygen concentration = 20 %)

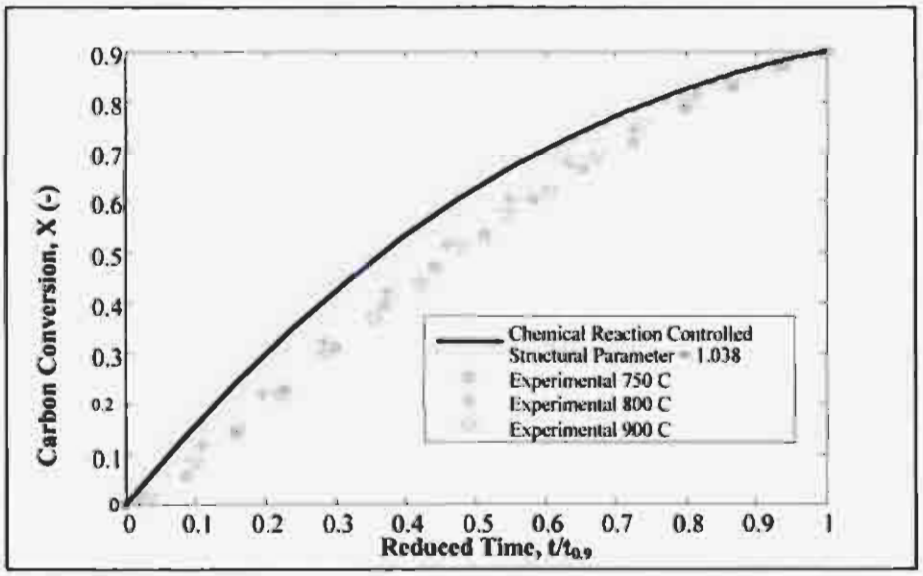

Figure 7.23: Deviation of experimental results at high temperatures from chemical reaction controlled reaction (Pressure = 287.5 kPa, Oxygen concentration = 20 %)

7.4.3.3 Determination of Initial Thiele Modulus

The evaluation of the initial Thiele Modulus from the reduced time plots for a known value of the structural parameter, which was determined from the carbon dioxide reaction (Chapter 6) experiments, was applied to the experimental results determined at 287.5 kPa and at temperatures 450, 500 and 600°C. Comparisons between the experimental and model results using reduced time plots are shown in Figures 7.24 to

7.26 with the initial Thiele moduli reported in Table 7.3. The model result was determined by manual regression with the Thiele modulus as the unknown and correlation coefficients larger than 0.95 were obtained. The good comparison between the experimental and model results confirms the validity of the structural model (without the intrinsic reaction kinetics) and the pore diffusion effect incorporated in the overall model.

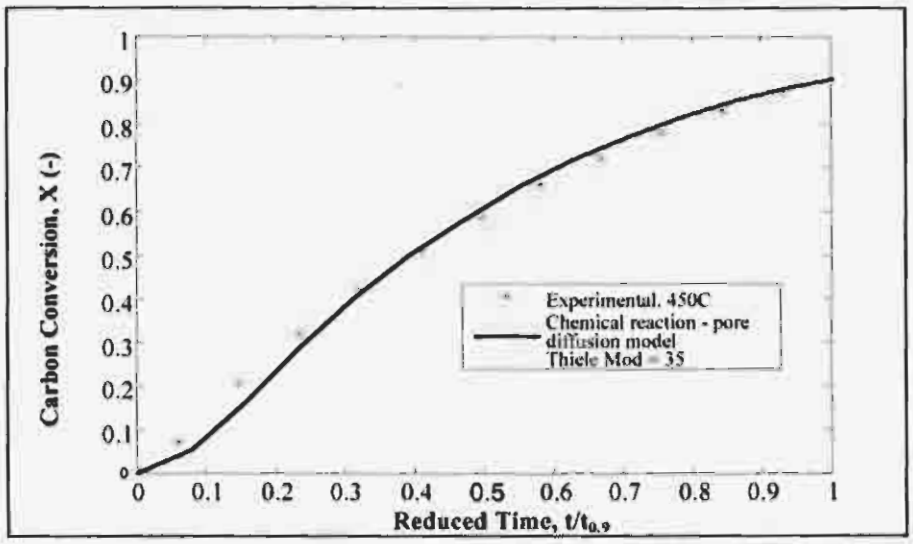

Figure 7.24: Comparison of experimental and model results at 450°C and 2.875 kPa

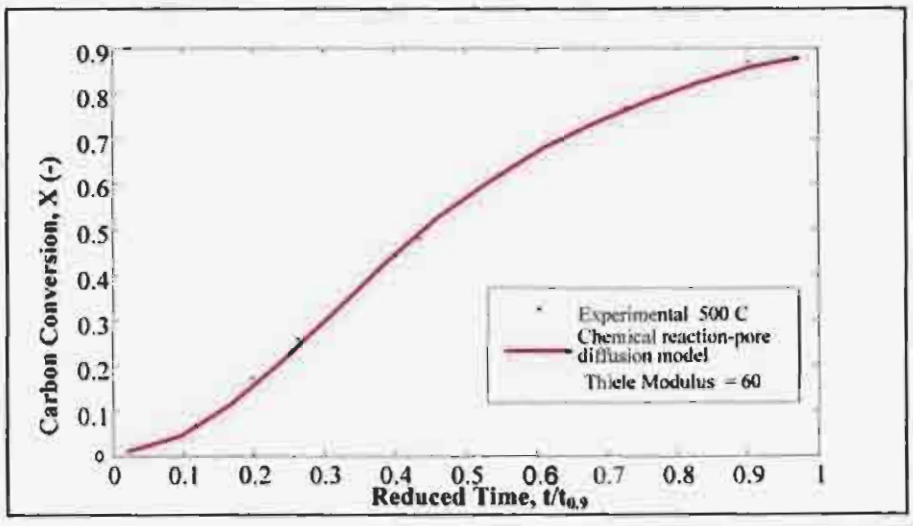

Figure 7.25: Comparison of experimental and model results at 500°C and 287.5 kPa

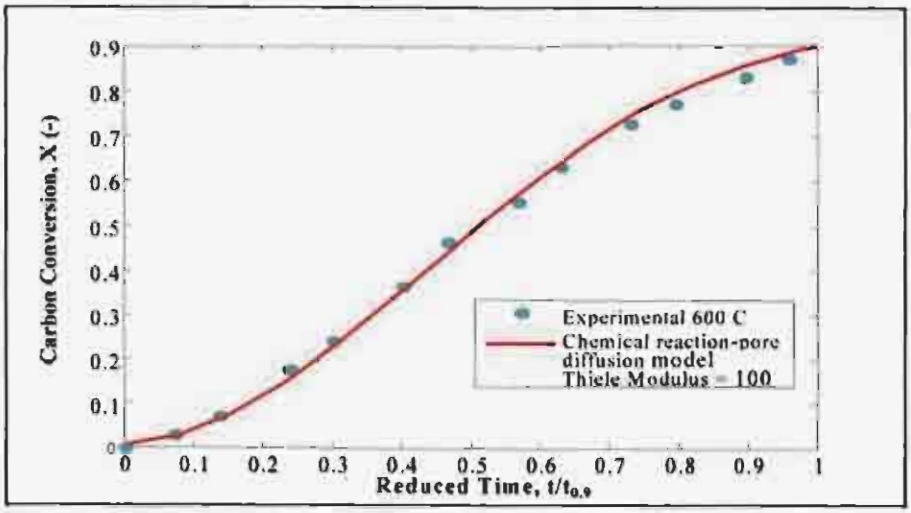

Figure 7.26: Comparison of experimental and model results at 600°C and 287.5 kPa

7.4.3.4. Determination of reaction rate constants

For determination of all the intrinsic reaction parameters, the following procedure was adopted; (1) with known values of the structural parameter from the carbon dioxide experiments for chemical reaction controlled conditions and initial Thiele moduli determined from the reduced time experimental results plots (Section 7.4.3.3) the time factor t_f using the model based on real time was evaluated by regression; (2) from the evaluated time factor, which can be derive from Equations (3.21) and (3.23), namely

$$t_f = \frac{k_{so} \exp(-E/RT) C_o S_o}{1-\varepsilon_o} \qquad (7.1)$$

The activation energy E and the pre-exponential factor grouping $k_{so} S_o/(1-\varepsilon_o)$ were calculated from a plot of the $\log(t_f/C_o)$ versus 1/T using the slope and intercept respectively determined by linear regression.

Time factor t_f: Time factors were evaluated for the results addressed above and results consisting of the comparison of experimental and model results are shown in Figures 7.27 to 7.29 with the time factors reported in Table 7.3. Correlation coefficients larger than 0.99 were obtained from the experimental results and regressed predictions. These results also confirm the validity of the overall chemical reaction-pore diffusion model.

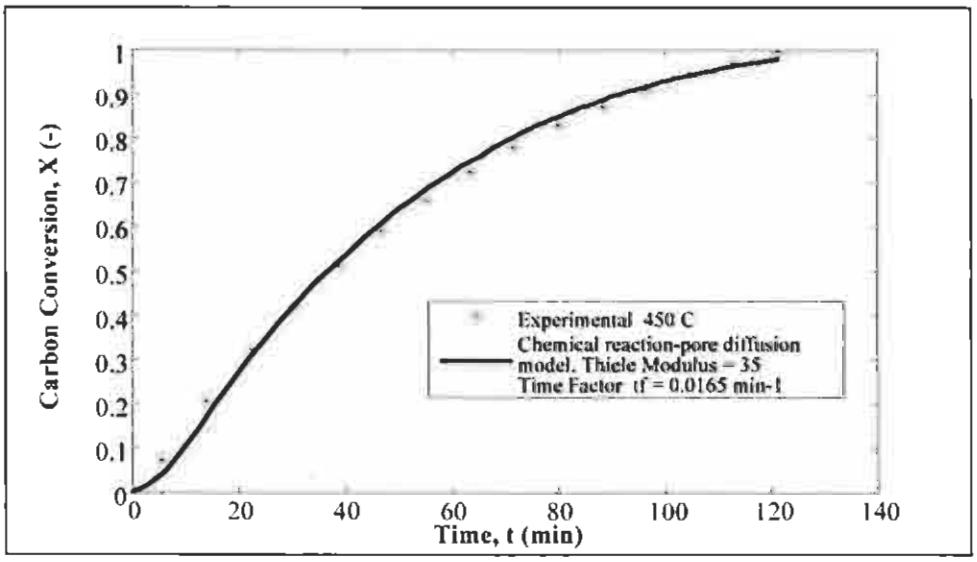

Figure 7.27: Determination of time factor at 450°C and 287.5 KPa

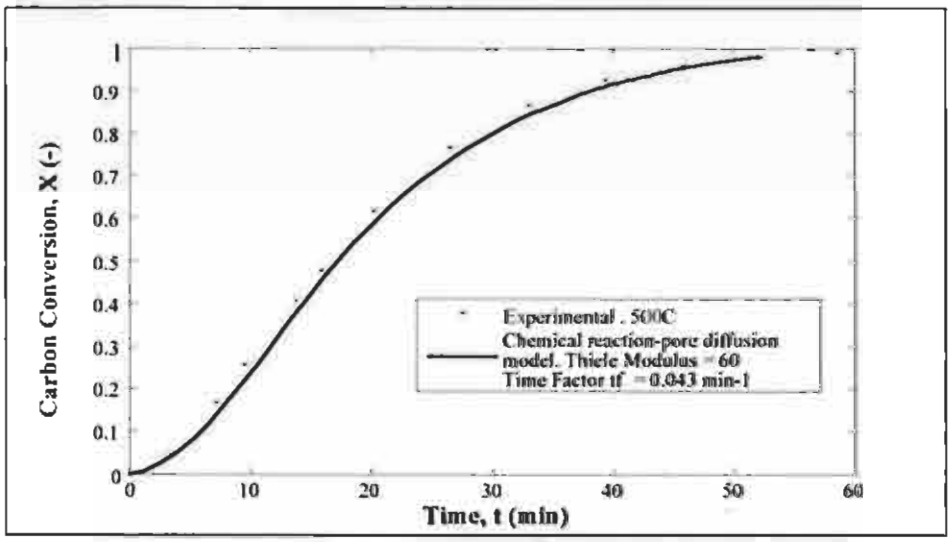

Figure 7.28: Determination of time factor at 500°C and 287.5 kPa

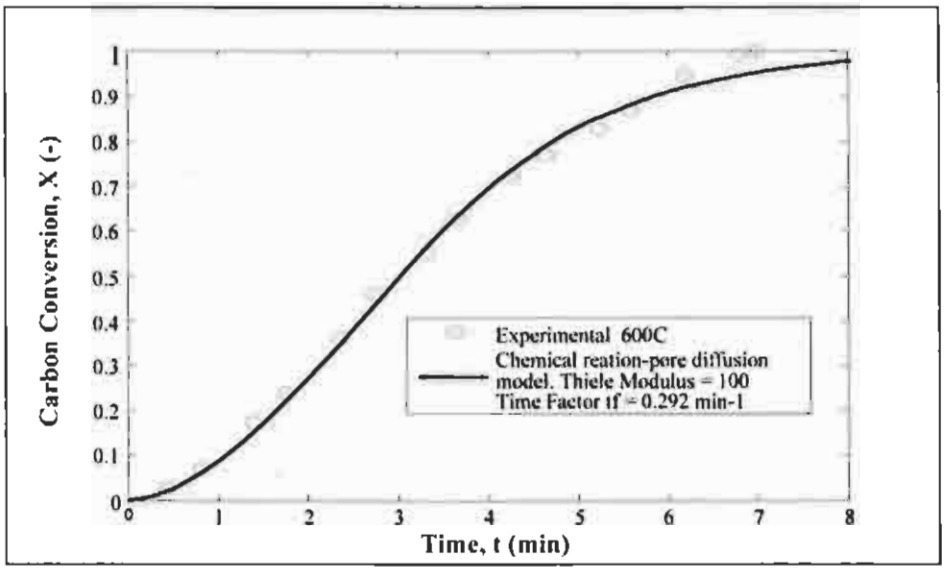

Figure 7.29: Determination of time factor at 600°C and 287.5 KPa

Activation Energy and pre-exponential factor: The activation energies and the pre-exponential factor were determined (involving three temperatures only) and reported in Table 7.3. These values were determined from results shown in Figure 7.30 involving a linear regression and time factor results determined above. Despite the limited number of points, there is a distinct linear relationship (Arrhenius equation) with realistic reaction rate parameters over the temperature range 450 to 600°C.

The inclusion of results over the high temperature range (750 – 900°C) based on a chemical reaction-pore diffusion model showed a distinct break above approximately 600°C with a lower apparent activation energy (approximately less than 40 $kJmole^{-1}$). These results above 600°C are not reported on Figure 7.30 as they were considered incomplete since film diffusion was not accounted for, which seriously affects the assessment of the initial Thiele modulus. Thus, it is possible with the thermogravimetric analyser used to estimate intrinsic reaction rate constants in the presence of pore diffusion in the temperature range 450 to 600°C. This has not been achieved by any other investigator according to open literature, which consists of incorporating the basic random pore model in the chemical reaction-pore diffusion model. The activation energies obtained are lower than that reported by Williams *et*

al. (2000) and Russell *et al.* (1998), being 155 kJmole^{-1} and 120-140 kJmole^{-1}, respectively. The results reported by these authors were deduced from many investigations involving many different parent coal samples with unknown maceral composition and in many cases different chars structures, which makes a meaningful comparison somewhat difficult. Gopalakrishnan and Bartholomew (1998) published results for combustion of chars derived from sub-bituminous coals containing significant amounts of calcium minerals and reported activation energies of the order of 109 kJmole^{-1} similar to that obtained in this investigation. The activation energy is also lower than that reported by Everson *et al.* (2006), who obtained a value of 133 kJmole^{-1} using a pulverised form of a char prepared from an identical parent coal, but with a charring temperature of 700°C, which indicates that the char properties, which are dependant on the charring temperature, determines the reaction kinetics. This argument also applies to the value of the pre-exponential factor.

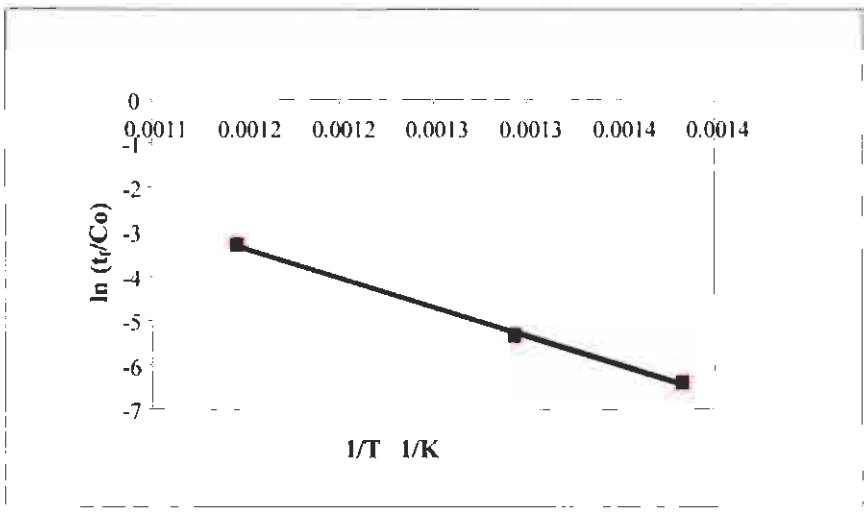

Figure 7.30: Intrinsic reaction rate constants for combustion at 287.5 kPa

Table 7.3: Parameters determined for reaction-diffusion model at 287.5 kPa

Variable	Experimental Temperature		
	450°C	500°C	600°C
Structural Parameter ψ	1.04	1.04	1.04
Initial Thiele Modulus ϕ_o	35(±3)	60(±5)	100(±10)
Effective Diffusion Co-efficient (Initial value) D_{eo} ($m^2 s^{-1}$)	$1.75 \cdot 10^{-9}$(±0.12)	$1.93(\pm 0.14) \cdot 10^{-9}$	$4.48(\pm 0.21) \cdot 10^{-9}$
Time Factor tf: min^{-1}	0.016(±0.001)	0.043(±0.002)	0.29(±0.001)
Determined Effective Diffusion Coefficient (Knudsen diffusion) D_{eo} ($m^2 s^{-1}$)	$7.14 \cdot 10^{-9}$	$7.39 \cdot 10^{-9}$	$7.85 \cdot 10^{-9}$
Activation Energy E kJ $mole^{-1}$	109(±11)		
Pre-exponential factor (lumped) $k'_{so} S_o/(1-\varepsilon_o)$ m^3 $mole^{-1} \cdot min^{-1}$	$1.16(\pm 0.18) \cdot 10^5$		

7.4.3.5 Determination of diffusion coefficient

The effective diffusion coefficients at different temperatures were estimated from the experimentally determined Thiele moduli and reaction rate constants using equation (3.18) defining the Thiele modulus. For this purpose the BET-surface area and particle density was used and the corresponding results are reported in Table 7.3. These results increase with temperature and are compared with calculated effective diffusion coefficients consisting of the Knudsen diffusion equation only. The equations used are the following (Froment and Bischoff, 1990):

$$D_{k,i} = \frac{2}{3} r_i \sqrt{\frac{8RT}{\pi M_A}} \qquad (7.2)$$

and $$D_{k,i,e} = \frac{\varepsilon}{\tau} \qquad (7.3)$$

For this calculation the pore size and pore volume determined from the BET measurements (Table 4.12) were used with an assumed tortuosity equivalent to 2. The comparison of the experimental and predicted results is good which confirms the presence of a char structure consisting mainly of micropores, which determines the initial overall reaction kinetics.

7.5 Conclusions

The combustion reactivity of the char prepared at 700°C is larger than the char prepared at 900°C that correlates with a decreasing vitrinite- and total maceral reflectance and an increasing amount of dense char. This is in agreement with published results.

The combustion reactivity increases with increasing oxygen concentration (5 to 40 %), temperature (450 to 600°C) and pressure (87.5 to 287.5 kPa), which is expected as a result of the dominant intrinsic reaction rate. At higher temperatures (750 to 900°C), however, pore and film diffusional effects appear to have an effect.

Initial particle size has a significant effect on the combustion reactivity with larger particles showing a larger diffusion effect. Char particles also do not change in size during combustion mainly due to the high ash content.

The numerical method used for solving the partial differential and algebraic equations describing the chemical reaction pore diffusion model was successfully solved and validated against simplified cases with analytical solutions. The method involves essentially an iteration routine for determining the reacting gas profile in a spherical particle dependant on the Thiele modulus, followed by a subsequent determination of the solid phase conversion using a reaction rate equation.

The general set of equations describing the chemical reaction-pore diffusion model was expanded to incorporate features characteristic of combustion which include the following:

- Variation of the porosity during the reaction, which is accounted for in terms of the diffusivity coefficient.
- The presence and effect of a high ash content on the porosity of the coal char.
- Pore growth and coalescence affecting essentially the active surface area available for chemical reaction. The random pore model is applicable under these conditions.

These features were successfully introduced into the model, which could only be solved with an advanced numerical algorithm.

The solutions of the chemical reaction-pore diffusion model were examined with respect to the effect of parameters involved and a quadratic diffusivity–porosity relationship. It was found that:

- During a reaction period, a transition from a chemical reaction pore diffusion reaction regime to a chemical reaction-controlled regime can occur depending on the initial value of Thiele modulus. This phenomenon is called transitional reaction diffusion control behaviour.
- The initial Thiele modulus appearing in the reaction diffusion model is much larger than that experienced with conventional catalytic reactions simply because of the presence of an exceedingly fast combustion reaction (rate constant) and low diffusion rates (coefficients) as a result of the micropores present.

It was found necessary to develop a new routine for the determination of the unknown parameters that are characteristic of the model, namely the structural parameter, the initial Thiele modulus and the intrinsic reaction rate parameters. By plotting the carbon conversion versus a reduced time quantity, defined as the actual time divided by the time for 90% conversion ($t/t_{0.9}$), the effect of the intrinsic reaction rate is eliminated. This makes it possible to determine the structural parameter alone in the case of reaction controlling and the structural parameter with the Thiele modulus for a chemical reaction pore diffusion case.

It was found that the transitional chemical reaction–pore diffusion model was applicable for combustion reactions with 20 % oxygen between above 450 and 600°C. The reactions at 750 and 900°C are exceedingly fast with 20 % oxygen and film diffusion becomes a controlling factor.

Since the combustion reactions at low temperatures were found to include diffusional effects, an evaluation of the initial Thiele modulus using the reduced time plots would require a simultaneous evaluation of the structural parameter. This is undesirable, as regression with two unknowns would be required. This can be overcome by conducting experiments at conditions so that reaction controlled conditions exists, which can be achieved with a slower reaction. Experiments with carbon dioxide, which is a slow reaction as reported in Chapter 6, were accordingly used and the parameter value obtained was used for the modeling of combustion reaction. Using the structural parameter value reported for the carbon dioxide reaction (Chapter 6) initial Thiele moduli were evaluated over carbon conversion ranges from zero to 90%

from experimental results. Initial Thiele moduli vary from 35 to 100 for the quadratic diffusion-porosity relationship over the temperature range 450 to 600°C at 287.5 kPa were obtained.

With the known structural parameter from the carbon dioxide experiments and the initial Thiele moduli determined from the reduced time plots for the combustion experiments, the intrinsic reaction rate parameters were determined successfully from the real time plots. A first order of the reaction with respect to the concentration of oxygen was found to be satisfactory and the quadratic diffusion–porosity relationships were found to give good comparisons of experimental and model results especially at high carbon conversions. This confirms the transition to a common chemical reaction-controlling model. The activation energies and pre-exponential factors were found to be slightly lower than those reported in the literature.

Diffusion coefficients were calculated from the results obtained from the experimental results and compared with results obtained from theoretical equations published in the literature for Knudsen diffusion. It was found that the experimental results are of the same order of magnitude, which confirms the major role of the micro-pores. As the pores grow in size during the reaction, it would be necessary to include molecular diffusion in addition to Knudsen diffusion (Liu *et al.*, 2000b).

CHAPTER 8: GENERAL CONCLUSIONS AND RECOMMENDATIONS

8.1 General Conclusions

This thesis presents results concerning the characterisation of a typical South African high ash, inertinite rich discard and chars derived from that coal prepared at different temperatures, followed by the determination of the gasification and combustion characteristics and reaction rate controlling regimes of a char prepared at 900°C at reaction temperatures up to 900°C. The conclusions from this investigation are the following:

(1) The coal sample examined is characterised as a high ash, bituminous Medium Rank C coal with a low calorific value and above-average total sulphur content. Petrographically, the coal sample has a high total inertinite and a low vitrinite content with a very low liptinite composition. The intermediate microlithotypes (di- and tri-macerals) are relatively low whereas the proportion of combined mineral/maceral particles is high and even greater than the mineral-rich fraction. It is clear that this coal sample is very different to coal feedstock used in conventional pulverised coal combustion boilers and certainly different to coal feedstock used in operating fluidised bed combustors developed elsewhere in the world (especially in the Northern Hemisphere).

(2) The determination of char properties involved chars prepared from this high ash inertinite rich coal whereas results published in the literature on char properties have been confined almost exclusively to chars prepared from vitrinite rich coal samples and in most cases with low ash contents. For this purpose a carbon form analysis was used consisting of the assessment of true char, coke, inorganic matter, non-reacted and partially reacted coal fractions. Two chars were prepared at 700 and 900°C and were characterised in detail followed by reactivity measurements of the char prepared at the highest temperature. This char was chosen in order to ensure that the gasification and combustion experiments at reaction temperatures below 900°C were confined to a common char.

(3) The properties of the chars prepared at 700 and 900°C were found to be very different. The important changes that can have an influence on reactivity are the following:

The devolatisation and reflectance properties of the two chars differed as expected, but the order of magnitude of the changes with respect to reflectance of the vitrinite and of the total macerals is most noteworthy. The low temperature char experienced a minor increase in vitrinite reflectance, while the total maceral reflectance scans showed a more dramatic change. This is indicative of a greater change of the non-vitrinite fraction of the coal at 700°C whereas this did not happen at the high temperature where there was a complete conversion of all macerals with the occurrence of a large fraction of low porosity dense char.

For the low temperature char it was found that very little dense char was formed and that more than half of the pure vitrinite and nearly all the inertinite retained its original coal structure. The char prepared at 900°C experienced marked devolatilisation with complete conversion of all macerals and consisting of a large fraction of dense char originating from the inertinite. The dense phase has a very low porosity and is likely to restrict pore diffusion under certain conditions.

The major minerals present in the chars are kaolinite (53%) and quartz (18%) with nearly equal amounts of pyrite and calcite (8%) all reported on a carbon free basis. A high proportion of all the minerals (52%) occur in extraneous particles, defined as particles with more than 60 % minerals and only 13% of the minerals are included in carbon-rich particles defined as particles with minerals less than 20%.

Direct determination of structural properties (surface areas and porosities) was carried out with a BET adsorption apparatus using nitrogen and exceedingly low surface areas and pore volumes were obtained, which confirmed the low porosity of the resultant chars corresponding to the char properties obtained and reported. The structural values obtained, however, gave exceedingly large values for the structural parameter required for use in the random pore model. These values were considered meaningless as predictions based on these values gave reaction rate behaviour very different from those obtained

experimentally and were consequently not used. An alternative method for estimation of the structural parameter was consequently developed and used in the modeling procedure.

It was found that the chars experienced thermal cracking irrespective of the charring temperature (above 700°C) due to thermal stress fracturing (passive deflagration) occurring in maceral mixtures and minerals/maceral associations. This leads to cracks of different sizes, which contributes to increased porosity. It is postulated that this effect together with minute pores formed from reactive macerals in the parent coal contributes to the occurrence of a significant porous overall structure which could affect the overall reaction rate and should be accounted for in developing a model.

(4) The effect of reaction conditions, which includes temperature, pressure, gas composition and particle size on the gasification and combustion performance of the char prepared at 900°C was examined and the qualitative trends observed were consistent with what was to be expected and in agreement with published results That is, the carbon conversion rate during the gasification reaction increased with increasing carbon dioxide concentration, temperature and total pressure.

The results from the combustion experiments were found to be generally in the order of 100 times faster than the gasification reactions and these display somewhat different trends at higher temperatures. The combustion results in the high range do not appear to be as temperature dependant as over the low temperature range, which is an indication of increased diffusion effects such as pore and film diffusion. This has been analysed and confirmed with the aid of reaction rate modeling (accounting for pore diffusion) in this investigation. The decreasc of reaction rates with total pressure observed by some investigators was not found at the pressures of 87.5 and 287.5 kPa.

(5) The gasification reaction rate with carbon dioxide-nitrogen mixtures was found to be chemical reaction controlled and adequately described with the random pore model for results obtained at 750 to 900°C and 87.5 and 287.5 kPa. This model and the structural parameter characterising the pore behaviour during the gasification process were evaluated by using a plot of carbon conversion versus a reduced time parameter (real time/time for 90%

conversion) which enables evaluation and estimates of the structural parameter to be made from results determined at different temperatures and pressures (independent of the intrinsic reaction rate). This can also be deduced from the theory of the random pore model. In addition. the evaluation was confined to carbon conversion levels up to 90% (mass) in order to overcome the uncertainty of results (asymptotic) near the end of the reaction period.

A low value (mean regressed value) for the structural parameter was obtained by regression from many experimental results, which indicated that the reaction does not display a maximum when plotted against carbon conversion and that pore coalescence was the main structural mechanism. This behaviour indicates that the intrinsic reaction rate of the carbon dioxide-char reaction is very low in comparison with diffusion rates present at temperatures up to 900°C and pressures up to 287.5 kPa. Thus, the reaction rate behaviour of the char prepared at 900°C with its very low porosity can still be chemical reaction controlling for the gasification reaction involving carbon dioxide at concentrations as low as 20 % and pressures as high as 287.5kPa.

An intrinsic reaction rate equation based on power law dependence with an order equivalent to 0.5 with respect to partial pressure of carbon dioxide was found to be suitable. An activation energy and pre-exponential factor higher than that reported in the literature was obtained. which can be attributed to the specific carbon surface formed from a high inertinite coal. The high ash content appeared not to have a significant catalytic effect.

(6) The general chemical reaction-pore diffusion model for gas-solid reactions adapted to include results accounting for the particular properties of the char was found to be valid for the combustion results at temperatures between 450 and 600°C at 287.5 kPa. These properties include (1) the consumption of carbon and the ash content which affects the porosity and the maintenance of a stable particle size as a result of dominance of the mineral phase; (2) a porous structure with an initial low porosity due to the devolatilisation of a small fraction of reactive macerals (mostly vitrinite and reactive inertinites) in the parent coal and the pores/cracks formed as a result of thermal deflagration; (3) Knudsen diffusion as the initial controlling diffusion process as a result of the presence of a large fraction of micro-pores characteristic of the char structure;

(4) a varying pore structure according to the random pore model as confirmed with the same char for the gasification experiments in Chapter 6. The resulting char combustion chemical reaction-pore diffusion model equations were solved successfully with the aid of an advanced numerical algorithm (MATLAB©) and the validity of the results confirmed with known results for well-established simpler models.

For the validation of this model, it was assumed that the same structural parameter as evaluated for gasification with carbon dioxide (chemical reaction controlled) was applicable since the same char was used. The Thiele modulus was also obtained by regression using the unified carbon conversion versus reduced time plots and finally the intrinsic reaction parameters determined from the carbon versus real time plots by means of a step-wise regression procedure.

It was found that the experimental results at 450 to 600°C when plotted on the reduced time and real time plots agreed with model predictions (chemical reaction-pore diffusion) and that the reaction rate parameters and diffusion co-efficient obtained were in accordance with the Arrhenius equation and Knudsen diffusion equation respectively. This was, however, not the case for the results obtained in the temperature region 750 to 900°C which were attributed to the presence of film diffusion effects. This finding is consistent with the concept of different regimes as a function of temperature.

The results in the range 450 to 600°C are characterised by a high initial Thiele modulus, which decreases over the reaction period such that transition to chemical reaction controlling occurs near the end of the reaction period. The intrinsic reaction rate based on a first order power rate law was found to be valid and an activation energy slightly lower than that reported in the literature was assessed. The initial effective diffusivity is of the same order as that predicted according to the equation for Knudsen diffusion, which confirms the presence of mainly micro-pores.

8.2 Contributions to the knowledge base of coal science and technology

The following results originating from this investigation are considered important contributions:

(1) The relevant physical and chemical properties of a typical South African coal discard and that of corresponding chars formed under gasification and combustion conditions, which are required for predicting reaction rates were determined. These properties were found to be very different to properties of coal feedstock presently used in conventional combustion and gasification processes and to results reported in the literature. These properties can be useful for assessing the potential use of the coal in fluidised bed combustion and can be include in any international data bank on coal properties.

(2) The characterisation results of the chars formed at different temperatures derived from a high inertinite high ash coal in terms of reflectance measurements, total macerals and coal form analysis are most informative and have apparently not been examined in this manner by other investigators according to the open literature.

(3) The char analysis using CCSEM demonstrating the detailed interaction between different minerals and their associated carbon materials, with a quantitative assessment of the distribution of minerals provides a better insight into the effect of a high concentration of minerals on the char structure. The occurrence of thermal pores and cracks is attributed to the presence of different mineral/maceral associations which created a structure suitable for intra-particle diffusion.

(4) The modeling of gasification of a char at temperatures below 900°C using the random pore model for a char derived from a high inertinite coal, with a structural parameter derived according to a procedure using a reduced time parameter is considered novel. This procedure overcomes the problem associated with results obtained by adsorption and image analysis especially for char with very low porosities.

(5) The modelling of combustion of a char with chemical reaction-pore diffusion based on features of the char structure (qualitative and quantitative) and results obtained under chemical reaction controlled conditions are most noteworthy

and of great significance. This result is considered as the major achievement of this study.

(6) It was deduced that the devolatilisation of reactive macerals in the coal and the occurrence of thermal deflagration (cracking) produced a low porous structure, which introduced pore diffusion controlled conditions (in addition to chemical reaction) when combustion occurs. For the very slow carbon dioxide char reaction the pore diffusion rate is very fast in comparison with the intrinsic reaction rate and does not contribute to the overall reaction rate (chemical reaction controlled). This result has also not been published.

8.3 Recommendations for future investigations

The following recommendations based on the results of this investigation are proposed for further investigation, which can contribute to the expansion of the knowledge of the utilisation of discards rich in ash and with high inertinite content.

(1) An in-depth study confined to the characterisation and kinetics of chars formed by devolatilisation under reaction conditions prior to the actual char-gas gasification or combustion should be undertaken. These results will be more meaningful for industrial application since as it is well known that the initial period consisting of pyrolysis has a marked effect on the overall performance and this would depend on the raw coal properties.

(2) The effect of different inertinite forms and proportions larger than 50% (typical South African discards) and the presence of the other macerals on the reaction regimes for gasification and combustion with particular attention to the transition temperatures need to be investigated. The model developed in this investigation would have to be expanded to include film diffusion in order to establish regimes over a very wide range of temperatures.

(3) A detailed study of the composition of the minerals in the ash and the effect of intrinsic reaction rate kinetics in order to establish any catalytic effects. This would also be possible at high temperatures in the presence of pore diffusion according to the results obtained in this investigation. Coupled to this the

determination of thermal cracking with particular attention to the composition and mineral/maceral associations could be most useful.

(4) The determination of the structural properties for the very low porosity chars needs to be investigated in depth using other advanced techniques. These results have a great influence on of the validity of the random pore model and needs to be determined accurately for a meaningful validation of the model.

(5) Characterisation of the char to track changes during the reaction period could be most informative and could enhance the validation of theoretical predictions. This would involve terminating the reaction at different periods of time and analysing the samples with advanced analytical equipment. These measurements could consist, for example, of surface areas, porosity, coal form analysis and other relevant petrographic measurements.

REFERENCES

ADSCHIRI, T. AND FURUSAWA, T (1986). Relation between CO_2-reactivity of coal char and BET surface area, *Fuel* 65:1688.

AHN, D.H. GIBBS, K.H. AND KIM, J.J. (2001). Gasification kinetics of an Indonesian sub-bituminous coal-char with CO_2 at elevated pressure. *Fuel* 80:1651-1658.

ALONSO, M.J.G. BORREGO, A.G. ALVAREZ, D. PARRA, J.B. AND MENENDEZ, R. (2001a). Influence of pyrolysis temperature on char optical texture and reactivity. *Jour. Anal. Appl. Pyrolysis* 58-59:887-909.

ALONSO, M.J.G. BORREGO, A.G. AND MENENDEZ, R. (2001b). A reactivity study of chars obtained at different temperatures in relation to their petrographic characteristics. *Fuel Processing Technology* 69:257-272.

Association for the study of peak oil and gas. Newsletter 28, December (2004). www.peakoil.net.

AUSMAN, J.M. AND WATSON, C.C. (1962). Mass transfer in a catalyst pellet during regeneration. *Chemical Engineering Science* 17:323.

AVRAMI, M. (1940). Kinetics of phase change: II Transformation-time relations for random distribution of nuclei. *Journal of Chemical Physics* 8:212.

BAILEY, J.G. TATE, A.G., DIESSEL, C.F.K. AND WALL, T.F. (1990). A char morphology system with applications to coal combustion, *Fuel* 69:225.

BALLAL, G. AND ZYGOURAKIS, K. (1987a). Evolution of pore surface area during non-catalytic gas-solid reactions 1. Model development. *Ind. Eng. Chem. Res.* 26 (5):911-920.

BALLAL, G. AND ZYGOURAKIS, K. (1987b). Evolution of pore surface area during non-catalytic gas-solid reactions 1. Experimental results and model validation. *Ind. Eng. Chem. Res* 26 (5):1787-1796.

BAUM, M.M. AND STREET, P.J. (1971). Predicting the combustion behaviour of coal particles. *Combustion Science and Technology* 3:231.

BEND, S.L. EDWARDS, I.A.S. AND MARSH, H. (1991). Coal provincialism, coal characterisation and char formation. *Fuel* 70(10):1147.

BEND, S.L. EDWARDS, I.A.S. AND MARSH, H. (1992). The influence of rank upon char morphology and combustion. *Fuel* 71:493-501.

BEAMISH, B.B. SHAW, K.J. RODGERS, K.A. AND NEWMAN, J. (1998). Thermogravimetric determination of the carbon dioxide reactivity of char from New Zealand coals and its association with inorganic geochemistry of the parent coal. *Fuel Processing Technology* 53:243.

BERKOWITZ, N. (1985). The chemistry of coal. Amsterdam, New York.

BENFELL, K.E. (2001). Assessment of char morphology in high-pressure pyrolysis and combustion. Doctoral Thesis. The University of Newcastle. Australia.

BHATIA, S.K. AND PERLMUTTER, D.D. (1980). A random pore model for fluid-solid reactions: I. Isothermal, kinetic control. *AIChE Journal* 26. (3):379-385.

BHATIA, S.K. AND PERLMUTTER, D.D. (1981). A random pore model for fluid solid reactions: II. Diffusion and Transport Effects, *AIChE Journal* 27(2):247.

BHATIA, S.K. AND GUPTA, G.R. (1992). Mathematical modeling of gas-solid reactions: Effect of pore structure. *Reviews Chemical Engineering* 8:177-258.

BHATIA, S.K. (1998). Reactivity of chars and carbons: New insights trough molecular modeling. *AIChE Journal* 44 (11):2478.

BLACKWOOD, J.D. AND INGEME, A.J. (1960). Reaction of carbon with carbon dioxide at high pressure. *Australian Journal of Chemistry* 13:194.

BREM, G. AND BROUWERS, J.J.H. (1990). Analytical solutions for non-linear conversion of a porous solid particle in a gas. *Chemical Engineering Science* 45(7):1905-1924.

Broadbent, S.R. and Hammersley, J.M. (1957) Percolation processes I crystal and mazes. Proceedings of Cambridge Philosophical Society. 53:629.

BRUNAUER, S. DEMING, L.S. DEMING, W.S. AND TELLER, E. (1940). On a theory of the van der Waals adsorption of gases. *AIChE Journal* 62:1723-1732.

CAI, H.-Y. GUELL, A.J. CHATZAKIS, I.N. LIM, J.-Y. DUGWELL, D.R. AND KANDIYOTI, R. (1996). Combustion reactivity and morphology changes in coal chars: effect of pyrolysis temperature, heating rate and pressure *Fuel* 75:15-24.

CAI, H.-Y. MEGARITIS, A. MESSENBOCK, R. DIX, M. DUGWELL, D.R. AND KANDIYOTI, R. (1998) Pyrolysis of coal maceral concentrates under Pf combustion conditions (1). Changes in volatile release and char combustibility as a function of rank. *Fuel* 77 (12):1273-1282.

CALO, J.M. AND SUURBERG, E.M. (1999). High pressure/temperature thermogravimetric apparatus report. Brown University. U.S.A.

CHILDLESS, J.M. (2005). The world gasification industry (2000-2004, 2005-2010): Major factors and treads driving growth. Proceedings of 22nd Annual International Pittsburgh Coal Conference. Pittsburgh. September 22-15.

CHORNET, E., BALDASANO, J.M. AND TARKI, H.T. (1979). Kinetic expressions for coal char-gas reactions. *Fuel* 58(5):395-396.

CLOKE, M. AND LESTER, E. (1994). Characterisation of coals for combustion using petrographic analysis. A review. *Fuel* 73:315-320.

CRELLING, J.C. SKORUPSKA, N.M. AND MARSH, H. (1988). Reactivity of coal macerals and lithotypes. *Fuel* 67:781-785.

CRELLING, L.C. HIPPO, E.J. WOERNER, B.A. AND WEST, D.P. (1992). Combustion characteristics of selected whole coals and macerals. *Fuel* 71:151-158.

DAVIES, K.A. HOURT, R.H. YANG, N.Y.C. AND HEADLEY, T.J. (1995). Evolution of char chemistry, crystallinity, and ultrafine structure during pulverised-coal combustion. *Combustion and Flame* 100:31.

DEPARTMENT OF MINERALS AND ENERGY. (2003). South Africa's Mineral Industry 2002/2003. Pretoria, South Africa: Government Printer.

Du CANN, V.M. (2005a). Test Report P160-2004. SABS, Pretoria South Africa. June.

DU CANN, V.M. (2005b). Test Report P112-2004, SABS, Pretoria South Africa, February.

DUTTA, S. WEN, C.Y. AND BELT, R.J.J. (1977). Reactivity of coals and char. 1. In carbon dioxide atmosphere. *Ind Eng Chem. Process* 16(1):20-30.

ESSENHIGH, R.H. (1982). Fundamentals of coal combustion in Chemistry of Coal Utilization: Second Supplementary Volume. Elliot, M.A., Ed. Wiley and sons, Inc., New York. Pp1153-1313.

ESSENHIGH, R.H. (1991). Rate equations for the carbon-oxygen reaction: an evaluation of the Langmuir adsorption isotherm at atmospheric pressure. *Energy and Fuels* 5:41.

ESSENHIGH, R.H. AND MESCHER, A.M. (1997). Mechanism of carbon combustion: relative influence of adsorption, desorption and boundary layer diffusion as a function of pressure. *Combustion and Flame* 111:350.

EVERSON, R.C. NEOMAGUS, H.W.J.P. AND KAITANO, R. (2005). The modeling of the combustion of high-ash particles suitable for pressurized fluidised bed combustion: shrinking reacted core model. *Fuel* 84:1136-1143.

EVERSON, R.C. NEOMAGUS, H.W.J.P. KASAINI, H. AND NJAPHA, D. (2006). Reaction kinetics of pulverised coal-chars derived from inertinite-rich coal discards: Characterisation and combustion. *Fuel*.88 (7-8):1067-1075.

FALCON, R.M.S. AND SNYMAN, C.P. (1986). An introduction to coal petrology. Atlas of petrographic constituents in the bituminous coals of Southern Africa. The Geological Society of South Africa. Review Paper Number 2.

FROMENT, G.F. AND BISCHOFF, K.B. (1990). Chemical Reactor Analysis and design. John Wiley and Sons. USA.

FU, W.B. AND WANG, Q.H. (2001). A general relationship between the kinetic parameters for the gasification of coal chars with CO_2 and coal type. *Fuel Processing Technology*, 72:63-77.

GALE, T.K. BARTHOLOMEW, C.H. AND FLETCHER, T.H. (1995). Decreasing in the swelling and porosity of bituminous coals during devolatilisation at high heating rates. *Combustion and Flame* 100:94.

GARDNER, N.C. SAMUELS, E. AND WILKS, K. (1979). Modeling of coal combustion. Advanced Chemistry Series 131:217-220.

GAN, H. NANDI, S.P. AND WALKER, JR., P.L. (1972). Nature of the porosity in American coals. *Fuel* 51:272.

GAVALAS, G.R. (1980a). A random capillary model with application to char gasification at chemically controlled rates. *AIChE Journal* 26(4): 577.

GAVALAS, G.R AND WILKS, K.A. (1980b). Intraparticle mass and transfer in coal pyrolysis. *AIChE Journal* 26:201.

GAVALAS. G.R. (1981). Analysis of char combustion including the effect of pore enlargement. *Combustion Science and technology* 24:197.

GOMEZ-BAREA, A. OLLERO, P. AND ARJONA, R. (2005). Reaction –diffusion model of TGA gasification experiments for estimating diffusional effects. *Fuel* 84:1695-1704.

GOODARZI, F. AND VLEESKENS, J.M. (1988). Reactivity of bituminous semi-anthracitic coals: reflected light study of their combustion residues (fly ash). *Journal of Coal Quality*. 7: 80-85.

GOPALAKRISHNAN, R. AND BARTHOLOMEW, C.H. (1996). Effects of CaO. High temperature treatment, carbon structure and coal rank on intrinsic char oxidation rates. *Energy and Fuels* 10:689-695.

GREGG, S.J. AND SING, K.S.W. (1982). Adsorption, surface area and porosity. Second Edition. Academic Press. London.

GRIFFIN, L.P. HOWARD, J.B. AND PETERS, W.A. (1994). Pressure and temperature effects in bituminous coal pyrolysis: experimental observations and a transient lumped parameter model. *Fuel* 73:591.

GURIERREZ, M.D.C. CUKIERMAN, A.L. AND LEMCOFF, N.O. (1988). Study of sub-bituminous coal chars. Effect of heat treatment on their structural characteristics. *Journal. Chem. Tech. Biotechnology*. 41:85.

GUPTA, J.S. AND BHATIA, S.K. (2000) A modified discrete random pore model allowing for different initial surface reactivity. *Carbon* 38:47-58.

HASHIMOTO, K. MIURA, K. YOSHIKAWA, F. AND IMAI, I. (1979) Change in pore structure of carbonaceous materials during activation and adsorption performance of

activated carbon. *Industrial Engineering Chemistry, Process Design Development* 18:72.

HASHIMOTO, K. MIURA, K. AND UEDA, T. (1986). Correlation of gasification rates of various coals measured by rapid heating method in a steam atmosphere at relatively low temperature. *Fuel* 65:1516.

HIPPO, E. AND WALKER, P.L. jr. (1972) Reactivity of Heat Treated Coals in Carbon Dioxide at 900°C. *Fuel* 54:245.

HURT, R.H. SAROFIM, A.F. AND LONGWELL, J.P. (1991). Effect of non-uniform surface reactivity on the evolution of pore structure and surface area during carbon gasification. *Energy and Fuels* 5:463.

HURT, R.H. DAVIS, K.A. YANG, N.Y.C. HEADLY, T.J. AND MITCHELL, G.D. (1995). Residual carbon from pulverised coal fired boilers: 2. Morphology and physicochemical properties. *Fuel* 74:1297.

HURT, R.H. AND GIBBINS, J.R. (1995). Residual carbon from pulverised coal fired boilers: Size distribution and combustion reactivity. *Fuel* 74:471.

HURT, R. SUN, K.K. AND LUNDEN, M. (1998). A kinetic model of carbon burning in pulverised coal combustion. *Combustion and Flame* 113:181.

HURT, R.H. (1998). Structure, properties and reactivity of solid fuels. Proceedings of the Combustion Institute 27:2887-2904.

HURT, R.H. AND CALO, J.M. (2001). Semi-global intrinsic kinetics for char combustion modeling. *Combustion and Flame* 125:1138-1149.

HURT, R.H. AND HAYES, B.S. (2005). On the origin of the power- law kinetics in carbon oxidation. Proceedings of the Combustion Institute. 30:2161-2168

HUTTINGER, K.J. AND NATTERMANN, C. (1994). Correlation between coal reactivity and inorganic matter content for pressure gasification with steam and carbon dioxide. *Fuel* 73:1682

International Standard. ISO 7404-3 (1994). Methods for the petrographic analysis of bituminous coal and anthracite. Part 3: Method of determining maceral group composition.

ISHIDA, M. AND WEN, C.Y. (1968). Comparison of kinetic and diffusional models for solid-gas reactions. *AIChE. Journal* 14(2):311-317.

JOHNSON, J.L. (1979a). Kinetics of bituminous coal char gasification with gases containing steam and hydrogen. *Advances in Chemistry* 137:145-178.

JOHNSON, J.L. (1979b). Kinetics of coal gasification. Wiley and Sons, Inc., New York. 283p.

JOHNSON J.L. (1981). Fundamentals of coal gasification, In: Chemistry of Coal Utilisation, Second Sup. Volume, Wiley Inter-science, New York: 1591-1598.

JONES, R.B. MCCOURT C.B. MORLEY, C. AND KING, K. (1985a). Macerals and rank influence on the morphology of coal char, *Fuel* 64:460.

JONES, R.B. MORLEY, C AND MCCOURT, C.B. (1985b). Maceral effects on the morphology and combustion of coal char, Proceedings of 1985 International Conference on Coal Science, Sydney, Australia, p. 669.

KAJITANI, S. SUZUKI, N. ASHIZAWA, M. AND HARA, S. (2006). CO_2 gasification rate analysis of coal char in entrained flow coal gasifier. *Fuel* 85:539.

KASAOKA, S. SAKATA, Y. AND TONG, C. (1985). Kinetic evaluation of the reactivity of various coal chars for gasification with carbon dioxide in comparison with steam. *International Chemical Engineering* 25:160.

KAWAHATA, M. AND WALKER, P.L. (1992). Mode of porosity development in activated anthracite. Proceedings of the Fifth Carbon Conference, Pergamon Press, New York. Vol 2:251-263

KHAN, M.R. AND JENKINS, R.G. (1986). Swelling and plastic properties of coal devolatilised at elevated pressures: an examination of the influences of coal type. *Fuel.* 65:725-731.

KHAN M.R. AND JENKINS, R.G. (1989). Chemistry of coal weathering. Elsevier. Amsterdam.

KIDENA, K. KATSUYAMA, M. MURATA, S. NOMURA, M. AND CHIKADA. (2002). Study on plasticity of maceral concentrates in terms of their structural features. *Energy and Fuels* 16(5):1231-1238.

KNIGHT, A.T. AND SERGEANT, G.D. (1982). Reactivity of Australian coal-derived chars to carbon dioxide. *Fuel* 71:879.

KUHL, H. KASHANI-MOTAGH, M.M. MUHLEN, H.J. and Van HEEK, K. H. (1992). Controlled gasification of different carbon materials and development of pore structure. *Fuel* 71:879.

KWON, H. KIM, S.D. AND FUNG, D.P.C. (1988). Reaction kinetics of char-CO@ gasification. *Fuel* 67:530.

LAINE, N. R. VASTOLA, F.J AND WALKER, P. L. (1963). The importance of active surface area in the carbon-oxygen reaction. *Journal of Physical Chemistry* 67:2030-2034.

LAURENDEAU, N. M. (1978). Heterogeneous kinetics of coal char gasification and combustion. *Progress in Energy and Combustion Science* 4:221.

LESTER, T.W. SEEKER, W.R. AND MERKLIN, J. (1981). The influence of oxygen and total pressure on the surface oxidation of bituminous coal. Proceedings of the Combustion Institute. 18:1257.

LESTER, E. AND CLOKE, M. (1999). The characterisation of coals and their respective chars formed at 1300 C in a drop tube furnace. *Fuel*. 78:1645-1658.

LEWELLEN, (1975). Product decomposition effects of coal pyrolysis. Doctoral Thesis. Cambridge Massachusetts Institute of Technology. USA.

LEWIS, P.F. AND SIMONS, G.A. (1979). Car gasification: Part II. Oxidation results. *Combustion Science and Technology* 20:117.

LIGHTMAN, P. AND STREET, P.J. (1968). Microscopical examination of heat treated pulverised coal particles. *Fuel* 47:7-28.

LILIEDAHL T AND SJÖSTRÖM, K (1997). Modeling of char-gas reaction kinetics. *Fuel* 76(1):2937.

LIU, G.S. (1999). Mathematical modelling of coal char reactivity in a pressurised entrained flow gasifier. Doctoral Thesis. University of Newcastle, Australia.

LIU, G. BENYON, P. BENFELL, K.E. BRYANT, G.W. TATE, A.G. BOYD, R.K. HARRIS, D.J. AND WALL, T.F. (2000a). The porous structure of bituminous coal chars and its influence on combustion and gasification under chemically controlled conditions. *Fuel* 79:617-626.

LIU, G. TATE, A.G. BRYANT, G.W. AND WALL, T.F. (2000b) Mathematical modeling of coal char reactivity with CO_2 at high pressures and temperatures. *Fuel* 79:1145-1154.

LIU, Y.I. GUPTA, R. SHARMA, A. WALL, T. BUTCHER, A. MILLER, GOTTLIEB, AND FRENCH, D. (2005) Mineral matter-organic matter association characterisation by QEMSCAN and application in coal utilization. *Fuel* 84:1259-1267.

LIU, G.S. AND NIKSA, S. (2004). Coal conversion submodels for design applications at elevated pressures: Part II: Char gasification. *Progress in Energy and Combustion Science* 30:679-717.

LU, G.Q. (1995). Preparation and characterisation of an effective sorbet for SO_2 and NO_x removal using coal washery reject. Doctoral Thesis. University of Queensland, Australia.

LU, G.Q. AND DO, D.D. (1992). A kinetic study of coal reject-derived char activation with CO_2, H_2O and air. *Carbon*. 30 (1): 21-29.

LU, G.Q. AND DO, D.D. (1994) Comparison of structural models for high-ash char gasification. *Carbon*. 32 (2):247-263.

LU, L., SAHAJWALLA, D. AND HARRIS, D. (2000). Characteristics of chars prepared from various pulverised coals at different temperatures using drop tube furnace. *Energy and Fuels*. 14:869-676.

MARQUEZ, F.M. CORDERO, T. MIRASOL, J.R. AND RODRI'IGUEZ, J.J. (2002). CO_2 and steam gasification of grapefruit skin char. *Fuel* 81:423-429.

MARSH, H. AND KUO, K. (1989). Kinetics and catalysis of carbon gasification. Introduction to carbon science. Ed. Marsh H. Butterworths. London

MELENDEZ, R.B. (2001). The characterisation and combustion of South American Coals. Doctoral thesis. University of Nottingham. UK.

MESSENBOCK, R.C. DUGWELL, D.R. AND KANDIYOTI, R. (1999). CO_2 and steam-gasification in high-pressure wire-mesh reactor: the reactivity of Daw Mill coal and combustion reactivity of its chars. *Fuel* 78:781-793.

MENDEZ, L. B. BORREGO, A.G. MARTINEZ-TARAZONA, M.R. AND MENENDEZ, R. (2003) influence of petrographic and mineral matter composition of coal particles on their combustion reactivity. *Fuel* 82:1875-1882.

MENENDEZ, R. VLEESKENS, J.M. AND MARSH, H. (1993). The use of scanning electron microscopy for classification of coal-chars during combustion. *Fuel* 72:611-617.

MENENDEZ, R. ALVAREZ, D. AND FUERTES, A.B. (1994). Effects of clay minerals on char texture and combustion. *Energy and Fuels* 8:1007-1015.

MIURA, K. HASHIMOTO, K. AND SILVESTON, P.L. (1989). Factors affecting the reactivity of coal chars during gasification, and indices representing reactivity. *Fuel* 68:1461.

MOHANTY, K.K. OTTINO, J.M. AND DAVIS, H.T. (1982). Reaction and transport in disordered media: introduction of percolation concepts. *Chemical Engineering Science* 37:905-924.

MONSON, C.R., GERMANE, G.J. BLACKHAM, A.J. AND SMOOT, L.D. (1995). Char oxidation at elevated pressure. *Combustion and Flame*, 100:387

MUHLEN, H.J. VAN HEEK, K.H. AND JUNTGEN, H. (1985). Kinetic studies of steam gasification in the presence of H_2O, CO_2 and CO. *Fuel* 64:944.

MÜHLEN, H.J. AND SULIMA, A. (1986). Thermogravimetric apparatus for characterisation of coal with regard to pyrolysis and gasification under pressure up to 100bar. Coal characterisation for conversion processes 1986. Proceedings of the first international Roluduc Symposium on Coal Science. April 28-May 1, 1986, Rolduc. The Netherlands.

MÜHLEN, H.J. AND SOWA, F. (1995). Factors influencing the ignition of coal particles-studies with a pressurized heated-grid apparatus. *Fuel* 74:1551-1554.

MURILLO, R. NAVARRO, M.V. LÓPEZ, J.M. GARCÍA, T. CALLÉN M.S. AYLÓN, E AND MASTRAL, A.M. 2006. Activation of pyrolitic lignite char with CO_2. Kinetic study. *Energy & Fuels* 20:11-16.

NIKSA, S. LIU, G.S. AND HURT, R.H. (2003). Coal conversion submodels for design applications at elevated pressures. Part 1. Devolatilisation and char combustion. *Progress in Energy and Combustion Science* 29:425-477.

NJAPHA, D. (2003). Determination of the kinetic models and associated parameters for the low temperature combustion and gasification of high-ash coal chars. Doctoral Thesis. North-West University.

NOMURA, M. KIDENA, M. HIRO, M. AND MURATA, S. (2000) Mechanistic study on the plastic phenomena of coal. *Energy and Fuels*. 14:904-909.

NOZAKI, T. ADSCHIRI, T. AND FUJIMOTO, K. (1992). Coal char gasification under pressurized CO_2 atmosphere. *Fuel* 71,213.

O'BRIEN, G. JENKINS, B. ESTERLE, J. AND BEATH, H. (2003). Coal characterisation by automated coal petrography. *Fuel* 82:1067-1073.

OKA, N. MURAYYAMA, T. YAMADA, S. YAMADA, T. SHINOZAKI, S. SHINOZAKI, M. AND THOMAS, C.G. (1987). The influence of rank and maceral composition on ignition and char burnout of pulverised coal. *Fuel Processing Technology* 15:384.

PETERSEN, E.E. (1957). Reaction of porous solids. *AIChE Journal* 3:443-448.

RADOVIC, L.R. STECZKO, K. WALKER, P.L. AND JENKINS, R.G. (1985). Combined effects of inorganic constituents and pyrolysis conditions on the gasification reactivity of coal chars. *Fuel Processing Technology* 10:311.

REYES, S. AND JENSEN, K.F. (1986). Percolation concepts in modeling of gas-solid reactions: Application to char gasification in the kinetic regime. *Chemical Engineering Science* 41:333.

RICHARD, J.R. MAJTHOUB, M.A. AHO, M.J. PIRKONEN, P.M. (1994). Separate effects of pressure and some other variables and char combustion under fixed bed combustion. *Fuel* 73:485.

ROBERTS, D.G. AND HARRIS, D.J. (2000a). Char gasification with O_2, CO_2 and H_2O : effects of pressure on intrinsic reaction kinetics. *Energy and Fuels* 14:483.

ROBERTS, D.G. HARRIS, D.J. AND WALL, T.F. (2000b). Total pressure effects on chemical reaction rates of chars with O_2, CO_2 and H_2O. *Fuel* 79:1997-1998.

ROSENBERG, P. PETERSEN, H.I. AND THOMSEN, E. (1996a). Combustion char morphology related to combustion temperature and coal petrography. *Fuel* 75(9):1082-1996.

ROSENBURG, P. PETERSEN, H.I. AND THOMSEN, E. (1996b). Combustion char morphology related to combustion temperature and coal petrography, *Fuel* 9:739.

SALATINO, P. AND SENNECA, O. (1998). Loss of gasification reactivity of coal chars upon thermal annealing. International Conference on ash behaviour control in energy conversion systems. Pacifico Yokohama, Japan.

SANDMANN, C.W. AND ZYGOURAKIS. (1986). Evolution of pore structure during gas-solid reactions: Discrete models. *Chemical Engineering Science* 41(4):733-739.

SATTERFIELD, C.N. (1970). Mass Transfer in heterogeneous catalysis. M.I.T Press, Cambridge, Mass.

SCHUMACHER, W. MUHLEN, H.J. VAN HEEK, K.H. AND JUNTGEN, H. (1986). Kinetics of K-catalysed steam and CO_2 gasification in the presence of product gases. *Fuel* 65:1360-1363.

SCHOBERT, H.H. (2006) Penn State University, USA., Private communication.

SENNECA, O. SALATINO, P. AND MASI, S. (1998). Microstructural changes and loss of gasification reactivity of chars upon heat treatment. *Fuel*. 77:1483.

SHUFEN, L. AND RUIZHENG, S. (1994). Kinetic studies of alignite char pressurised gasification with CO_2, H_2 and steam. *Fuel* 73 (3):413.

SIMON, I.W. (1980). The unified coal-char reaction. *Fuel* 59(2):143-144.

SIMON, G.A. (1983). The role of pore structure in coal pyrolysis and gasification. *Progress in Energy Combustion Science* 9:227.

SINGLA, P.K. MIURA, S. HUDGINS, R. AND SILVESTON, P.L. (1981). Pore development during carbonization of coals. *Fuel* 62:645.
SMITH, I.W. (1982). The combustion rates of coal chars: review. Proceedings of the Combustion Institute. 19:1095-1065

SMITH, W.H. ROUX, H.J. AND STEYN, J.G.H. (1983). The classification of coal macerals and their relation to certain chemical and physical parameters of coal. Special publication of Geological Society of South Africa. 7:111-115.

SMOOT, L.D. AND SMITH, P.J. (1985). Coal gasification and combustion. Plenum Press. New York and London.

SOLOMAN, P.R. AND FLETCHER, T.H. (1994). Impact of coal pyrolysis on combustion. Proceedings of the Combustion Institute. 25:405.

SORENSON, H.S. ROSENBERG, P. PETERSEN, H.I. AND SORENSEN, L.H. (2000). Char porosity characterisation by scanning electron microscopy and image analysis. *Fuel* 79:1379-1388.

STANELY-WOOD, N.G. AND LINES, R.W. (1992). Particle size analysis. Royal society of Chemistry. University of Technology, Loughborough, UK.

SU, J. L. AND PERLMUTTER, D. D. (1985). Effect of pore structure on char oxidation kinetics. *AIChE Journal* 31(6):973-981.

TANG, L. GUPTA, R. SHENG, C. AND WALL, T. (2005a). The char structure characterisation from the coal reflectogram. *Fuel* 84:1268-1276.

TANG, L. GUPTA, R., SHENG, C. AND WALL, T. (2005b). The estimation of the char reactivity from coal reflectogram. *Fuel* 84:127-134.

TSAI, S.C. (1982). Fundamentals of Coal Beneficiation and Utilisation. Elsevier, Amsterdam. 292p.

Van KREVELEN, D.W. (1981). Coal: Topology, Physics, Chemistry, Constitution. Elsevier. Amsterdam.

Van KREVELEN, D.W, HUNTJENS, F.J. AND DORMANS, H.N.M. (1956). Chemical structure and properties of coal. XVI. Plastic behaviour on heating *Fuel* 35:462-475.

VASSILEV, S. V. AND TASCON, J.M.D. (2003). Methods for characterisation of inorganic and mineral matter in coal; A critical overview. *Energy and Fuels* 17:271-281.

VLEESKENS, J.M., MENENDEZ, R.M., ROOS, C. AND THOMAS, C.G. (1993). Combustion in the burnout stage: the fate of inertinite. *Fuel Processing Technology* 36:91-99.

Van ALPHEN, C. (2005a). Description of selected char samples. V*an Alphen Consultancy .Research Report*. Johannesburg, South Africa.

Van ALPHEN, C. (2005b). Van Alphen Consultancy Research Report, October.

WAKAO, N. AND SMITH, J.M. (1962). Diffusion in catalyst pellets. *Chemical Engineering Science* 17:825.

WALKER, P.L., RUSINKO, F. AND AUSTIN, L.G. (1959). Gas reactions of carbon. Advances in catalysis and related subjects. Academic Press, New York. 11: 133-221.

WALKER, P.L. MATSUMOTO, S. HANZAWA, T. MUIRA, AND ISAMAIL, I.M.K. (1983). Catalysis of gasification of coal-derived cokes and chars. *Fuel* 62:140.

WALKER, P.L. AND MAHAJAN, O. (1993) Pore structure in coals. *Energy and Fuels* 7:749.

WELLS, W.F. AND SMOOT, L.D. (1985). Particle size dependence of coal reactivity. *Combustion and Flame 68*:481.

WEEDA, M. ADCOUWER, H.H. KAPTEIN, F. AND MOULIJN, J.A. (1993). Steam gasification kinetics and burn-off behaviour for a bituminous coal derived in the presence of H_2. *Fuel Processing Technology* 36:81.

WEEDA, M. ERMERS, F.V.D. LINDEN, B. KAPTEIJN, F. AND MOULIJN, J.A. (1993). Anomalous carbon dioxide gasification behaviour of high temperature coal chars. *Fuel Processing Technology* 36:243-250.

WEEDA, M. (1995). Kinetics of coal gasification under industrial conditions. Doctoral thesis. University of Amsterdam. Netherlands.

WEISZ, P.B. AND GOODWIN, R.D. (1963). Combustion of carbonaceous deposits within porous catalyst particles. *Journal of Catalysis* 2:397.

WHEELER, A. (1951). Reaction rates and selectivity in catalyst pores. Advances in Catalysis. Academic Press Inc.

WEN, C.Y. (1968). Non catalytic heterogeneous solid fluid reactions. *Industrial Engineering Chemistry* 60:34-54.

WIGLEY, F., WILLIAMSON, J. AND GIBB, W.H. (1997). The distribution of mineral matter in pulverised coal particles in relation to burnout behaviour. *Fuel*. 26:1283-1288.

WILLIAMS, A. POURKASHANIAN, M AND JONES, J.M. (2000). The combustion of coal and some other solid fuels. Proceedings of the Combustion Institute. 28:2141-2162

YANG, A. AND WATKINSON, A.P. (1994). Gasification reactivity of some Western Canadian coals. *Fuel* 73:193.

YE, D.P. AGNEW, J.B. AND ZHANG, D.K. (1998). Gasification of a South Australian low-rank coal with carbon dioxide and steam: kinetics and reactivity studies. *Fuel* 77(11):1209-1219.

YOUNG, B.C. AND SMITH, I.W. (1987). Carbon combustion: the order of reaction in oxygen. International conference on coal science. Elsevier Science Publishers. The Netherlands. p793.

YU, J. (2002). A mechanistic study of coal swelling and char structure evolution during pyrolysis – Experimental and model predictions. Doctoral Thesis. The University of Newcastle, Australia.

ZHU, J. (2007) University of Queensland, Australia. Private communication.

ZYGOURAKIS, K. (1993). Effect of pyrolysis conditions on the macropore structure of coal-derived chars. *Energy and Fuels* 7(1):33-41.

APPENDICES

APPENDIX A: Char preparation

The char was prepared as described in Chapter 4. The char was derived from the parent coal via pyrolysis using a Packed Bed Balance Reactor, (PBBR). A sketch of the PBBR reactor is given in Figure A1.

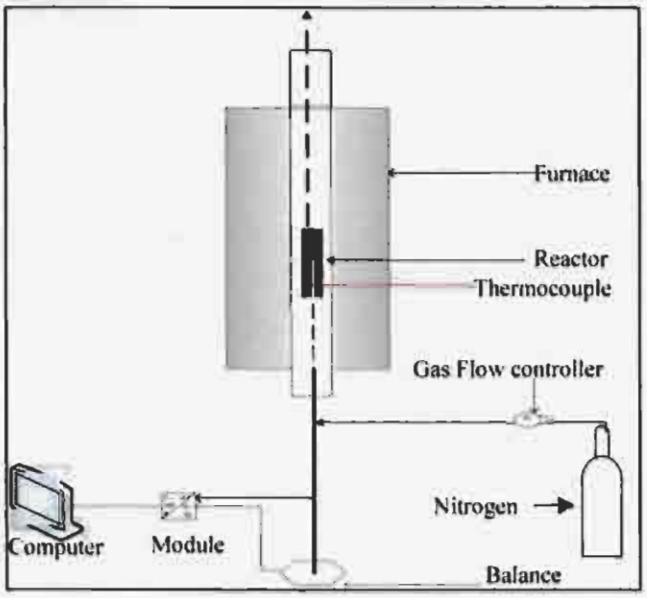

Figure A1: Experimental set up for char preparation

APPENDIX B: Classification system for char forms

The microscopic constituents of the samples were assessed by virtue of their colour, reflectance, and degree of anisotropy, size, morphology and extent of devolatilisation. The relative proportions of the carbon-rich constituents/inorganic materials in each case were established on the basis of a 500 point-count according to the method set out in the ISO Standard 7404 - 3, 1994.

The following system of main groups and categories was used:

GROUP A

The components included in this group all showed relatively very high reflectances in normal white light. Oxidation effects were minimal or absent.

Category 1: DENSE CHAR

Mainly originating from inert inertinites; low porosity

Category 2 and 3: NETWORKS

Mainly formed from bi- and tri-macerite, the reactive macerals having devolatilised and "plastified" leaving a network of very highly reflecting material.

Fine walled - High porosity

Thick walled - Medium porosity

GROUP B

These components could be classified as "Coke", i.e. continuous carbon matrices formed from vitrinites and reactive inertinites. The particles were highly reflecting. Oxidation features were minimal or absent.

Category 4 and 5: CIRCULAR ANISOTROPIC

Carbon textures exhibiting approximately circular regions of distinctly marked anisotropy.

Fine Circular Anisotropic - Anisotropy in the 0.5 to 1.0-micron size category.

Medium Circular Anisotropic - Anisotropy in the 1.0 to 1.5 micron size category.

Category 6: INCIPIENT ANISOTROPIC

Anisotropic forms showing less well-developed textures with domain size of less than 0.5 microns.

Category 7: ISOTROPIC

Derived from vitrinite in the original coal; no developed texture.

GROUP C

These constituents all exhibited relatively lower reflectances and marked oxidation features, in most cases very distinct oxidation rims.

Category 8: "OXIDISED" - mainly from vitrinite

Category 9:" OXIDISED" - mainly from inertinite

Category 10:"OXIDISED" - low reflecting network

GROUP D

Original coal macerals, which have been little affected by the process

Category 11: ORIGINAL COAL - unaffected

Category 12: ORIGINAL COAL - partially affected

GROUP E

Category 13: INORGANIC MATTER - apparently derived from the minerals in the parent coal

Category 14: INORGANIC MATTER - apparently additive to the original coal

GROUP F

Category 15: PROCESS-DERIVED DEPOSITIONAL CARBONS

Including pyrolytic and spherulitic carbons

APPENDIX C: Abbreviations and terms used in petrographic analysis

1. Maceral analysis (% by volume)

The abbreviations used are defined as follows:

VIT	Vitrinite
PV	Pseudovitrinite
TV	Total vitrinite
S/R/C	Sporinite/resinite/cutinite
ALG	Alginite
TOT L	Total liptinite (formerly referred to as exinite)
RSF	Reactive semifusinite
ISF	Inert semifusinite
F/SEC	Fusinite/secretinite
MIC	Micrinite
R INT	Reactive inertodetrinite
I INT	Inert inertodetrinite
TOT I	Total inertinite

Total reactive macerals = Vitrinite + liptinite + RSF + reactive inertodetrinite

2. Reflectance measurements

The abbreviations used are defined as follows:

Rr %	Random reflectance of vitrinite, oil immersion
Rsc%	Reflectance of total maceral scan
σ	Standard deviation

3. Microlithotype analysis (% by volume)

Definitions of the Microlithotypes and carbominerites are as follows:

VITRITE	Vitrinite > 95 %
LIPTITE	Liptinite > 95 %
INERTITE	Inertinite > 95 %
CLARITE	Vitrinite + Liptinite > 95 %)
DURITE	Inertinite + Liptinite > 95 %)
VITRINERTITE	Vitrinite + Inertinite > 95 %)
TRIMACERITE	Vitrinite, Inertinite, Liptinite > 5 %)
CARBOMINERITE	Total inorganic/organic microlithotypes
MINERITE	> 60 Vol. % minerals

4. Carbominerite analysis (% by volume)

Definitions of the Carbominerites are as follows:

CARBARGILITE	Coal + 20 to 60 Vol. % clay minerals
CARBOSILICITE	Coal + 20 to 60 Vol. % quartz
CARBOPYRITE	Coal + 5 to 20 Vol. % sulphides
CARBANKERITE	Vol. % carbonates
CARBOMINERITE	Total inorganic/organic microlithotypes

APPENDIX D: Carbon dioxide gasification experimental results

Experimental and char conversion model results are presented in this Appendix. All the experiments were conducted at temperature range of between 850°C and 900°C, pressure of 87.5 and 287.5kPa. The CO_2 concentration was varied between 20 and 100 %.

D.1: Effect of gas composition on char gasification at 87.5kPa

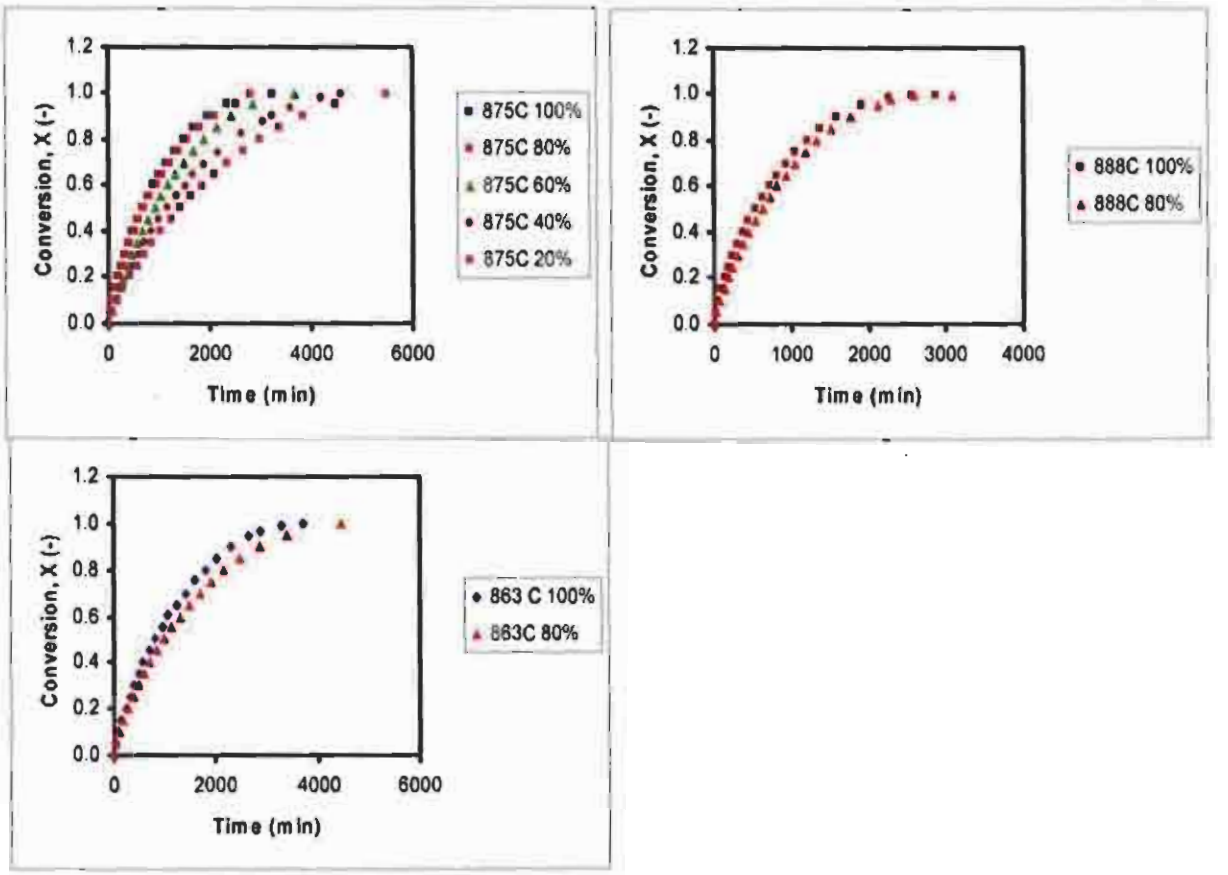

Figure D1: Effect of gas composition on gasification of char at different temperatures and a fixed pressure of 87.5kPa

D.2: Effect of gas composition on char gasification at 287.5kPa

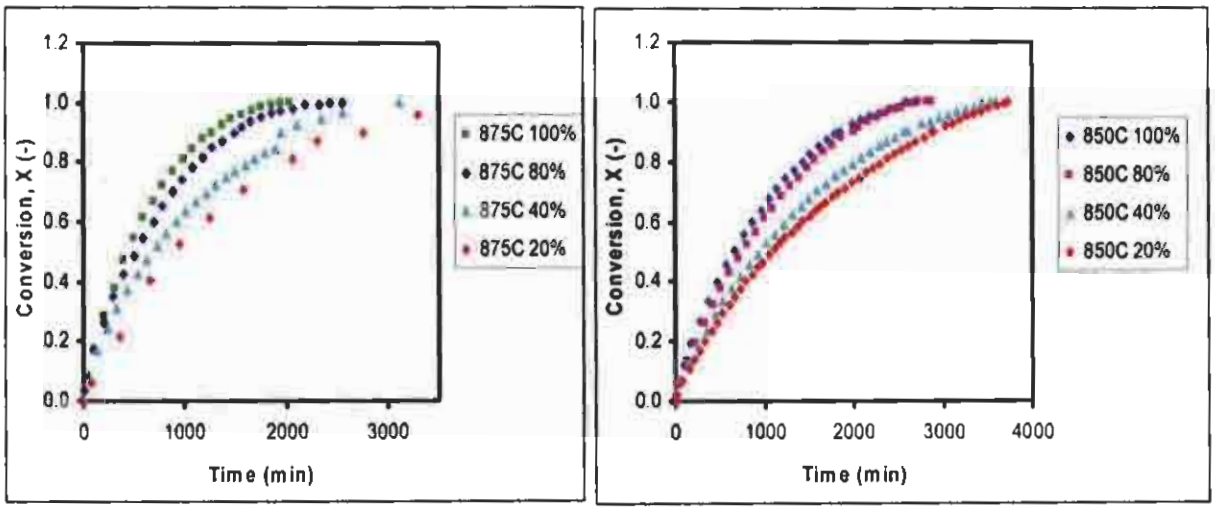

Figure D2 Effect of gas composition on gasification of char at different temperatures and a fixed pressure of 287.5kPa

D.3: Effect of temperature on char gasification at 87.5kPa

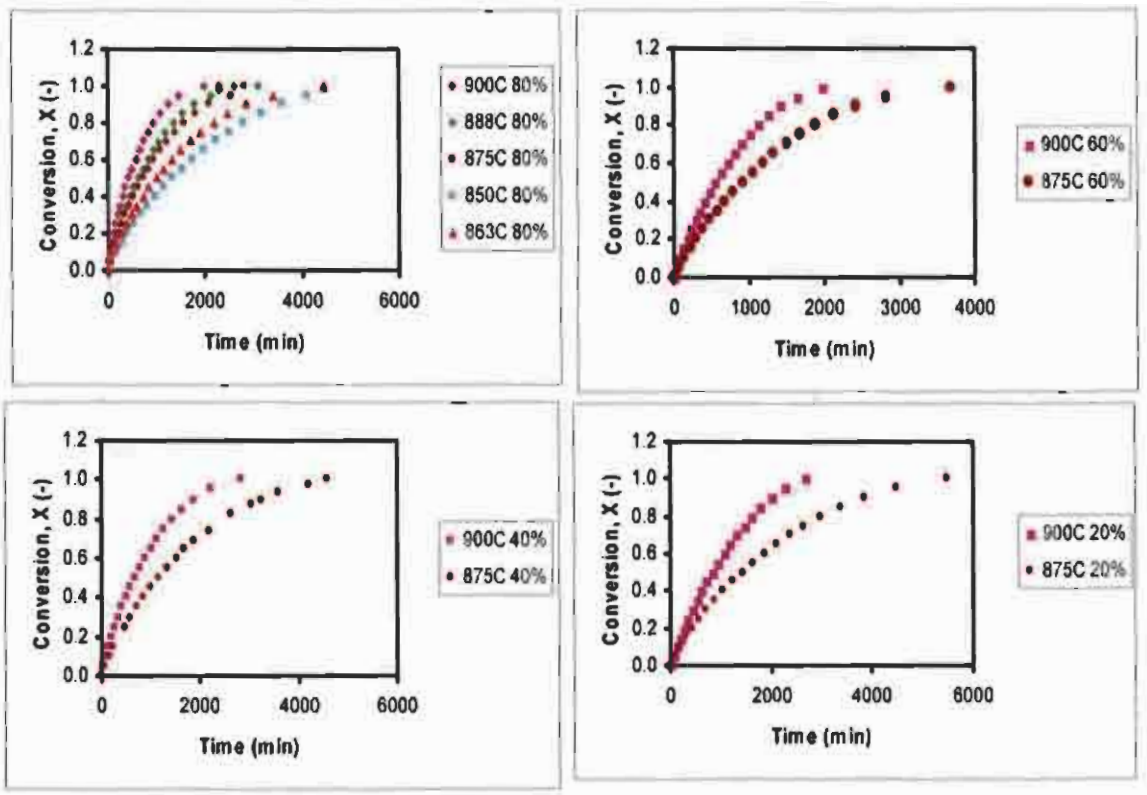

Figure D3 Effect of temperature on gasification of char at a fixed gas composition and pressure of 87.5kPa

D.4: Effect of temperature on char gasification at 287.5kPa

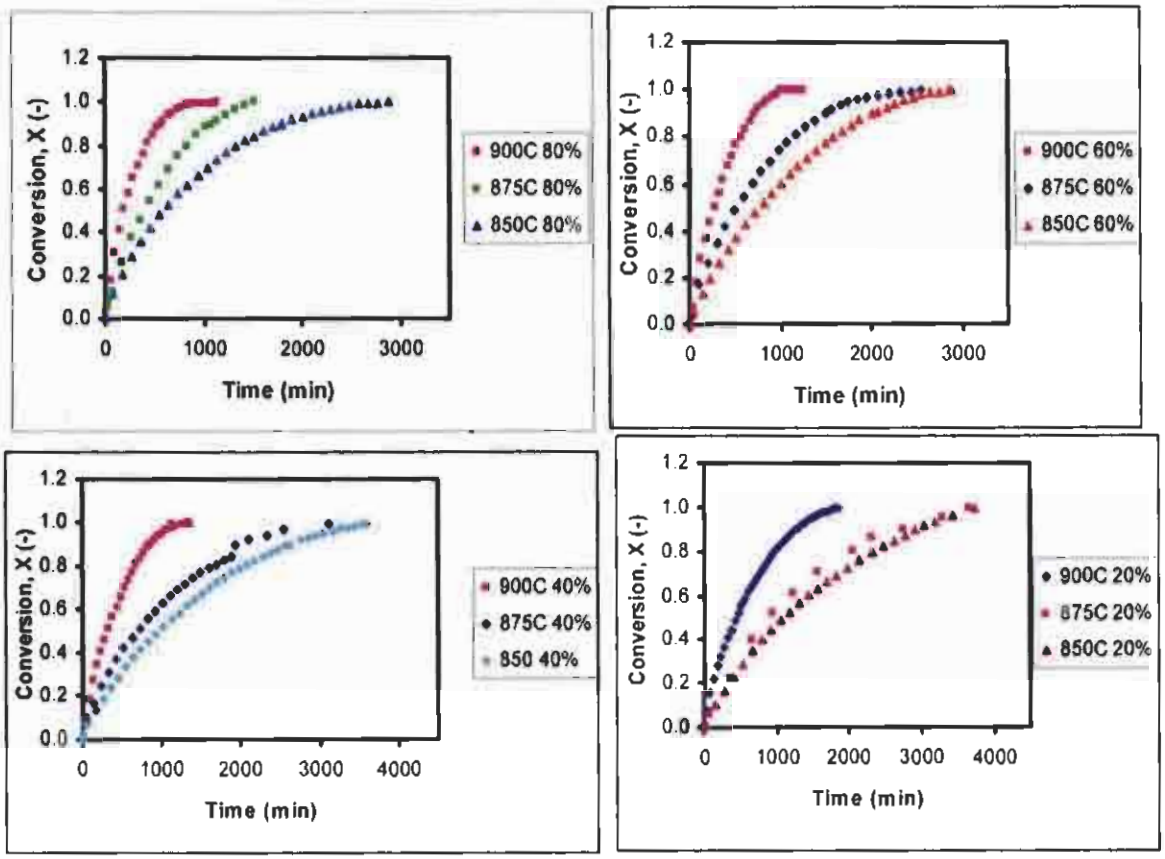

Figure D4 Effect of temperature on gasification of char at a fixed gas composition and pressure of 287.5kP*a*

D.5: Effect of pressure on char gasification

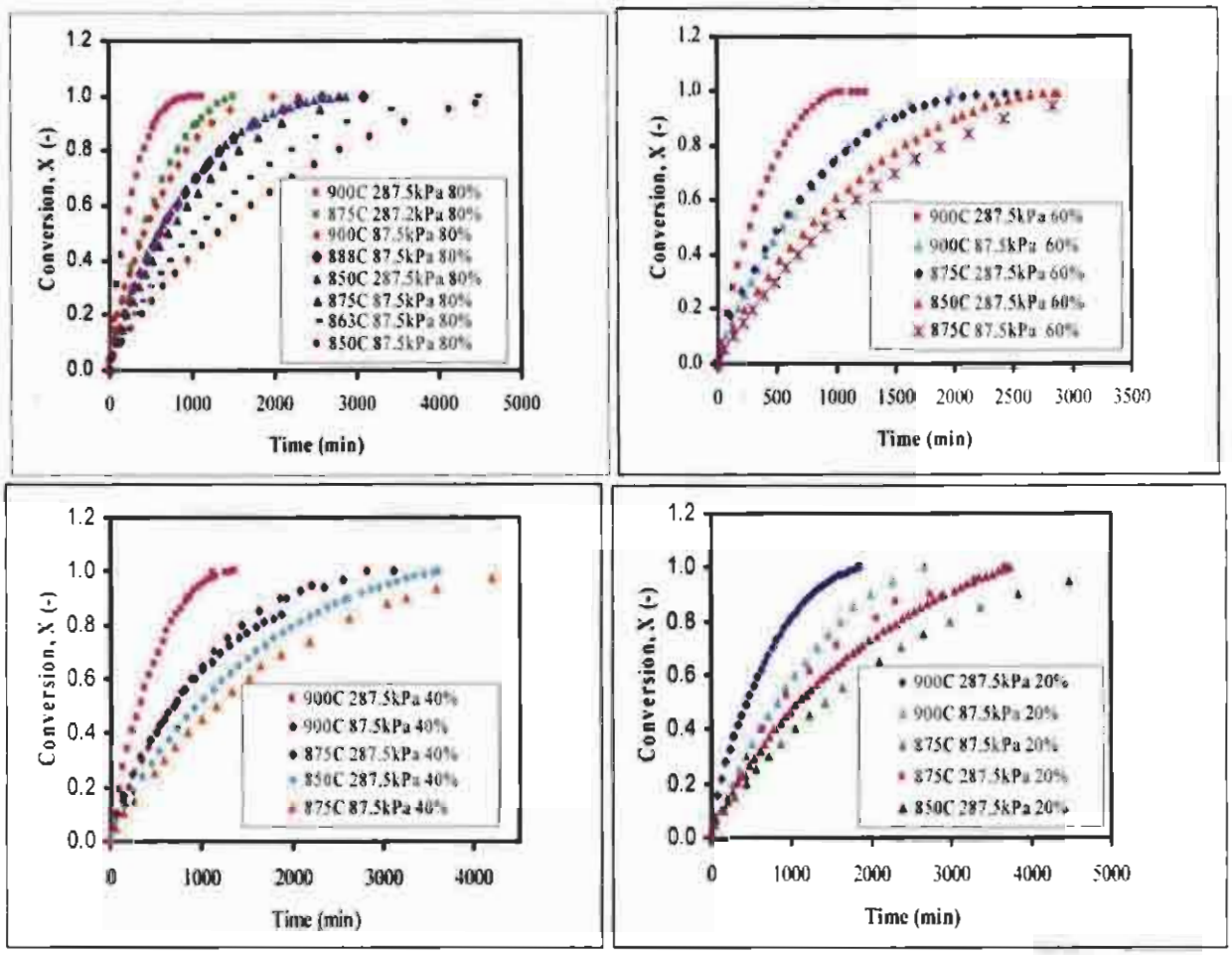

Figure D5 Effect of pressure on gasification of char at a fixed gas composition

D.6 Determination of the order of the gasification reaction at different temperatures

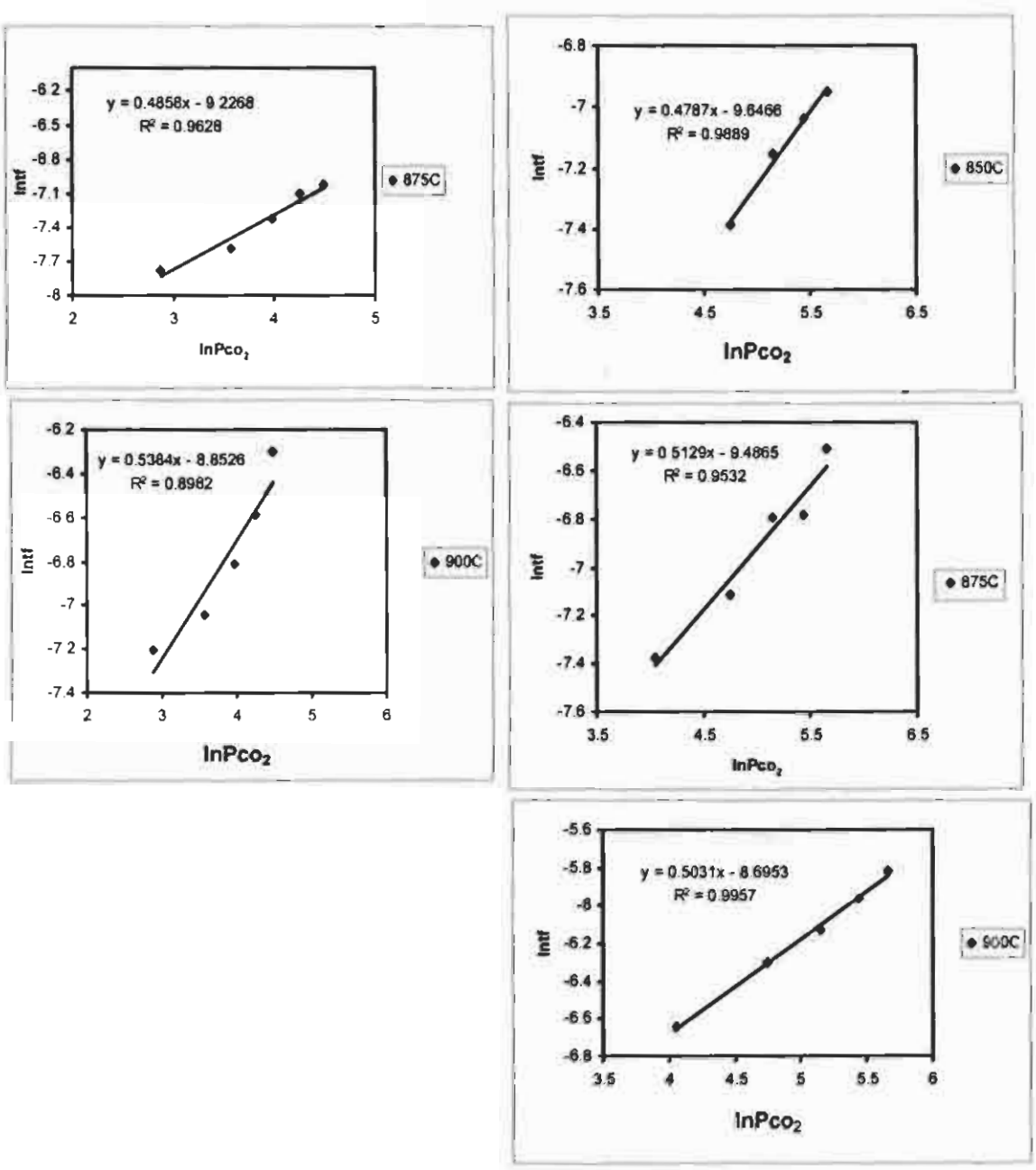

Figure D6: Determination of the order of the gasification reaction at different temperatures.

D.7: Determination of gasification activation energy (E) at 287.5kPa and different CO_2 partial pressures

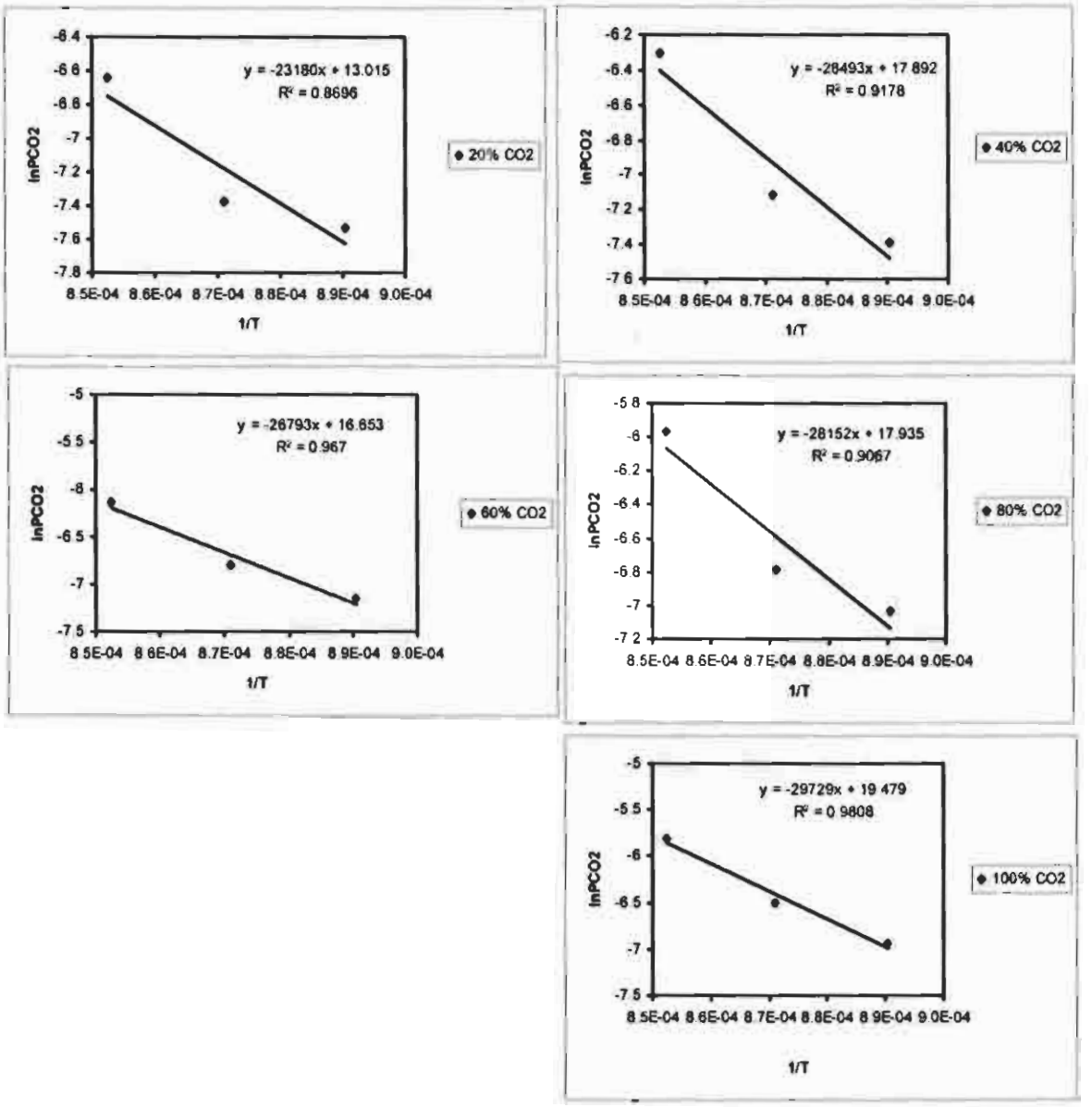

Figure D7: Determination of activation energy at different carbon dioxide partial pressures

D.8: Char conversion model for CO_2 gasification at 87.5kPa

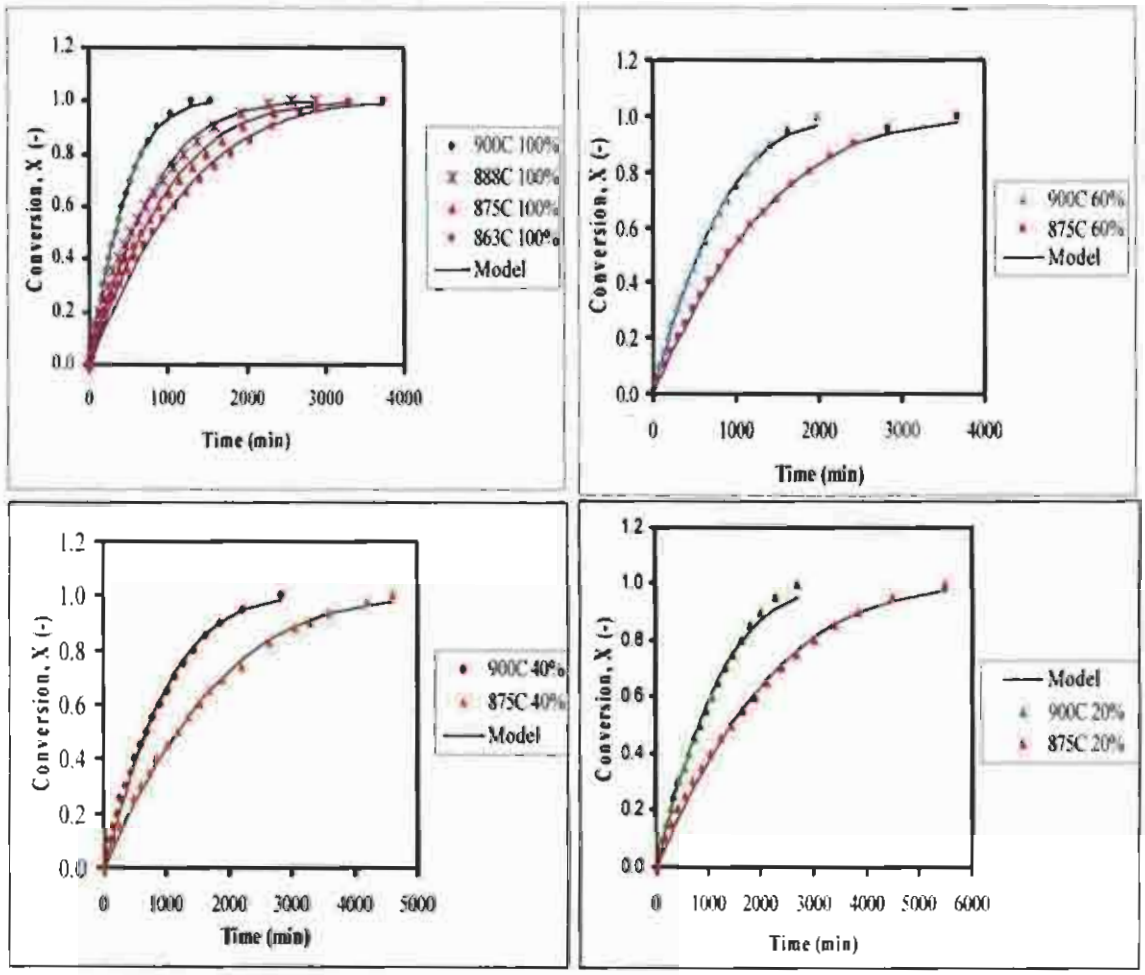

Figure D8: Comparison of experimental data with model data at different temperatures

APPENDIX E: Combustion experimental results

Char combustion experimental results are presented in this Appendix. The experiments were conducted at temperature range of between 450 and 950°C, pressure of 87.5 and 287.5kPa. The O_2 concentration was varied between 5 and 40%.

E.1: Effect of char preparation temperature on combustion

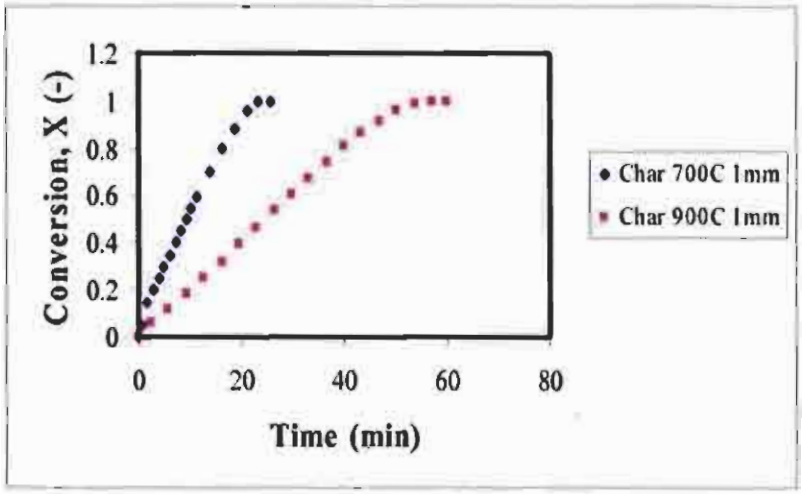

Figure E1: Conversion versus time curve showing the effect of char preparation temperature on combustion (char combusted in 20% Oxygen and at a pressure of 87.5kPa)

E.2: Effect of gas composition on char combustion

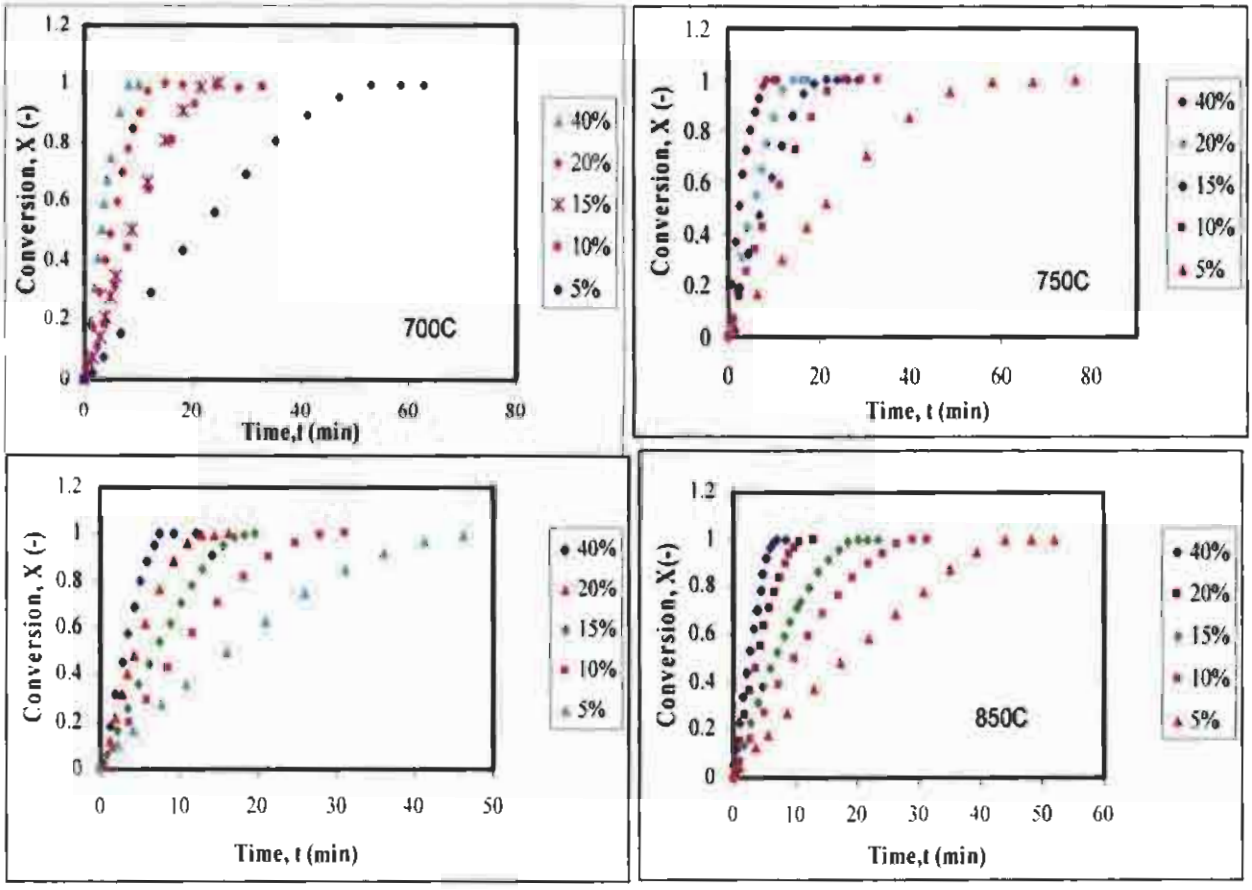

Figure E2: Effect of gas composition on char900 combustion at different temperatures at a pressure of 287.5kPa

E.3: Effect of temperature on char combustion

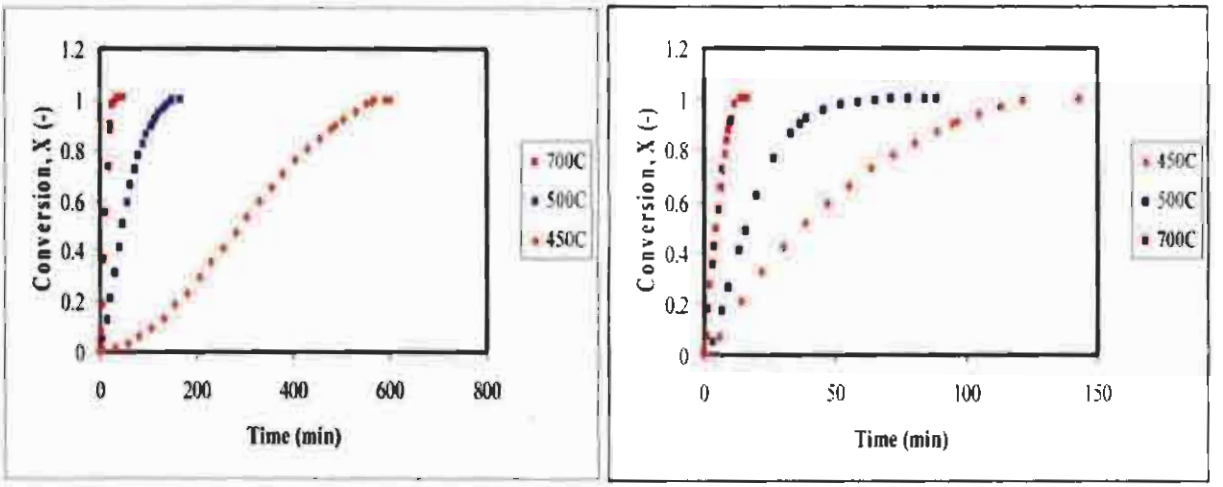

(a) Conversion versus time at 87.5kPa *(b)Conversion versus time at 287.5kPa*

Figure E3: Char combustion in 20% oxygen at (a) 87.5kPa (L) and (b) 287.5kPa all in 20% Oxygen

E.4: Effect of pressure on char combustion

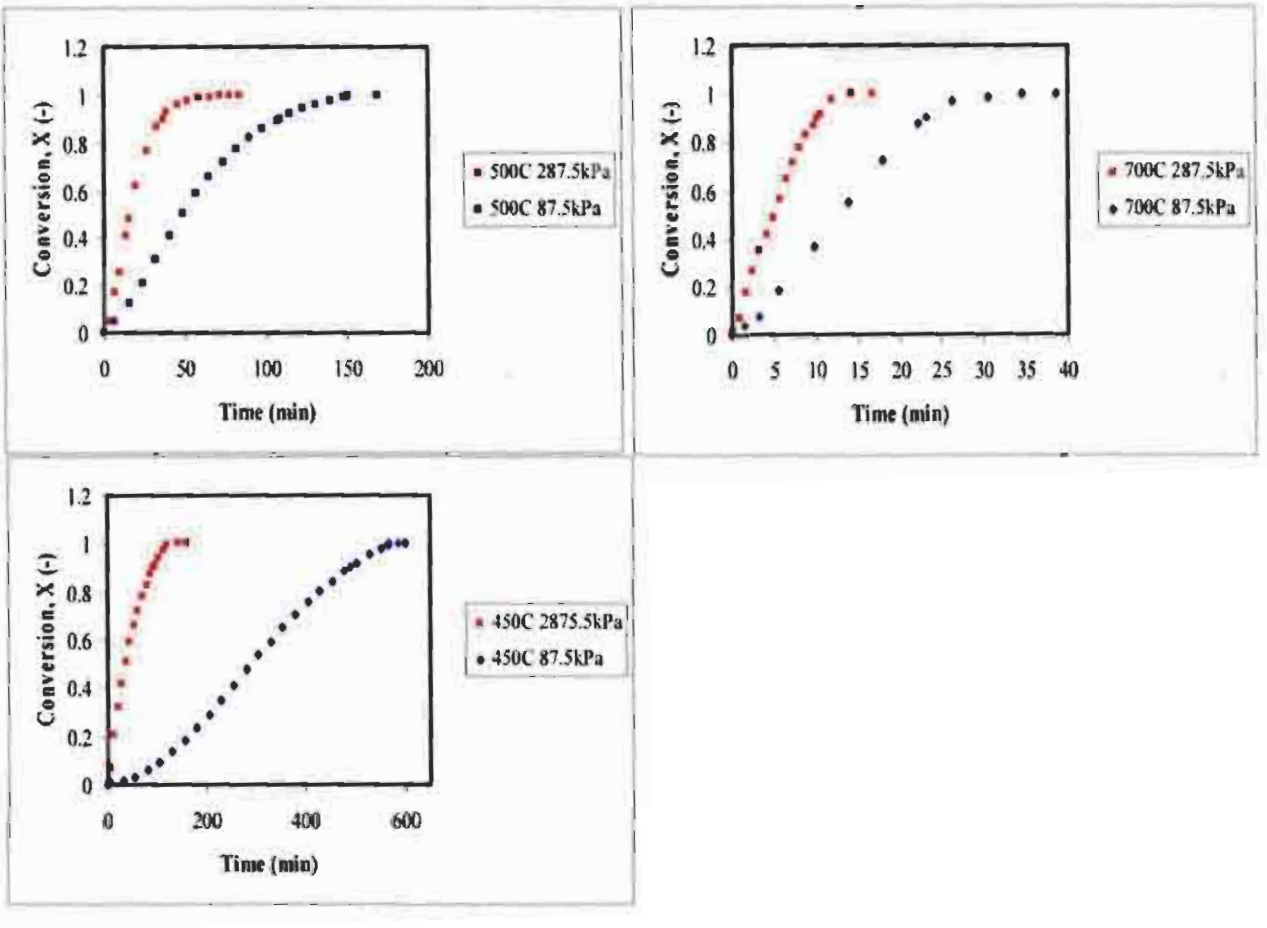

Figure E4: Effect of pressure on combustion of 1mm char900 in 20% Oxygen at different temperatures by plotting conversion versus time

E.5: Effect of particle size on char combustion

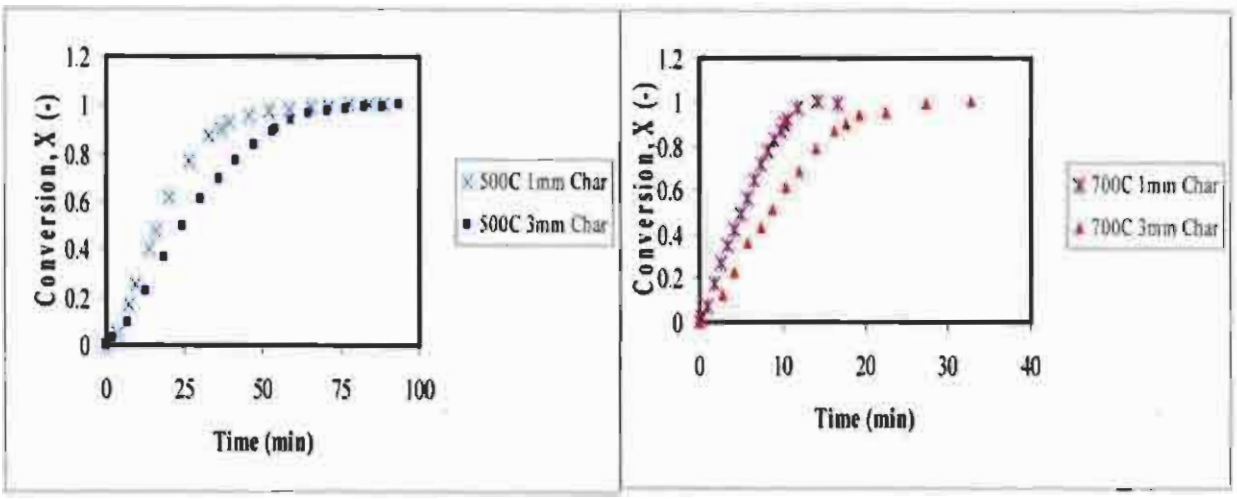

Figure E5: Effect of particle size on char combustion in 20% Oxygen at 287.5kPa.